NONLINEAR DYNAMICS AND SYSTEMS THEORY
An International Journal of Research and Surveys

Volume 19   Number 3   2019

CONTENTS

NONLINEAR DYNAMICS & SYSTEMS THEORY

Volume 19,   No. 3,   2019

Nonlinear Dynamics and Systems Theory

An International Journal of Research and Surveys

INSTRUCTIONS FOR CONTRIBUTORS

(1) General. Nonlinear Dynamics and Systems Theory (ND&ST) is an international journal devoted to publishing peer-refereed, high quality, original papers, brief notes and review articles focusing on nonlinear dynamics and systems theory and their practical applications in engineering, physical and life sciences. Submission of a manuscript is a representation that the submission has been approved by all of the authors and by the institution where the work was carried out. It also represents that the manuscript has not been previously published, has not been copyrighted, is not being submitted for publication elsewhere, and that the authors have agreed that the copyright in the article shall be assigned exclusively to InforMath Publishing Group by signing a transfer of copyright form. Before submission, the authors should visit the website:

http://www.e-ndst.kiev.ua

for information on the preparation of accepted manuscripts. Please download the archive Sample_NDST.zip containing example of article file (you can edit only the file Samplefilename.tex).

(2) Manuscript and Correspondence. Manuscripts should be in English and must meet common standards of usage and grammar. To submit a paper, send by e-mail a file in PDF format directly to

Professor A.A. Martynyuk, Institute of Mechanics,
Nesterov str.3, 03057, MSP 680, Kiev-57, Ukraine
e-mail: journalndst@gmail.com

or to one of the Regional Editors or to a member of the Editorial Board. Final version of the manuscript must typeset using LaTex program which is prepared in accordance with the style file of the Journal. Manuscript texts should contain the title of the article, name(s) of the author(s) and complete affiliations. Each article requires an abstract not exceeding 150 words. Formulas and citations should not be included in the abstract. AMS subject classifications and key words must be included in all accepted papers. Each article requires a running head (abbreviated form of the title) of no more than 30 characters. The sizes for regular papers, survey articles, brief notes, letters to editors and book reviews are: (i) 10-14 pages for regular papers, (ii) up to 24 pages for survey articles, and (iii) 2-3 pages for brief notes, letters to the editor and book reviews.

(3) Tables, Graphs and Illustrations. Each figure must be of a quality suitable for direct reproduction and must include a caption. Drawings should include all relevant details and should be drawn professionally in black ink on plain white drawing paper. In addition to a hard copy of the artwork, it is necessary to attach the electronic file of the artwork (preferably in PCX format).

(4) References. Each entry must be cited in the text by author(s) and number or by number alone. All references should be listed in their alphabetic order. Use please the following style:

Journal: [1] H. Poincare, Title of the article. *Title of the Journal* **volume**
(issue) (year) pages. [Language]

Book: [2] A.M. Lyapunov, *Title of the Book.* Name of the Publishers, Town, year.

Proceeding: [3] R. Bellman, Title of the article. In: *Title of the Book.* (Eds.).
Name of the Publishers, Town, year, pages. [Language]

(5) Proofs and Sample Copy. Proofs sent to authors should be returned to the Editorial Office with corrections within three days after receipt. The corresponding author will receive a sample copy of the issue of the Journal for which his/her paper is published.

(6) Editorial Policy. Every submission will undergo a stringent peer review process. An editor will be assigned to handle the review process of the paper. He/she will secure at least two reviewers' reports. The decision on acceptance, rejection or acceptance subject to revision will be made based on these reviewers' reports and the editor's own reading of the paper.

NONLINEAR DYNAMICS AND SYSTEMS THEORY

CONTENTS

NONLINEAR DYNAMICS AND SYSTEMS THEORY

An International Journal of Research and Surveys

Impact Factor from SCOPUS for 2017: SNIP – 0.707, SJR – 0.316

Nonlinear Dynamics and Systems Theory (ISSN 1562–8353 (Print), ISSN 1813–7385 (Online)) is an international journal published under the auspices of the S.P. Timoshenko Institute of Mechanics of National Academy of Sciences of Ukraine and Curtin University of Technology (Perth, Australia). It aims to publish high quality original scientific papers and surveys in areas of nonlinear dynamics and systems theory and their real world applications.

AIMS AND SCOPE

Nonlinear Dynamics and Systems Theory is a multidisciplinary journal. It publishes papers focusing on proofs of important theorems as well as papers presenting new ideas and new theory, conjectures, numerical algorithms and physical experiments in areas related to nonlinear dynamics and systems theory. Papers that deal with theoretical aspects of nonlinear dynamics and/or systems theory should contain significant mathematical results with an indication of their possible applications. Papers that emphasize applications should contain new mathematical models of real world phenomena and/or description of engineering problems. They should include rigorous analysis of data used and results obtained. Papers that integrate and interrelate ideas and methods of nonlinear dynamics and systems theory will be particularly welcomed. This journal and the individual contributions published therein are protected under the copyright by International InforMath Publishing Group.

PUBLICATION AND SUBSCRIPTION INFORMATION

Nonlinear Dynamics and Systems Theory will have 4 issues in 2019, printed in hard copy (ISSN 1562–8353) and available online (ISSN 1813–7385), by InforMath Publishing Group, Nesterov str., 3, Institute of Mechanics, Kiev, MSP 680, Ukraine, 03057. Subscription prices are available upon request from the Publisher, EBSCO Information Services (mailto:journals@ebsco.com), or website of the Journal: http://e-ndst.kiev.ua. Subscriptions are accepted on a calendar year basis. Issues are sent by airmail to all countries of the world. Claims for missing issues should be made within six months of the date of dispatch.

ABSTRACTING AND INDEXING SERVICES

Papers published in this journal are indexed or abstracted in: Mathematical Reviews / MathSciNet, Zentralblatt MATH / Mathematics Abstracts, PASCAL database (INIST–CNRS) and SCOPUS.

Robust Output Feedback Stabilization and Boundedness of Highly Nonlinear Induction Motors Systems Using Single-Hidden-Layer Neural-Networks

H. Ait Abbas [1*], A. Seghiour [2], M. Belkheiri [3] and M. Rahmani [3]

[1] *Laboratory of Materials and Durable Development-LM2D, Electrical Engineering Department, Faculty of Sciences and Applied Sciences, University of Bouira, (10000) Bouira, Algeria.*
[2] *Electrical Engineering Department, Higher School of Electrical Engineering and Energetic, (31000) Oran, Algeria.*
[3] *Laboratory of Telecommunications Signals and Systems, Amar Telidji University – Laghouat, BP G37 Road of Ghardaia (03000 Laghouat), Algeria.*

Abstract: This paper presents a new single-hidden-layer neural-network (SHL NN)-based adaptive input-output feedback linearization control (IOFLC) to handle the flux and speed tracking problems of the induction motor (IM) subjected to unknown parametric uncertainty, modelling errors and external load disturbances. In this approach, we first apply the IOFLC to divide the IM dynamics into two decoupled subsystems. The resulted controller is then augmented via an on-line SHL NN in order to overcome effects of both the neglected dynamics and the modeling errors. The NN is lunched over input-output signals of the controlled system. The adaptive laws augmented using NN parameters are expressed in terms of the estimated tracking error dynamics of the nominal systems. Of main interest, Lyapunov's direct method is involved to exhibit the ultimate boundedness of the error signals. Computer simulations are presented to emphasize the practical potential of the proposed approach.

Keywords: *nonlinear systems; feedback control; perturbations; adaptive or robust stabilization; neural nets and related approaches; stability; boundedness; simulation.*

Mathematics Subject Classification (2010): 93C10, 93B52, 93C73, 93D21, 62M45, 70K20, 34C11, 37M05.

---

* Corresponding author: mailto:h.aitabbas@univ-bouira.dz

1 Introduction

The IMs are widely used as electromechanical actuators due to their being rugged, free of maintenance, low cost and generally less expensive than other electrical machines [2, 5]. These motors have been utilized for more and more extensive industrial applications such as electric railways and robots, where advanced dynamic performance is claimed. However, the IM considered as a multivariable system has such characteristics as high-coupling and high nonlinearity, which implies that it is very difficult to control.

In the past two decades, trajectory tracking control of the IM systems has been amply studied due to the exigency of high performance in the context of excellent tracking accuracy, rejection of both structured (external disturbances) and unstructured uncertainties (parameter variations and unmodelled dynamics) [2]. For that purpose, the field-oriented control (FOC) scheme will be applied for the IM nonlinear system so as to achieve similar performance characteristics of a separately excited DC motor, such fast, precise tracking, which makes the control task easy [5]. However, some drawbacks such as the coupling between speed and flux and unmodelled dynamics subjugate thoughtful constraints for the FOC and effect the performance speed tracking accuracy. Further, since unknown parametric uncertainties often exist in IM dynamics and they are source of instability, it is meaningful to consider control problems of the corresponding nonlinear IM model [2,5].

Nowadays, practical issues narrow down the choice and give a significant advantage to the input-output feedback linearization control (IOFLC) that is among the most powerful techniques to perform an exact decoupling between both speed and flux dynamics, and higher power efficiency [12]. Furthermore, with the developments of nonlinear control theory and methods (sliding-mode control [14,18], backstepping approach [7,16], and nonlinear feedback linearization control [5,8,17]), the control of IMs subjected to uncertainties has become an important research topic. Specifically, substantial attention has been focused on the use of SHL NN in the system modelling and control applications due to their advantageous features including high potential to identify nonlinear behaviors, powerful nonlinear mapping between inputs and outputs without faithful knowledge of the system model [20].

Moreover, the adaptive control results motivate researchers to find new structures that do not rely on completely knowing the system nonlinearities by using approximation property of NNs and fuzzy logic approximators [4, 9, 19]. The author in [13] presents a new adaptive controller which rules out the effect of uncertainties in order to achieve precise position-tracking performance of IMs using a radial basis function neural network (RBF NN). In [6], the authors develop a new adaptive backstepping controller of a nonlinear IM that achieves global asymptotic speed tracking for the full-order, despite the uncertainty in rotor resistance and external disturbance (load torque). The work presented in [16] deals the tracking control problem of IMs subject to disturbances in practical applications, in which both fuzzy logic control scheme is involved to identify the term of nonlinearities and an adaptive backstepping method is employed to elaborate an adaptive term that eliminates theses nonlinarities. An adaptive fuzzy vector controller (AFVC) is established in the paper [10] to cover the speed and torque tracking problem of a doubly-fed IM, in which the control conception is carried thanks to an appropriate backstepping method that ensures inherently the stability of the control system.

Motivated by the aforesaid discussion, we propose to combine SHL NNs that show strong potentials in approximating uncertainties, with the IOFLC methodology in order to originate a variety of control schemes within the context of NN-based adaptive input-

output feedback control, which can be extended for an extensive class of nonlinear systems with unmodeled dynamics. The elaborated controller takes on dynamic compensator to stabilize the linearized system. Note that the vector that contains the measured tracking error and compensator states is exploited to adapt the NN weights. The input vector to the NN is composed of input/output data, and the adaptive terms adjust on-line for high nonlinearities using nonlinearly parameterized SHL NN. The stability analysis is presented in order to both build the NN adaptation law using only unappropriated measurement as a training signal, and reveal boundedness of all the error signals of the controlled system.

The rest of the paper is organized as follows. The IM model and problem statement are presented in Section 2. Section 3 contains the FOC and IOFLC. NN augmentation and the design control for the IM are detailed in Section 4. Section 5 describes the SHL NN implementation. The stability analysis is detailed in Section 6. The effectiveness of the proposed IM control system is demonstrated through simulation results in Section 7.

2 Induction Motor Modeling and Problem Statement

2.1 Mathematical model of the IM

The IM is represented by the model [12]

$$
\begin{cases}
\dfrac{dw}{dt} = \dfrac{n_p L_m}{J L_r}\big(i_{sb}\psi_{ra} - i_{sa}\psi_{rb}\big) - \dfrac{f}{J}w - \dfrac{\tau_L}{J}, \\[2mm]
\dfrac{d\psi_{ra}}{dt} = -\dfrac{R_r}{L_r}\psi_{ra} - n_p w\psi_{rb} + \dfrac{R_r}{L_r}L_m i_{sa}, \\[2mm]
\dfrac{d\psi_{rb}}{dt} = n_p w\psi_{ra} - \dfrac{R_r}{L_r}\psi_{rb} + \dfrac{R_r}{L_r}L_m i_{sb}, \\[2mm]
\dfrac{di_{sa}}{dt} = \dfrac{L_m R_r}{\sigma L_s L_r^2}\psi_{ra} + \dfrac{n_p L_m}{\sigma L_s L_r}w\psi_{rb} - \left(\dfrac{L_m^2 R_r + L_r^2 R_s}{\sigma L_s L_r^2}\right)i_{sa} + \dfrac{1}{\sigma L_s}u_{sa}, \\[2mm]
\dfrac{di_{sb}}{dt} = -\dfrac{n_p L_m}{\sigma L_s L_r}w\psi_{ra} + \dfrac{L_m R_r}{\sigma L_s L_r^2}\psi_{rb} - \left(\dfrac{L_m^2 R_r + L_r^2 R_s}{\sigma L_s L_r^2}\right)i_{sb} + \dfrac{1}{\sigma L_s}u_{sb}.
\end{cases} \tag{1}
$$

Notice that i, ψ, u_s denote current, flux linkage and stator voltage input to the machine. The variable w denotes the speed of the rotor, while θ is the rotor position. $L_r, L_s,$ and L_m denote the rotor, stator, and mutual inductances, R_r and R_s are the rotor and stator resistances, J is the rotor's moment of inertia, f denotes the coefficient of viscous friction, τ_L is the load torque, and n_p is the number of pole pairs; the subscripts "s" and "r" stand for the stator and rotor; (a, b) represent vector components with respect to a fixed stator reference frame in which $\sigma = 1 - L_m^2/(L_s L_r)$. From now on we will skip the subscripts "r" and "s" since we will only utilize the state variables of rotor fluxes (ψ_{ra}, ψ_{rb}) and stator currents (i_{sa}, i_{sb}).

Let $x = (w, \psi_a, \psi_b, i_a, i_b)^T$ be the state vector, and

$$
p = (\delta_1, \delta_2, \delta_3)^T = (\tau_L - \tau_{LN}, R_r - R_{rN}, R_s - R_{sN})^T \tag{2}
$$

be the unknown parameter deviations from the nominal values τ_{LN}, R_{rN} and R_{sN} of the load torque τ_L, rotor resistance R_r and stator resistance R_s. However, τ_L is typically unknown, whereas R_r and R_s may have a range of variations of $\pm 100\%$ around their nominal values due to ohmic heating. Let $u = (u_a, u_b)^T$ be the control vector. Let $\alpha =$

R_{rN}/L_r, $\beta = L_m/(\sigma L_s L_r)$, $\gamma = (L_m^2 R_{rN}/\sigma L_s L_r^2) + (R_{sN}/\sigma L_s)$, $\mu = n_p L_m/(JL_r)$, $G = (\sigma L_s)$, be a reparameterization of the IM model, where $\alpha, \beta, \gamma, \mu, G$ are known parameters depending on the nominal values R_{rN} and R_{sN}. System (1) can be reformulated in compact form as

$$\dot{x} = f(x) + u_a g_a + u_b g_b + \delta_1 f_1(x) + \delta_2 f_2(x) + \delta_3 f_3(x), \qquad (3)$$

where the vector fields $f, g_a, g_b, f_1, f_2, f_3$ are

$$f(x) = \begin{pmatrix} \mu(i_b \psi_a - i_a \psi_b) - \dfrac{f}{J} w - \dfrac{\tau_{LN}}{J}, \\ -\alpha \psi_a - n_p w \psi_b + \alpha L_m i_a, \\ n_p w \psi_a - \alpha \psi_b + \alpha L_m i_b, \\ \alpha \beta \psi_a + n_p \beta w \psi_b - \gamma i_a, \\ -n_p \beta w \psi_a + \alpha \beta \psi_b - \gamma i_b. \end{pmatrix}, \quad f_1(x) = \begin{pmatrix} -\dfrac{1}{J} \\ 0 \\ 0 \\ 0 \\ 0 \end{pmatrix},$$

$$f_2(x) = \begin{pmatrix} 0 \\ -\dfrac{1}{L_r}\psi_a + \dfrac{L_m}{L_r} i_a \\ -\dfrac{1}{L_r}\psi_b + \dfrac{L_m}{L_r} i_b \\ \dfrac{L_m}{\sigma L_s L_r^2}\psi_a - \dfrac{L_m^2}{\sigma L_s L_r^2} i_a \\ \dfrac{L_m}{\sigma L_s L_r^2}\psi_b - \dfrac{L_m^2}{\sigma L_s L_r^2} i_b \end{pmatrix}, f_3(x) = \begin{pmatrix} 0 \\ 0 \\ 0 \\ -\dfrac{1}{G} \\ -\dfrac{1}{G} \end{pmatrix}, g_a = \begin{pmatrix} 0 \\ 0 \\ 0 \\ \dfrac{1}{G} \\ 0 \end{pmatrix}, g_b = \begin{pmatrix} 0 \\ 0 \\ 0 \\ 0 \\ \dfrac{1}{G} \end{pmatrix}.$$

2.2 Control problem statement

This paper focuses on the study of tracking control $((w \to w^*)$ and $(\psi_d = \sqrt{\psi_{ra} + \psi_{rb}} \to \psi_d^*))$ for the field-oriented IM subject to external disturbances (load torque) and parameter uncertainties. For that matter, we contribute to develop an adaptive input-output feedback linearization technique to elaborate controllers in which SHL NNs are used to approximate terms of nonlinearity.

3 Field-Oriented and Input Output Linearization Control

3.1 Conventional field-oriented control

The control objective is to conceive a controller in which the stator voltages are choosen to adjust the torque, speed and/or position of the motor. To achieve the field-oriented control, we perform the transformation of the vectors (i_a, i_b) and (ψ_a, ψ_b) in the fixed stator frame (a, b) into vectors in a frame (d, q) which rotate along with the flux vector $((\psi_a, \psi_b))$. Therefore, the stator phase currents and voltages are then expressed in this new coordinates as follows [7]

$$\begin{bmatrix} i_d \\ i_q \end{bmatrix} = \begin{bmatrix} \cos \rho & \sin \rho \\ -\sin \rho & \cos \rho \end{bmatrix} \begin{bmatrix} i_{sa} \\ i_{sb} \end{bmatrix}, \quad \begin{bmatrix} u_d \\ u_q \end{bmatrix} = \begin{bmatrix} \cos \rho & \sin \rho \\ -\sin \rho & \cos \rho \end{bmatrix} \begin{bmatrix} u_{sa} \\ u_{sb} \end{bmatrix}$$

in which we define $(\rho = \arctan\left(\frac{\psi_b}{\psi_a}\right))$, where ψ_d and ρ are just "polar coordinates" for the ordered pair (ψ_a, ψ_b). The term "field-oriented" affects this new rotating coordinate

system in which the angular position is ρ so that $\psi_q \equiv 0$, and i_d and i_q are called the direct and quadrature currents, u_d and u_q are called the direct and quadrature voltages, respectively.

When we refer to the fixed stator (d, q) reference frame, the electromagnetic dynamic model of the induction motor can be developed yielding

$$
\begin{cases}
\dfrac{dw}{dt} = \mu\psi_d i_q - \dfrac{f}{J}w - \dfrac{\tau_L}{J}, \\[2mm]
\dfrac{d\psi_d}{dt} = -\alpha\psi_d + \alpha L_m i_d, \\[2mm]
\dfrac{di_d}{dt} = -\gamma i_d + \alpha\beta\psi_d + n_p w i_q + \alpha L_m \dfrac{i_q^2}{\psi_d} + \dfrac{1}{G}u_d, \\[2mm]
\dfrac{di_q}{dt} = -\gamma i_q - \beta n_p w\psi_d - n_p w i_d - \alpha L_m \dfrac{i_d i_q}{\psi_d} + \dfrac{1}{G}u_q, \\[2mm]
\dfrac{d\rho}{dt} = n_p w + \alpha L_m \dfrac{i_q}{\psi_d}.
\end{cases}
\tag{4}
$$

Now, it is clear that the electromagnetic torque $\tau_e = J\mu\psi_d i_q$ is just proportional to the product of two state variables ψ_d and i_q. Unfortunately, in the state space model of the IM presented in (4), differential equations for i_d and i_q nevertheless include plenty high nonlinearities. For that, one possibility to make simpler these dynamics is to involve the nonlinear state feedback control

$$
\begin{bmatrix} u_d \\ u_q \end{bmatrix} = G \begin{bmatrix} \gamma i_d - \alpha\beta\psi_d - n_p w i_q - \alpha L_m \frac{i_q^2}{\psi_d} + \overline{v}_d \\[2mm] \gamma i_q + \beta n_p w\psi_d + n_p w i_d + \alpha L_m \frac{i_d i_q}{\psi_d} + \overline{v}_q \end{bmatrix}.
\tag{5}
$$

Then, the resulting closed-loop IM system is written as

$$
\begin{cases}
\dfrac{dw}{dt} = \mu\psi_d i_q - \dfrac{f}{J}w - \dfrac{\tau_L}{J}, \\[2mm]
\dfrac{di_q}{dt} = \overline{v}_q, \\[2mm]
\dfrac{d\psi_d}{dt} = -\alpha\psi_d + \alpha L_m i_d, \\[2mm]
\dfrac{di_d}{dt} = \overline{v}_d, \\[2mm]
\dfrac{d\rho}{dt} = n_p w + \alpha L_m \dfrac{i_q}{\psi_d},
\end{cases}
\tag{6}
$$

where $\psi_d(t)$ and $w(t)$ are output signals of the IM that will be controlled to achieve the tracking accuracy.

3.2   Input-output linearization control

In the above FOC scheme, the speed w and flux ψ_d are only asymptotically decoupled. Consequently, the speed is linearly related to i_q only after ψ_d is constant. However, field weakening (i.e., decreasing ψ_d) is necessary for high speeds so as not to saturate the stator voltages. Since field-weakening depends on speed, the dynamics of ψ_d may interfere with the dynamics of w, especially when the speed varies rapidly [12].

As a solution to the presented problem, we suggest to introduce an input-output linearization controller that will be designed for the full order (voltage command) system model (6). Specifically, the transformation ($\eta = \mu\psi_d i_q$, $\psi_d = \psi_d$, $\xi = -\alpha\psi_d + \alpha L_m i_d$) is introduced for (6), resulting in

$$
\begin{cases}
\dfrac{dw}{dt} = \eta - \dfrac{f}{J}w - \dfrac{\tau_L}{J}, \\[2mm]
\dfrac{d\eta}{dt} = \mu\xi i_q + (\mu\psi_d)\overline{v}_q, \\[2mm]
\dfrac{d\psi_d}{dt} = \xi, \\[2mm]
\dfrac{d\xi}{dt} = -\alpha\xi + (\alpha L_m)\overline{v}_d, \\[2mm]
\dfrac{d\rho}{dt} = n_p w + \alpha L_m \dfrac{\eta}{\mu\psi_d^2},
\end{cases}
\tag{7}
$$

in which v_d and v_q are two new inputs, the application of the feedback

$$
\begin{cases}
\overline{v}_d = \dfrac{\xi}{L_m} + \dfrac{v_d}{\alpha L_m}, \\[3mm]
\overline{v}_q = -\dfrac{\mu\xi i_q}{\mu\psi_d} + \dfrac{v_q}{\mu\psi_d}
\end{cases}
\tag{8}
$$

results in the input-output linearized system

$$
\begin{cases}
\dfrac{dw}{dt} = \eta - \dfrac{f}{J}w - \dfrac{\tau_L}{J}, \\[2mm]
\dfrac{d\eta}{dt} = v_q + \delta_q, \\[2mm]
\dfrac{d\psi_d}{dt} = \xi, \\[2mm]
\dfrac{d\xi}{dt} = v_d + \delta_d, \\[2mm]
\dfrac{d\rho}{dt} = n_p w + \alpha L_m \dfrac{\mu\eta}{\psi_d^2},
\end{cases}
\tag{9}
$$

where both δ_d and δ_q denote inversion errors. To explain, assuming that all parametric uncertainties terms for each subsystem are an error signal δ_i (δ_d and δ_q)), we take into account the motor parameters R_r and R_s that can vary appreciably due to the Ohmic heating while the magnetic saturation can cause variations of L_r and L_s [6].

It is clear that the system (9) is linear from the inputs v_d, v_q to the outputs w, ψ_d. Consequently, the IM dynamics has a straightforward structure since the conceived controller is the $input-output$ linearization controller. However, since the designed controller relies completely on the exact values of the IM parameters with total knowledge of the model, the robustness to parametric uncertainty cannot be ensured. Much work in the literature on robust control have been consecrated to handle such problems. The authors in [8, 15] developed an adaptive output feedback controller augmented via a SHL NN for highly complex nonlinear systems to eliminate the effect of unknown variations in plant parameters and structure that can be unknown but bounded, and provided the stability analysis of the closed loop system using the Lyapunov method.

In the present paper, taking the advantage that the flux dynamics is decoupled from the speed dynamics after IOFLC, and inspired by the control ideas in [8,15] that exploit SHL NNs for their approximation ability, we aim to develop a control law that augments the IOFLC scheme by only SHL NNs to sensibly approximate the uncertainties existing in the IM.

4 Adaptive Controller Design

4.1 Control design

Taking advantage from the fact that the IM dynamics (9) is divided into two linear subsystems, we contribute to synthesize adaptive control laws augmented via NN that utilize the available measurements (ψ_d and w) so that the outputs ($\psi_d(t)$ and $w(t)$) track smooth bounded reference trajectories ($\psi_d^*(t)$ and w^*), respectively, with bounded error. That is, the first four equations of (9) may be written as two decoupled linear subsystems, flux dynamics

$$\begin{cases} \dfrac{d\psi_d}{dt} = \xi, \\ \dfrac{d\xi}{dt} = v_d + \delta_d \end{cases} \tag{10}$$

and speed dynamics

$$\begin{cases} \dfrac{dw}{dt} = \eta - \dfrac{f}{J}w - \dfrac{\tau_L}{J}, \\ \dfrac{d\eta}{dt} = v_q + \delta_q, \end{cases} \tag{11}$$

where v_d and v_q are the inputs chosen to force the linear systems (10) and (11) to track a given reference trajectories ψ_d^* and $w^*(t)$, respectively.

Note that both flux and speed subsystems are partially known, and their outputs ψ_d and w have relative degrees equal to 2. Therefore, the output dynamics ($y_d = \psi_d$) and ($y_q = w$) given by (10) and (11), respectively, will be reformulated as

$$\begin{cases} y_d^{(2)} = \ddot{\psi}_d = v_d + \delta_d, \\ y_q^{(2)} = \ddot{w} = v_q + \delta_q, \end{cases} \tag{12}$$

on suggest exploit SHL NNs for their efficiency and ease of implementation in order to deal with the effect of uncertainties (δ). Therefore, the control strategy will be improved by adding adaptive neural network components u_{ad}, u_{aq} in the expressions of the control laws v_d, v_q in order to identify nonlinearities δ_d and δ_q, respectively. The global block diagram of the designed control scheme is illustrated in Figure (1).

Consequently, the pseudocontrols v_d and v_q are chosen to have the form

$$\begin{cases} v_d = \ddot{\psi}_d^* + D_{cd} - u_{ad}, \\ v_q = \ddot{w}^* + D_{cq} - u_{aq}, \end{cases} \tag{13}$$

where $y_c^{(r)} = (\ddot{\psi}_d^*, \ddot{w}^*)$ are the second derivatives ($r = 2$) of the input signals generated by the stable command filters, D_{cd} and D_{cq} denote outputs of the linear dynamic compensators, u_{ad} and u_{aq} represent the adaptive control signals designed to overcome δ_d and δ_q, respectively.
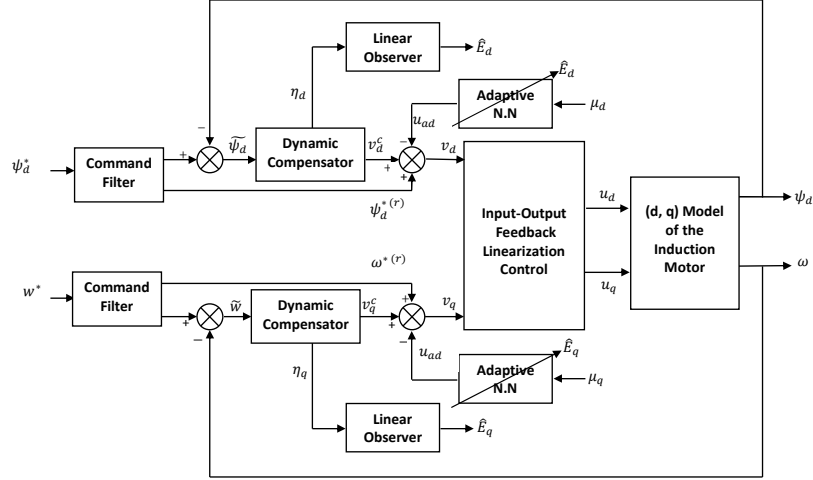
Figure 1: Adaptive inpout-output feedback linearization controller-based SHL NN architecture.

With (13), the dynamics in (12) reduce to

$$\begin{cases} y_d^{(2)} = \ddot{\psi}_d = \ddot{\psi}_d^* + D_{cd} - u_{ad} + \delta_d, \\ y_q^{(2)} = \ddot{w} = \ddot{w}^* + D_{cq} - u_{aq} + \delta_q. \end{cases} \tag{14}$$

Accordingly, one challenge is to design adaptive input-output feedback linearization controllers, whose adaptive terms u_{ad} and u_{aq} adjust on-line for unknown nonlinearities δ_d and δ_q using nonlinearly parameterized SHL NNs for the flux and speed subsystems, respectively.

Consequently, with (14), the two subsystems (10) and (11) can be rewritten, respectively, as in (15) and (16)

$$\begin{cases} \dfrac{d\psi_d}{dt} = \xi, \\ \dfrac{d\xi}{dt} = \ddot{\psi}_d^* + D_{cd} - u_{ad} + \delta_d, \end{cases} \tag{15}$$

$$\begin{cases} \dfrac{dw}{dt} = \eta - \dfrac{f}{J}w - \dfrac{\tau_L}{J}, \\ \dfrac{d\eta}{dt} = \ddot{w}^* + D_{cq} - u_{aq} + \delta_q. \end{cases} \tag{16}$$

The two subsystems are almost identical, for the rest of the paper we will treat only the dynamics of the flux subsystem to simplify writing

$$\begin{cases} \dfrac{d\psi_d}{dt} = \xi, \\ \dfrac{d\xi}{dt} = \ddot{\psi}_d^* + D_{cd} - u_{ad} + \delta_d. \end{cases} \tag{17}$$

4.2   Design of the dynamic compensator and error dynamics

The output tracking errors is defined as $(\widetilde{\psi}_d = \psi_d^* - \psi_d)$. Then the dynamics in (14) can be rewritten as

$$\ddot{\widetilde{\psi}}_d = -D_{cd} + u_{ad} - \delta_d. \tag{18}$$

The following linear compensator is introduced to stabilize the dynamics in the ideal case $(\delta_d = 0, \, u_{ad} = 0)$

$$\begin{cases} \dot{\eta}_d = \alpha_d \eta_d + \beta_d \widetilde{\psi}_d, \\ D_{cd} = \chi_d \eta_d + \varrho_d \widetilde{\psi}_d, \end{cases} \tag{19}$$

where η_d needs to be at least of dimension $(r - 1 = 1)$ [1,3,11], while the gains $\alpha_d, \beta_d, \chi_d$ and ϱ_d should be designed such that $\overline{A}$ is Hurwitz.

Notice that the tracking error dynamics is formed from the combination of the vector $e_d = [\widetilde{\psi}_d \quad \dot{\widetilde{\psi}}_d]^T$ mutually with the compensator state η_d

$$\begin{cases} \dot{E}_d = \overline{A} E_d + \overline{b}[u_{ad} - \delta_d], \\ z_d = \overline{C} E_d, \end{cases} \tag{20}$$

where $E_d = [e_d^T \quad \eta_d^T]^T, \overline{A} = \begin{bmatrix} A - \varrho_d bc & -b\chi_d \\ \beta_d c & \alpha_d \end{bmatrix}, \overline{b} = \begin{bmatrix} b \\ 0 \end{bmatrix}, \overline{c} = \begin{bmatrix} c & 0 \\ 0 & I \end{bmatrix}, A = \begin{bmatrix} 0 & 1 \\ 0 & 0 \end{bmatrix}, b = \begin{bmatrix} 0 \\ 1 \end{bmatrix}, c = \begin{bmatrix} 1 \\ 0 \end{bmatrix}^T$, and z_d is the vector of available measurements.

4.3   Design and analysis of an observer for the error dynamics

A minimal-order observer of dimension $(r - 1 = 1)$ may be designed for the dynamics in (20). However, to streamline the subsequent stability analysis, in what follows, we consider the case of a full-order observer of dimension $(2r - 1 = 3)$ [4, 15, 21].

To this end, consider the following linear observer for the tracking error dynamics in (20):

$$\begin{cases} \dot{\widehat{E}}_d = \overline{A} \widehat{E}_d + K(z_d - \widehat{z}_d), \\ \widehat{z}_d = \overline{C} \widehat{E}_d, \end{cases} \tag{21}$$

where K is a gain matrix, and should be chosen such that $\widetilde{A} = (\overline{A} - K\overline{C})$ is asymptotically stable. Then, introduce the observer error signal $\widetilde{E}_d = (\widehat{E}_d - E_d)$ and write the observer error dynamics

$$\begin{cases} \dot{\widetilde{E}}_d = \widetilde{A} \widetilde{E}_d - \overline{b}[u_{ad} - \delta_d], \\ \widetilde{z}_d = \overline{C} \widetilde{E}, \end{cases} \tag{22}$$

where $\widetilde{z}_d = (\widehat{z}_d - z_d)$.

5   SHL NN Approximation of the Inversion Error

5.1   Neural network approximation

Assume that there exists a neural network with only one single hidden layer that approximates the term of uncertainties δ_d. This NN has an output given by

$$y_i = \sum_{j=1}^{N_2} \left[m_{ij} \Phi \left(\sum_{k=1}^{N_1} n_{jk} x_k + \theta_{nj} \right) + \theta_{mi} \right], \quad x \in \Re^{N_1}, \quad i = 1, ..., N_3, \qquad (23)$$

where $\Phi(.)$ is an activation function, n_{jk} are the first-to-second layer interconnection weights, m_{ij} are the second to third layer interconnection weights, N_2 is associated with the number of neurons in the hidden layer, θ_{nj} and θ_{mi} denote bias terms.

Theorem 5.1 *Given $\epsilon^* > 0$, there exists a set of bounded weights Ψ and N such that the model inversion error $\delta(x, u)$ can be approximated over a compact set $\mathcal{D} \subset \Omega X \mathcal{R}$, by an SHL NN*

$$\delta(\xi_d, v_d) = \Psi^T \Phi(N^T \mu_d) + \epsilon(d, \mu_d), \quad |\epsilon| < \epsilon^*, \qquad (24)$$

using the input vector

$$\mu_d(t) = [\nu_d^T(t) \quad \psi_d^T(t)]^T \in \mathcal{D}, \quad \|\mu_d\| \le \mu_d^*, \quad \mu_d^* > 0. \qquad (25)$$

5.2   Adaptive element

The output of an SHL NN defines the adaptive signal

$$u_{ad} = \widehat{\Psi}^T \Phi(N^T \mu_d) + \epsilon(d, \mu_d), \qquad (26)$$

where $\widehat{\Psi}$ and $\widehat{N}$ are estimates of Ψ and N that are updated as follows:

$$\begin{aligned}
\dot{\widehat{\Psi}} &= -F_d[2(\widehat{\Phi} - \widehat{\Phi'} N^T \mu_d)\widehat{E}_d^T P\overline{b} + k_d(\widehat{\Psi} - \Psi_0)], \\
\dot{\widehat{N}} &= -G_d[2\mu_d \widehat{E}_d^T P\overline{b}\widehat{\Psi}^T \widehat{\Phi'} + k_d(\widehat{N} - N_0)]
\end{aligned} \qquad (27)$$

in which Ψ_0 is the initial value of Ψ, N_0 is the initial value of the hidden layer weights vector N, $\widehat{\Phi} = \Phi(N^T \mu_d)$, $\widehat{\Phi'}$ denotes the Jacobian matrix, P is the solution of the Lyapunov equation

$$\overline{A}^T P + P\overline{A} = -Q \qquad (28)$$

for some $Q > 0$, $k_d > 0$, and F_d, G_d are adaptation gain matrices.

Using (24) and (26), the error dynamics in (20) can be reformulated as

$$\begin{cases} \dot{E}_d = \overline{A} E_d + \overline{b}[\widehat{\Psi}^T \Phi(\widehat{N}^T \mu_d) - \Psi^T \Phi(N^T \mu_d) - \epsilon], \\ z_d = \overline{C} E_d. \end{cases} \qquad (29)$$

Define

$$\widetilde{\Psi} = \widehat{\Psi} - \Psi, \quad \widetilde{N} = \widehat{N} - N, Z_d = \begin{bmatrix} \Psi & 0 \\ 0 & N \end{bmatrix}, \widetilde{Z}_d = \begin{bmatrix} \widetilde{\Psi} & 0 \\ 0 & \widetilde{N} \end{bmatrix} \qquad (30)$$

and note that $||\widehat{\Psi}|| < ||\widetilde{\Psi}|| + \Psi^*, ||\Psi|| < \Psi^*, ||\widehat{N}||_F < ||\widetilde{N}||_F + N^*, ||N||_F < N^*$, where Ψ^* and N^* are the upper bounds for the weights in (24), and the subscript F denotes the Frobenius norm. Therefore, the mismatch between the adaptive signal and the inversion errors

$$u_{ad} - \delta_d = \widehat{\Psi}^T \Phi(\widehat{N}^T \mu_d) - \Psi^T \Phi(N^T \mu_d) - \epsilon \tag{31}$$

allows for the following upper bound for some computable α_a, α_b

$$|u_{ad} - \delta_d| \leq \alpha_a ||\widetilde{Z}_d||_F + \alpha_b, \quad \alpha_a > 0, \quad \alpha_b > 0. \tag{32}$$

Since the weights are adjusted online, we will need the following representation for the stability proof : $\widehat{\Psi}^T \Phi(\widehat{N}^T \mu_d) - \Psi^T \Phi(N^T \mu_d) = \widetilde{\Psi}^T(\widehat{\Phi} - \widehat{\Phi'}\widehat{N}^T \mu_d) + \vartheta_b + \vartheta$, where $\vartheta = \widetilde{\Psi}^T \widehat{\Phi'} N^T \mu_d - \Psi^T \mathcal{O}(\widetilde{N}^T \mu_d)^2$, and $\vartheta_b = \widehat{\Psi}^T \widehat{\Phi'} \widetilde{N}^T \mu_d$.

Such a representation is achieved via the Taylor series expansion of $\Phi(N^T \mu_d)$ around the estimates $\widehat{N}^T \mu_d$. Taking account of the bound in (25), a bound for $(\vartheta - \epsilon)$ over a compact can be expressed as follows [1, 4, 15]

$$|\vartheta - \epsilon| \leq \gamma_a ||\widetilde{Z}_d||_F + \gamma_b, \quad \gamma_a > 0, \gamma_b > 0, \tag{33}$$

where γ_a and γ_b are computable constants, γ_a depends upon unknown constant μ_d^*, and γ_b upon ϵ^*. Thus, the forcing term in (17) can be written

$$u_{ad} - \delta_d = \widetilde{\Psi}^T(\widehat{\Phi} - \widehat{\Phi'}\widehat{N}^T \mu_d) + \widehat{\Psi}^T \widehat{\Phi'}\widetilde{N}^T \mu_d + \vartheta - \epsilon. \tag{34}$$

6 Stability Analysis

We confirm through Lyapunov's direct method that if the initial errors of the variables $E_d^T, \widetilde{E}_d^T, \widetilde{\Psi}$ and $\widetilde{N}$ belong to the presented compact set, then the composite error vector $\zeta_d = \begin{bmatrix} E_d^T & \widetilde{E}_d^T & \widetilde{Z}_d^T \end{bmatrix}^T$ is ultimately bounded. Notice that ζ_d can be viewed as a function of the state variables $\xi_d, \eta_d, \widetilde{E}_d, \widetilde{Z}_d$, the command vector $y_c = [\psi_d^* \quad \dot{\psi}_d^*]^T$, and a constant vector Z_d

$$\zeta_d = F(\xi_d, \eta_d, \widehat{E}_d, \widehat{Z}_d, y_c, Z_d). \tag{35}$$

The relation in(35) represents a mapping from the original domains of the arguments to the space of the error variables

$$F : \Omega_{\xi_d} \times \Omega_{y_c} \times \Omega_{\eta_d} \times \Omega_{\widehat{E}_d} \times \Omega_{\widehat{Z}_d} \times \Omega_{Z_d} \longrightarrow \Omega_{\zeta_d}. \tag{36}$$

Recall that (25) introduces the compact set $\mathcal{D}$ over which the NN approximation is valid. From (25), it follows that

$$\mu_d \in \mathcal{D} \Longleftrightarrow \xi_d \in \Omega_{\xi_d}, \quad v_d \in \Omega_{v_d}. \tag{37}$$

Also, notice that, since the observer in(21) is driven by the output tracking error $\widetilde{\psi}_d = \psi_d^* - \psi_d$ and compensator state η_d, having $\xi_d \in \Omega_{\xi_d}, y_c \in \Omega_{y_c}, \eta_d \in \Omega_{\eta_d}$ implies that $\widehat{E}_d \in \Omega_{\widehat{E}_d}$, the latter being a compact set.

According to (13)

$$v_d = F_{v_d}(\eta_d, \widehat{E}_d, \widehat{Z}_d, y_c), \tag{38}$$

where $F_{v_d} : \Omega_{\eta_d} \times \Omega_{\widehat{E}_d} \times \Omega_{\widehat{Z}_d} \times \Omega_{y_c} \longrightarrow \Omega_{v_d}$. Thus, (38), (37) and (35) ensure that Ω_{ζ_d} is a bound set. Introduce the largest ball, which is included in Ω_{ζ_d} in the error space

$$B_R = \{|\zeta_d| ||\zeta_d|| \leq R\}, \quad R > 0. \tag{39}$$

For every $\zeta_d \in B_R$, we have $\mu_d \in \mathcal{D}, Z_d \in \Omega_{Z_d}$, where both $\mathcal{D}$ and Ω_{Z_d} are bounded sets.

Assumption 6.1 Assume

$$R > \gamma\sqrt{\frac{T_M}{T_m}} \geq \gamma, \tag{40}$$

where T_M and T_m are the maximum and minimum eigenvalues of the following matrix

$$T = \begin{bmatrix} 2P & 0 & 0 & 0 \\ 0 & 2\widetilde{P} & 0 & 0 \\ 0 & 0 & F_d^{-1} & 0 \\ 0 & 0 & 0 & G_d^{-1} \end{bmatrix} \tag{41}$$

and

$\Upsilon = max(\sqrt{\frac{\|P\bar{b}\|^2\gamma_b^2+k_2^2+\overline{Z}_d}{\lambda_{min}(Q)-2}}, \sqrt{\frac{\|P\bar{b}\|^2\gamma_b^2+k_2^2+\overline{Z}_d}{\lambda_{min}(\widetilde{Q})-2}}, \sqrt{\frac{\|P\bar{b}\|^2\gamma_b^2+k_2^2+\overline{Z}_d}{\frac{k}{2}-k_1^2-\left[\gamma_a\|P\bar{b}\|\right]^2}})$, where $\overline{Z}_d = \frac{k_d}{2}\Big[\|\Psi -$

$\Psi_0\|\Big]^2, k_d > 2\Big[k_1^2+\gamma_a^2\|P\bar{b}\|^2\Big], k_1 = \Theta\alpha_a + \|P\bar{b}\|\gamma_a, k_2 = \Theta\alpha_b + \|P\bar{b}\|\gamma_b, \Theta = \|P\bar{b}\| + \|\widetilde{P}\bar{b}\|$

and $\widetilde{P}$ satisfies $\widetilde{A}^T\widetilde{P}+\widetilde{P}\widetilde{A} = -\widetilde{Q}$ for some $\widetilde{Q} > 0$ with minimum eigenvalues $\lambda_{min}(\widetilde{Q}) > 2$.

Theorem 6.1 *Let the assumption (6.1) hold, and let $\lambda_{min}(Q) > 2$ for Q introduced in (28). Then, if the initial errors belong to the compact set Ω_α, defined in (43), the feedback control law given by (5) and (13), along with (27), guarantees that the signals $E_d, \widetilde{E}_d, \widetilde{N}$ and $\widetilde{\Psi}$ in the closed-loop system are ultimately bounded.*

Proof. Consider the following Lyapunov function for the system in (22) and (29):

$$V = E_d^T P E_d + \widetilde{E}_d^T \widetilde{P}\widetilde{E}_d + \frac{1}{2}\widetilde{\Psi}^T F_d^{-1}\widetilde{\Psi} + \frac{1}{2}tr(\widetilde{N}^T G_d^{-1}\widetilde{N}). \tag{42}$$

The derivative of V along (22), (29), (34), and with the definition of $\widetilde{E}_d = \widehat{E}_d - E_d$, can be written as

$$\dot{V} = -E_d^T P E_d - \widetilde{E}_d^T \widetilde{Q}\widetilde{E}_d + 2\widehat{E}_d^T P\bar{b}[\vartheta - \epsilon] - 2\widetilde{E}_d^T(\widetilde{P}\bar{b} + P\bar{b})[u_{ad} - \delta_d]$$
$$- k_d\widetilde{\Psi}^T(\widehat{\Psi} - \Psi_0) - k_d tr[\widetilde{N}^T(\widehat{N} - N_0)].$$

Using upper bounds from (32) and (33), the following property for vectors $tr[\widetilde{N}^T(\widehat{N} - N_0)] = \frac{1}{2}\|\widetilde{N}\|_F^2 + \frac{1}{2}\|\widehat{N} - N_0\|_F^2 - \frac{1}{2}\|N - N_0\|_F^2$, and completing squares twice, the upper bound reduces to [15]

$$\dot{V} \leq -(\lambda_{min}(Q) - 2)\|E_d\|^2 + 2\gamma_b^2\|P\bar{b}\|^2 - (\lambda_{min}(\widetilde{Q}) - 2)\|\widetilde{E}_d\|^2 + k_2^2$$
$$- \big(\frac{k_d}{2} - k_1^2 - \big[\gamma_a\|P\bar{b}\|\big]^2\big)\|\widetilde{Z}_d\|_F^2 + \overline{Z}_d.$$

Either of the following conditions:

$\|E_d\| > \sqrt{\frac{\|P\bar{b}\|^2\gamma_b^2+k_2^2+\overline{Z}_d}{\lambda_{min}(Q)-2}}, \|\widetilde{E}_d\| > \sqrt{\frac{\|P\bar{b}\|^2\gamma_b^2+k_2^2+\overline{Z}_d}{\lambda_{min}(Q)-2}}, \|\widetilde{Z}_d\|_F > \sqrt{\frac{\|P\bar{b}\|^2\gamma_b^2+k_2^2+\overline{Z}_d}{\frac{k_d}{2}-k_1^2-\left[\gamma_a\|P\bar{b}\|\right]^2}}$ will

render $\dot{V} < 0$ outside a compact set: $B_\Upsilon = \big\{\zeta_d \in B_R, \|\zeta_d\| \leq \Upsilon\big\}$.

Note from (40) that $B_\Upsilon \subset B_R$. Then, consider the Lyapunov function candidate in (42) and write it as $V = \zeta_d^T T\zeta_d$. Let Γ be the maximum value of the Lyapunov function V on the edge of B_Υ: $\Gamma = \max_{\|\zeta_d\|=\Upsilon} V = \Upsilon^2 T_M$.

Introduce the level set $\Omega_\Upsilon = \{\zeta_d, V = \Gamma\}$. Let α_v be the minimum value of the Lyapunov function V on the edge of B_R: $\alpha_v = \min_{\|\zeta_d\|=R} V = R^2 T_m$. Define the level set

$$\Omega_\alpha = \{\zeta_d \in B_R, V = \alpha_v\}. \tag{43}$$

The condition in (40) ensures that $\Omega_\Upsilon \subset \Omega_\alpha$, and thus ultimate boundedness of ζ_d.

7 Simulation Results

In this section, computer simulations inquire the performances of the proposed control scheme in the presence of structured and unstructured uncertainties. The physical and electrical parameters of the two-phase IM under investigation are: $L_m = 0.0117H$, $R_r = 3.9\Omega$, $Rs = 1.7\Omega$, $L_r = 0.014H$, $L_s = 0.014H$, $f = 0.00014N.m/rad/sec$ and $J = 0.00011kg.m^2$ [12].

One has chosen the design parameters for the dynamic compensators as follows: $\alpha_d = -85$, $\beta_d = 10$, $\chi_d = -18005$ and $\varrho_d = 2376$, $\alpha_q = -105$, $\beta_q = 1$, $\chi_q = -324090$ and $\varrho_q = 3376$ in order to place the poles of both closed-loop error dynamics at $(-35, -25 \mp j)$ and $(-15, -45 \mp j)$, respectively (refer to [1,3] for more details). The observer dynamics in (29) was designed so that its poles are five times faster than those of the error dynamics. We implement ten neurons in the hidden layer of the neural network that approximate δ_d, while we employ eight neurons in the hidden layer of the NN that approximate δ_q. For the neural network, we use the following sigmoidal basis function $\Phi(x) = \frac{1}{1+e^{-ax}}$ with $a = 1$. The adaptation gains were set to $F_d = G_d = 2I$, with sigma modification gains $k_d = 0.365$.

7.1 Test of robustness of the adaptive control

To demonstrate that the proposed approach is successfully applicable for the nonlinear IM system in the presence of high uncertainties, the rate of (δ) will be varied with ($\pm 50\%$ then $\pm 100\%$) of its norm value. Once again, our perspective is to develop an adaptive controller for each subsystem of the decoupled dynamics of the IM using only one SHL NN, in which the adaptive terms (u_{ad} and u_{aq}) overcome the effects of inversion errors (δ_d and δ_q), what bring to force the system measurements (ψ_d) and (w) to track reference trajectories (ψ_d^*) and (w^*), respectively, with bounded errors.

The simulation results depicted in Figures 2 illustrate the performance comparison of the considered control systems for the case (δ is varied) without and with NN. In these figures, we illustrate clearly that the adaptive control augmented via only SHL NN works well, and excellent tracking accuracy is obtained. To explain, the tracking of the speed signal to its reference is close enough so that they are indistinguishable in Figure 2(b), which proves that the NN augmentation (u_{aq}) identifies successfully the inversion error (δ_q), as illustrated in Figure 3(a). Furthermore, Figure 2(d) reports that the flux response is compatible with respect the imposed flux reference trajectory. This is due essentially to the ability of a the SHL NN (u_{ad}) to model nonlinearities (δ_d) on-line, as presented in Figure 3(b). Moreover, from Figures 3(c) and 3(d) it is worth noticing that the proposed approach has achieved excellent responses both at transient and steady state process.

The proposed control system is able to achieve flux and speed tracking high accuracy with an admissible regulation performance with respect to load disturbances and adequate robustness against parameter variations.
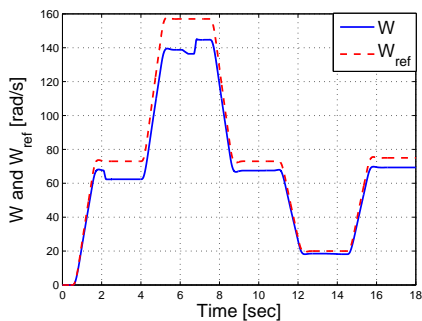
(a) W and W^* without NN.
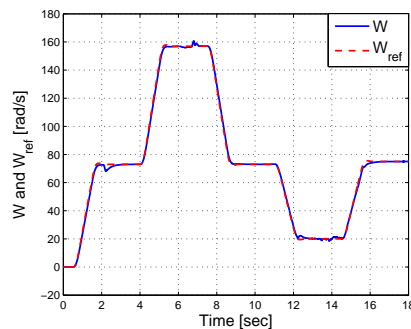
(b) W and W^* with SHL NN.

(c) ψ_d and ψ_d^* without NN.
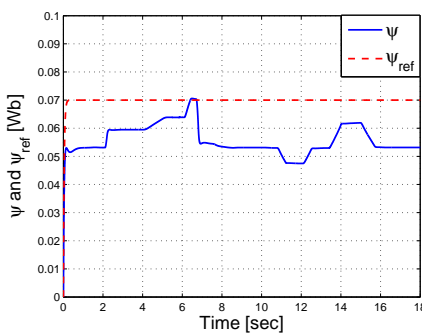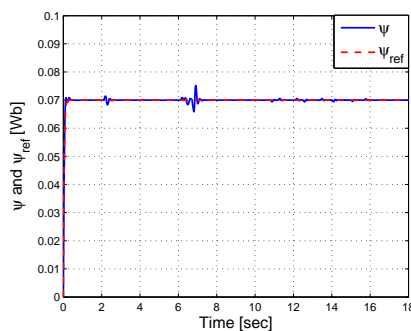
(d) ψ_d and ψ_d^* with SHL NN.
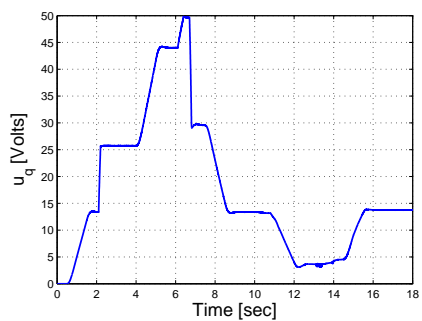
(e) u_q without NN.
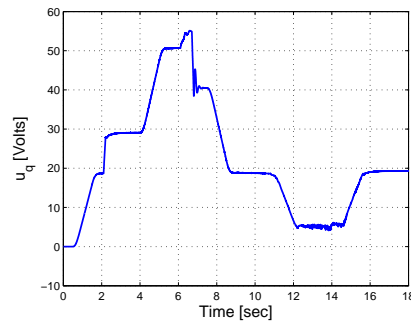
(f) u_q with SHL NN.
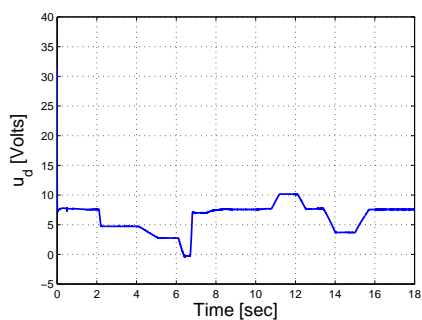
(g) u_d without NN.
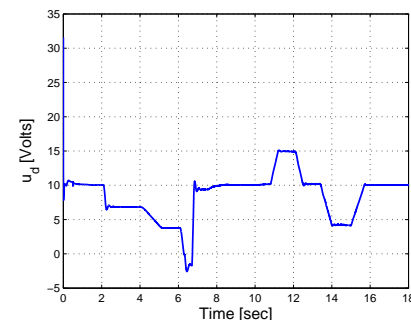
(h) u_d with SHLNN.

Figure 2: Simulation results with variation of uncertainties: without NN $((a),(c),(e),(g))$, and with NN $((b),(d),(f),(h))$.
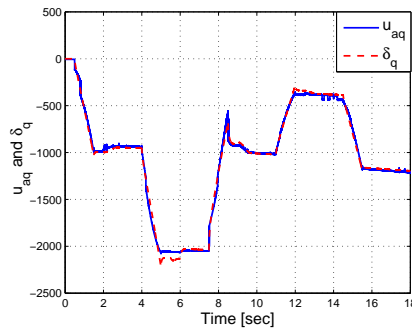
(a) u_q^a and Δ_q.
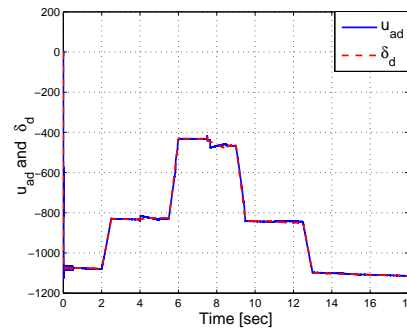
(b) u_d^a and Δ_d.
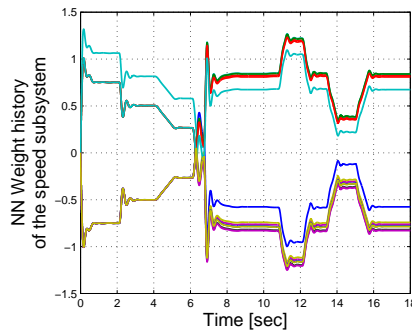
(c) NN weights history of speed subsystem.
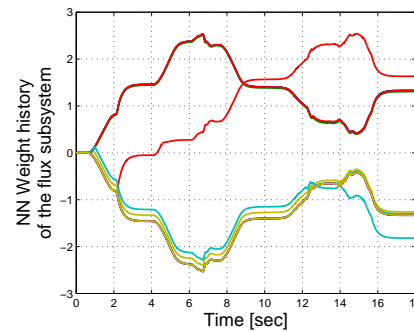
(d) NN weights history of flux subsystem.

Figure 3: $((a),(b))$ Identification of uncertainties (δ) by NN. $((c),(d))$ NN weight history.

8 Summary

The fundamental goal of this paper consisted in realizing a tracking accuracy for multi-inputs multi-outputs nonlinear induction motor in the presence of high uncertainties. First, an appropriate input-output feedback linearizing controller is applied to decouple the speed dynamics from the flux. Then, the nonlinear state feedback controller is involved as a linearizing control. After, the adaptive control augmented via only nonlinearly parameterized SHL NNs is introduced to cancel the uncertainties existing in the induction motor. A linear observer is introduced to estimate the derivatives of the tracking errors. These estimates are used as inputs to the NN and in the adaptation laws as an error signal. Of particular interest, ultimate boundedness of error signals is shown using Lyapunov's direct method. Finally, computer simulations are undertaken to highlight the effectiveness of the proposed adaptive controller. As a future research we will propose to add other NN structures for sensorless control.

References

[1] H. Ait Abbas, M. Belkheiri and Z. Boubakeur. Feedback Linearization Control for Highly Uncertain Nonlinear Systems Augmented by Single- Hidden-Layer Neural Networks. *Jour-*

nal of Engineering Science and Technology Review **8** (2) (2015) 215–224.

[2] H. A. Abbas, B. Zegnini, and M. Belkheiri. Neural network-based adaptive control for induction motors. In: *The 12th IEEE International Multi-Conference on Systems, Signals and Devices*, (DOI:10.1109/SSD.2015.7348180), (16-19 March 2015), Mahdia-Tunisia.

[3] H. A. Abbas, B. Zegnini, M. Belkheiri, and A. Rabhi. Radial basis function neural network-based adaptive control of uncertain nonlinear systems. In: *Control, Engineering and Information Technology (CEIT)*, 2015, 3rd International Conference on IEEE, (2015), 1–6.

[4] H. Ait Abbas, M. Belkheiri, and B. Zegnini. Robust Neural Output Feedback Tracking Control For a Class of Uncertain Nonlinear Systems Without Time-delay. *Nonlinear Dynamics and Systems Theory* **16** (2) (2016) 115–128.

[5] H. Ait Abbas, M. Belkheiri, and B. Zegnini. Feedback Linearization Control of an Induction Machine Augmented by Single Hidden Layer Neural Networks. *International Journal of Control*, (DOI. 10.1080/00207179.2015.1063162), **89** (1) (2016) 140–155.

[6] E. Arbin and M. Gregory. Adaptive Backstepping Control of a Speed-Sensorless Induction Motor Under Time-Varying Load Torque and Rotor Resistance Uncertainty. In: *Proc. of the 38th Southeastern Symposium on System Theory*, (March 5-7, 2006), 512–518, USA.

[7] M. Belkheiri and F. Boudjema. Neural network augmented backstepping control for an induction machine. *International Journal of Modelling, Identification and Control* **5** (4) (2008) 288–296.

[8] M. Belkhiri, H. Ait Abbas, & B. Zegnini. Feedback Linearization Control of Nonlinear Uncertain Systems Using Single Hidden Layer Neural Networks. In: *The 11th IEEE International Multi-Conference on Systems, Signals and Devices*, (DOI: 10.1109/SSD.2014.6808779), (February 11–14, 2014), Castelldefels-Barcelona, Spain.

[9] M. Benrejeb, M. Gasmi, and P. Borne. New stability conditions for TS fuzzy continuous nonlinear models. *Nonlinear Dynamics and Systems Theory* **5** (4) (2005) 369–379.

[10] N. Bounar, A. Boulkroune, F. Boudjema, M. M'Saad, M. Farza. Adaptive fuzzy vector control for a doubly-fed induction motor. *Neurocomputing* **151** (2) (2014) 756–769.

[11] J. Brasch, & J. Pearson. Pole placement using dynamic compensators. *IEEE Trans. Automat. Contr.* **AC-15** (Jan. 1970) 34–43.

[12] J. Chiasson. *Modeling and High Performance Control of Electric Machines*. John Wiley & Sons, New Jersey, 2005.

[13] L. Chuan-Kai. RBF neural network-based adaptive critic control of induction motors. *Applied Soft Computing* **11** (3) (2011) 3066–3074.

[14] N. Henini, L. Nezli, A. Tlemani and M. O. Mahmoudi. Improved Multimachine Multiphase Electric Vehicle Drive System Based on New SVPWM Strategy and Sliding Mode – Direct Torque Control. *Nonlinear Dynamics and Systems Theory* **11** (4) (2011) 425–438.

[15] N. Hovakimyan, F. Nardi, A. Calise and N. Kim, Adaptive Output Feedback Control of Uncertain Nonlinear Systems Using Single-Hidden-Layer NNs. *IEEE Trans. on Neural Networks* **13** (6) (2002) 1420–1431.

[16] Y. Jeon, B. Chen and H. Yu. Position tracking control of induction motors via adaptive fuzzy backstepping. *Energy Conversion and Management* **51** (11) (2010) 2345–2352.

[17] J. Zhou, C. Wen, and Y. Zhang. Adaptive Output Control of a Class of Time-Varying Uncertain Nonlinear Systems. *Nonlinear Dynamics and Systems Theory* **5** (3) (2005) 285–298.

[18] Z. Kardous and N. B. Braiek. Stabilizing Sliding Mode Control for Homogeneous Bilinear Systems. *Nonlinear Dynamics and Systems Theory* **14** (3) (2014) 303–312.

[19] S. Melliani, A. El Allaoui, and L. S. Chadli. Relation Between Fuzzy Semigroups and Fuzzy Dynamical Systems. *Nonlinear Dynamics and Systems Theory* **17** (1) (2017) 60–69.

[20] F.Nardi, F., & A. J. Calise. Robust adaptive nonlinear control using single hidden layer neural networks. In: *Proc. Conf. Decision Contr.* **4** (2000) 3825–3830.

[21] S. Xu, P. Shi, C. Feng, Y. Guo, and Y. Zou. Robust Observers for a Class of Uncertain Nonlinear Stochastic Systems with State Delays. *Nonlinear Dynamics and Systems Theory* **4** (3) (2004) 369–380.

Sumudu Decomposition Method for Solving Higher-Order Nonlinear Volterra-Fredholm Fractional Integro-Differential Equations

K. Al-Khaled* and M.H. Yousef

Department of Mathematics and Statistics, Jordan University of Science and Technology, P.O. Box (3030), Irbid (22110), Jordan

Abstract: In this paper, the Sumudu decomposition method is developed to solve the general form of the fractional nonlinear Volterra-Fredholm integro-differential equation. The fractional derivative is described in the Caputo sense. The proposed method is based on the application of the Sumudu transform to the fractional nonlinear Volterra-Fredholm integro-differential equation. The nonlinear term can easily be handled with the help of Adomian polynomials. Illustrative examples are given, and numerical results are provided to demonstrate the efficiency of the proposed method.

Keywords: *approximate Solutions; fractional integro-differential equation; Adomian decomposition; Sumudu transform.*

Mathematics Subject Classification (2010): 45J05, 45G10, 65R20, 65D20.

1 Introduction

Many problems in mathematical physics, theory of elasticity, visco-dynamics fluid and mixed problems of mechanics of continuous media can be reduced to the integral equation (Volterra or Fredholm) of the first or second kind. In [1, 2], the Adomian decomposition method was used to solve a higher-order nonlinear Volterra-Fredholm integro-differential equation of the form

$$\sum_{k=0}^{m} p_k(x)u^{(k)}(x) = f(x) + \lambda_1 \int_a^x \sum_{i=0}^{r} A_i(x,t)F_i(u(t))dt + \lambda_2 \int_a^b \sum_{j=0}^{s} B_j(x,t)G_j(u(t))dt \tag{1}$$

---

* Corresponding author: `mailto:kamel@just.edu.jo`

subject to the initial conditions

$$u^{(\ell)}(0) = \alpha_\ell, \ \ \ell = 0, 1, 2, ..., k - 1, \tag{2}$$

where $p_k(x)$ $(k = 0, 1, ..., m)$, $A_i(x, t)$ $(i = 0, 1, ..., r)$, $B_j(x, t)$ $(j = 0, 1, ..., s)$ and $f(x)$ all are given functions. $u^{(k)}$ indicates the $k-$th derivative of $u(x)$, $F(u(x))$ are non-linear functions. It is to be pointed out that $u(x), f(x)$ are assumed to be real, and $\lambda_1, \lambda_2, \ \alpha_\ell, \ell = 0, 1, ..., k - 1$ are all real finite constants.

It has turned out that many phenomena in engineering, physics and other sciences can be described very successfully by models using mathematical tools from fractional calculus. Integro-differential equations model many situations from science and engineering, for example, in circuit analysis. The activity of interacting inhibitory and excitatory neurons can be described by a system of integro-differential equations. For a better understanding of the phenomena, fractional derivatives provide more accurate models of real world problems than integer order derivatives do. Because of their many applications in scientific fields, fractional integro-differential equations are found to be an effective tool to describe certain physical phenomena. The most important advantage of using the fractional derivatives in mathematical modeling is due to the non-local property. It is well known that the integer-order differential operator possesses a local operator whereas the fractional order differential operator is non-local. This means that the next state of a system depends not only upon its current state but also upon all of its historical states [3]. In recent times, the fractional calculus is used in different physical and biological problems, see [4–6] and the references therein. Oldham and Spanier [4], Miller and Ross [7], Momani [8] and Podlubny [9] provide the history and a comprehensive treatment of this subject. To solve integro-differential equations, approximate solution and numerical solution methods are being used.

In this paper, we apply the Sumudu transform to solve the general form of the non-linear Volterra-Fredholm integro-differential equation

$$u^{(\alpha)}(x) = \frac{-1}{p_m(x)} \sum_{k=0}^{m-1} p_k(x) u^{(k)}(x) + f(x) + \lambda_1 \int_a^x \sum_{i=0}^{r} A_i(x, t) F_i(u(t)) dt$$

$$+ \lambda_2 \int_a^b \sum_{j=0}^{s} B_j(x, t) G_j(u(t)) dt, \ \ m - 1 < \alpha \le m. \tag{3}$$

The Sumudu transform was first proposed by Watugala [10, 11]. In [12, 13] some fundamental properties of the Sumudu transform were established in light of which the authors developed efficient and straightforward methodologies for treating differential equations. The Sumudu transform method is one of the most important transform methods, it is a powerful tool for solving many kinds of PDEs in various fields of science and engineering [12]. In [14], the authors start from the definition of the Sumudu transform on a general time scales to define the discrete Sumudu transform, and present its basic properties.

In [15], we used a reliable strategy, based on using the Adomian decomposition method (ADM), for solving the same system as in (3). Saadatmandi and Dehghan [17] applied the Legendre collocation method to find numerical solutions of a nonlinear fractional integro-differential equation of only Volterra type. For this current work, we implement the Adomian-Sumudu decomposition method (ASDM) for solving higher-order non-linear fractional Volterra-Fredholm integro-differential equations. The ASDM is an elegant

combination of the Sumudu transform method and the ADM. This technique is more powerful because we can combine the Sumudu method and the ADM to obtain the ASDM and it will provide exact and approximate analytical solutions for fractional non-linear equations. We would like to mention that the ASDM can provide high accuracy of numerical results, reduce the computational time and volume of the work. We would also like to point out that for obtaining the solution by using other methods, we need to solve the equation at other values of the parameter α, and we shall have to compute again for new α. In our method there is no need to perform such repetitive calculation. Against this backdrop, we would like to extend the previous results [1, 18], and also to generalize the results obtained in [15, 16] and to solve the fractional Volterra-Fredholm integro-differential equations (3).

The fractional differential operator $u^{(\alpha)}(x)$ describes the fractional derivatives of order α of equation (3). When $\alpha \in \mathbf{N}$, the equation (3) reduces to a linear integro-differential equation, while if $\lambda_1 = \lambda_2 = 0$, the equation reduces to linear fractional differential equations. Such kind of integro-differential equations is considered for generalizations of the work in [19]. The main objective of this paper is to study the behavior of the solution for equation (1) using the Sumudu decomposition method.

The layout of the paper is as follows. In Section 2, we briefly review some general concepts of the fractional theory and the Sumudu transform required for our subsequent development. In Section 3, we extend the application of the Sumudu-Adomian decomposition to construct our analytical approximate solutions for the general integro-differential equation (3). Finally, numerical experiments are presented and some comparisons are made in Section 4. The paper ends with some concluding remarks.

2   Basics of Fractional Calculus

This section is devoted to the description of the operational properties with the purpose of acquainting with sufficient fractional calculus theory. Many definitions and studies of fractional calculus have been proposed in the last two centuries. These definitions include the Riemman-Liouville, Weyl, Reize, Campos, Caputa, and Nishimoto fractional operators. Mainly, in this paper, we will re-introduce Section 2 of [20]. The Riemann-Liouville definition of fractional derivative operator J_a^α is stated as follows.

Definition 2.1 Let $\alpha \in \mathbf{R}_+$. The operator J^α, defined on the usual Lebesgue space $L_1[a, b]$ by

$$J_a^\alpha f(x) = \frac{1}{\Gamma(\alpha)} \int_a^x (x - t)^{\alpha-1} f(t)dt, \quad J_a^0 f(x) = f(x)$$

for $a \leq x \leq b$, is called the Riemann-Liouville fractional integral operator of order α.

Properties of the operator J^α can be found in [9], we mention the following: For $f \in L_1[a, b], \alpha, \beta \geq 0$ and $\gamma > -1$:

1. $J_a^\alpha f(x)$ exists for almost every $x \in [a, b]$.

2. $J_a^\alpha J_a^\beta f(x) = J_a^{\alpha+\beta} f(x)$.

3. $J_a^\alpha J_a^\beta f(x) = J_a^\beta J_a^\alpha f(x)$.

4. $J_a^\alpha x^\gamma = \frac{\Gamma(\gamma+1)}{\Gamma(\alpha+\gamma+1)}(x - a)^{\alpha+\gamma}$.

As mentioned in [8], the Riemann-Liouville derivative has certain disadvantages when trying to model real-world phenomena with fractional differential equations. Therefore, we shall introduce now a modified fractional differentiation operator D^α proposed by Caputo in his work on the theory of visco-elasticity [21].

Definition 2.2 The fractional derivative of $f(x)$ in the Caputo sense is defined as

$$D^\alpha f(x) = J^{m-\alpha} D^m f(x) = \frac{1}{\Gamma(m-\alpha)} \int_0^x (x-t)^{m-\alpha-1} f^{(m)}(t)dt, \qquad (4)$$

$m - 1 < \alpha \le m, m \in \mathbf{N}, x > 0.$

Also, we need here two of its basic properties.

Lemma 2.1 If $m - 1 < \alpha \le m$, and $f \in L_1[a, b]$, then $D_a^\alpha J_a^\alpha f(x) = f(x)$, and

$$J_a^\alpha D_a^\alpha f(x) = f(x) - \sum_{k=0}^{m-1} f^{(k)}(0) \frac{(x-a)^k}{k!}, \ x > 0.$$

The Caputo fractional derivative is considered in the Caputo sense. The reason for adopting the Caputo definition is as follows. To solve differential equations, we need to specify additional conditions in order to produce a unique solution. For the case of Caputo fractional differential equations, these additional conditions are just the traditional conditions, which are taken to the classical differential equations, and are therefore familiar to us. In contrast, for the Riemann-Liouville fractional differential equations, these additional conditions constitute certain fractional derivatives of the unknown solution at the initial point $x = 0$, which are functions of x. The initial conditions are not physical; furthermore, it is not clear how many quantities are to be measured from experiment, say, so that they can be appropriately assigned in an analysis. For more details on the geometric and physical interpretation for fractional derivatives of both Riemann-Liouville and Caputo types, see [8, 21].

Definition 2.3 For m to be the smallest integer that exceeds α, the Caputo fractional derivatives of order $\alpha > 0$ are defined as

$$D^\alpha u(x,t) = \frac{\partial^\alpha u(x,t)}{\partial t^\alpha} = \begin{cases} \frac{1}{\Gamma(m-\alpha)} \int_0^t (t-\tau)^{m-\alpha-1} \frac{\partial^m u(x,\tau)}{\partial \tau^m} d\tau, & m-1 < \alpha < m, \\ \frac{\partial^m u(x,t)}{\partial t^m}, & \alpha = m \in N. \end{cases}$$

For mathematical properties of fractional derivatives and integrals one can consult the mentioned references.

In the early 90s, Watugala [10, 11] introduced a new integral transform, named the Sumudu transform and applied it to the solution of ordinary differential equation in control engineering problems.

Definition 2.4 The Sumudu transform over the following set of functions

$$\mathbb{A} = \left\{ f(t) \mid \exists M, \ \tau_1, \tau_2 > 0, |f(t)| < Me^{\frac{|t|}{\tau_j}}, \ \text{if} \ t \in (-1)^j \times [0, \infty) \right\} \qquad (5)$$

is defined for $u \in (\tau_1, \tau_2)$ as

$$\mathbb{S}[f(t)] = F(u) = \int_0^\infty f(ut)e^{-t}dt = \int_0^\infty \frac{1}{u} f(t)e^{-t/u}dt, \qquad (6)$$

where u is a parameter and it may be real or complex, that is, independent of t. The inversion formula for the Sumudu transform is given by

$$\mathbb{S}[G(s)] = \frac{1}{2\pi i} \int_{\gamma-i\infty}^{\gamma+i\infty} e^{st} G(\frac{1}{s}) \frac{ds}{s}.$$

In Belgacem et al. [22], the Sumudu transform was shown to be the theoretical dual of the Laplace transform. Hence, one should be able to rival it to a great extent in problem solving. Given an initial $f(t)$, its Laplace transform $F(s)$ can be transformed into the Sumudu transform $F_s(u)$ of f by means of

$$\mathbb{S}(u) = \frac{F(\frac{1}{u})}{u}.$$

And its inverse is

$$F(s) = \frac{\mathbb{S}(\frac{1}{s})}{s}.$$

Every proven property of the Laplace transform may routinely be turned into a corresponding property of the Sumudu transform. Many of special properties of the Sumudu transform are mentioned and tabulated in [13,22]. Some special properties of the Sumudu transform are as follows:

1. $\mathbb{S}[1] = 1$.

2. $\mathbb{S}\left[\frac{t^n}{\Gamma(n+1)}\right] = u^n$, $n > 0$.

3. $\mathbb{S}[f(x) \mp g(x)] = \mathbb{S}[f(x)] \mp \mathbb{S}[g(x)]$.

Theorem 2.1 *[22] Let $G(u)$ be the Sumudu transform of $f(t)$ such that*

1. *$G(1/s)/s$ is a meromorphic function, with singularities having $Re(s) < \gamma$, and*

2. *there exists a circular region Γ with radius R and positive constants M and k with*

$$\left|\frac{G(1/s)}{s}\right| < MR^{-k},$$

then the function $f(t)$ is given by

$$f(t) = \mathbb{S}^{-1}[G(t)] = \frac{1}{2\pi i} \int_{\gamma-i\infty}^{\gamma+\infty} e^{st} G(\frac{1}{s}) \frac{ds}{s} = \sum residuse\left[e^{st} \frac{G(1/s)}{s}\right].$$

To solve fractional differential equations, the following lemma of the Sumudu transform will be needed.

Lemma 2.2 *[22] The Sumudu transform $\mathbb{S}[f(t)]$ of the fractional derivative introduced by Caputo is given by*

$$\mathbb{S}[D_t^\alpha f(t)] = \frac{G(u)}{u^\alpha} - \sum_{k=0}^{n-1} \frac{f^{(k)}(0)}{u^{\alpha-k}}, \quad where \ G(u) = \mathbb{S}[f(t)]. \tag{7}$$

3 Implementation of Sumudu Decomposition Method

In the analysis of the numerical method that follows, we will assume that problem (1)-(2) has a unique and sufficiently smooth solution. We apply the Sumudu-Adomian decomposition to find an approximate solution for the fractional integro-differential equations (3). We assume that $u(x)$ is sufficiently differentiable and that a unique solution of (3) exists. Take the Sumudu transform of both sides of equation (3)

$$\mathbb{S}[u^{(\alpha)}(x)] = \mathbb{S}\Big[\frac{-1}{p_m(x)}\sum_{k=0}^{m-1}p_k u^{(k)}(x)\Big] + \mathbb{S}[f(x)] + \mathbb{S}\Big[\lambda_1\int_a^x\sum_{i=0}^{r}A_i(x,t)F_i(u(t))dt\Big]$$

$$+ \mathbb{S}\Big[\lambda_2\int_a^b\sum_{j=0}^{s}B_j(x,t)G_j(u(t))dt\Big], \ m-1 < \alpha \le m.$$

Using the result of equation (7) on the left-hand side of the above equation we arrive at

$$u^{-\alpha}\mathbb{S}[u(t)] - \sum_{k=0}^{n-1}u^{-(\alpha-k)}u^{(k)}(0) = \mathbb{S}\Big[\frac{-1}{p_m(x)}\sum_{k=0}^{m-1}p_k u^{(k)}(x)\Big] + \mathbb{S}[f(x)]$$

$$+ \ \mathbb{S}\Big[\lambda_1\int_a^x\sum_{i=0}^{r}A_i(x,t)F_i(u(t))dt\Big] + \mathbb{S}\Big[\lambda_2\int_a^b\sum_{j=0}^{s}B_j(x,t)G_j(u(t))dt\Big], m-1 < \alpha \le m.$$

Solving for $\mathbb{S}[u(t)]$, we get

$$\mathbb{S}[u(t)] = u^{\alpha}\sum_{k=0}^{n-1}s^{\alpha-k-1}u^{(k)}(0) + u^{\alpha}\mathbb{S}\Big[\frac{-1}{p_m(x)}\sum_{k=0}^{m-1}p_k(x)u^{(k)}(x)\Big] + u^{\alpha}\mathbb{S}[f(x)]$$

$$+u^{\alpha}\mathbb{S}\Big[\lambda_1\int_a^x\sum_{i=0}^{r}A_i(x,t)F_i(u(t))dt\Big] + u^{\alpha}\mathbb{S}\Big[\lambda_2\int_a^b\sum_{j=0}^{s}B_j(x,t)G_j(u(t))dt\Big], m-1 < \alpha \le m.$$

Now, following [23, 24], the Sumudu decomposition method introduces the following expressions:

$$u(x) = \sum_{n=0}^{\infty}u_n(x) \tag{8}$$

for the solution of our problem, where the components $\mathbb{S}[u_n(t)]$ will be determined recurrently according to a recursive relation. Moreover, the method defines the nonlinear functions $F_i(u(x))$, $(i = 0, 1, ..., r)$, $G_j(u(x))$, $(j = 0, 1, ..., s)$ by the infinite series of polynomials

$$F_i(u(x)) = \sum_{n=0}^{\infty}(C_i)_n, \ \ G_j(u(x)) = \sum_{n=0}^{\infty}(D_i)_n \ \ \text{and} \ \ u^{(k)}(x) = \sum_{n=0}^{\infty}E_i, \tag{9}$$

where the $(C_i)_n, (D_j)_n, E_n$ are the Adomian polynomials which are generated according to specific algorithms set by Adomian [23,24], or by Wazwaz [25]. Substituting equations (8)-(9), yields

$$\mathbb{S}[\sum_{n=0}^{\infty}u_n(x)] = u^{\alpha}\sum_{k=0}^{n-1}u^{-(\alpha-k)}u^{(k)}(0) + u^{\alpha}\mathbb{S}\Big[\frac{-1}{p_m(x)}\sum_{k=0}^{m-1}p_k(x)\sum_{n=0}^{\infty}E_n\Big] + u^{\alpha}\mathbb{S}[f(x)]$$

$$+u^\alpha \mathbb{S}\Big[\lambda_1 \int_a^x \sum_{i=0}^r A_i(x,t) \sum_{n=0}^\infty (C_i)_n dt\Big] + u^\alpha \mathbb{S}\Big[\lambda_2 \int_a^b \sum_{j=0}^s B_j(x,t) \sum_{n=0}^\infty (D_i)_n dt\Big], m-1 < \alpha \le m.$$

It is useful to note that the recursive relation is constructed on the basis that the zeroth component $\mathbb{S}[u_0]$ is defined by all terms that arise from the initial conditions and from the source term $f(x)$, i.e.,

$$\mathbb{S}[u_0(x)] = u^\alpha \sum_{k=0}^{n-1} u^{-(\alpha-k)} u^{(k)}(0) + u^\alpha \mathbb{S}[f(x)]. \tag{10}$$

The remaining components of $\mathbb{S}[u(x)]$ can be completely determined so that each term is computed by using the previous terms as

$$
\begin{aligned}
\mathbb{S}[u_{k+1}(x)] &= u^\alpha \mathbb{S}\Big[\frac{-1}{p_m(x)} \sum_{k=0}^{m-1} p_k(x) \sum_{k=0}^\infty E_k\Big] \\
&+ u^\alpha \mathbb{S}\Big[\lambda_1 \int_a^x \sum_{i=0}^r A_i(x,t) \sum_{n=0}^\infty (C_i)_k dt\Big] \\
&+ u^\alpha \mathbb{S}\Big[\lambda_2 \int_a^b \sum_{j=0}^s B_j(x,t) \sum_{n=0}^\infty (D_i)_k dt\Big], \ k \ge 1.
\end{aligned}
$$

As a result, the components $u_0, u_1, u_2, ...$ are identified by applying the inverse Sumudu transform of the above equations to obtain

$$u_0(x) = \mathbb{S}^{-1}\Big[u^\alpha \sum_{k=0}^{n-1} u^{-(\alpha-k)} u^{(k)}(0)\Big] + \mathbb{S}^{-1}\Big[u^\alpha \mathbb{S}[f(x)]\Big] \tag{11}$$

and

$$
\begin{aligned}
u_{k+1}(x) &= \mathbb{S}^{-1}\Big(u^\alpha \mathbb{S}\Big[\frac{-1}{p_m(x)} \sum_{k=0}^{m-1} p_k(x) \sum_{k=0}^\infty E_k\Big]\Big) \\
&+ \mathbb{S}^{-1}\Big(u^\alpha \mathbb{S}\Big[\lambda_1 \int_a^x \sum_{i=0}^r A_i(x,t) \sum_{n=0}^\infty (C_i)_k dt\Big]\Big) \\
&+ \mathbb{S}^{-1}\Big(u^\alpha \mathbb{S}\Big[\lambda_2 \int_a^b \sum_{j=0}^s B_j(x,t) \sum_{n=0}^\infty (D_i)_k dt\Big]\Big), \ k \ge 1.
\end{aligned}
$$

Thus, the series solutions are entirely determined. However in many cases (when α is an integer) the exact solution in a closed form may be obtained [1]. The $n-th$ term approximation $\Phi_n = \sum_{k=0}^{n-1} u_k$ can be used to approximate the solution. The choice of (11) as the initial solution always leads to noise oscillation during the iteration procedure [19]. Also, the choice of $\mathbb{S}[u_0(x)]$ to contain minimal number of terms is giving more flexibility to solve complicated non-linear equations, especially in calculation of inverse Sumudu transform. A reliable modified form of the decomposition method has been introduced by Wazwaz [25]. The construction of the zeroth component of the decomposition series can be defined in a slightly different way. Wazwaz [25] assumed that if the zeroth component $\mathbb{S}[u_0(x)]$ depicted in (10) can be divided into two parts, then one part will be assigned to $\mathbb{S}[u_0(x)]$, while the second part of $\mathbb{S}[u_0(x)]$ can be included in the component of $\mathbb{S}[u_1(x)]$ among other terms.

4   Numerical Examples

In order to assess the advantages of the proposed method (the Sumudu-Adomian method) over the Adomian decomposition method [15] in terms of accuracy and efficiency for solving fractional integro-differential equations, we have applied the method to two different examples with known exact solutions at some values of α. The computations associated with the examples were performed using mathematica.

Example 4.1 Consider the following nonlinear fractional integro-differential equation [15]

$$D^\alpha u(t) = \frac{1}{\Gamma(1/2)}\Big(\frac{8}{3}t^{3/2} - 2t^{1/2}\Big) - \frac{t}{1260} + \int_0^1 xtu^4(x)dx,\ 0 \le t \le 1, \qquad (12)$$

where $u(0) = 0$, and $\alpha \in (0, 1]$.

Apply the Sumudu transform to both sides of equation (12). For the left-hand side $D^\alpha u(t)$ we use the initial condition together with equation (7), while for the first three terms on the right-hand side we use the fact that

$$\mathbb{S}\Big(\frac{t^{a-1}}{\Gamma(a)}\Big) = u^{a-1}, a > 0.$$

Upon passing simple calculations, we arrive at

$$\mathbb{S}[u(t)] = 2u^{\alpha+\frac{3}{2}} - 2u^{\alpha+\frac{1}{2}} - \frac{1}{1260}u^{\alpha+1} + u^\alpha \mathbb{S}\Big[\int_0^1 xtu^4(x)dx\Big].$$

Substituting the decomposition series (8) for $u(t)$, and the series $\sum_{n=0}^\infty A_n(t)$ for the nonlinear term $u^4(t)$, we have

$$\mathbb{S}[\sum_{n=0}^\infty u_n(t)] = 2u^{\alpha+\frac{3}{2}} - 2u^{\alpha+\frac{1}{2}} - \frac{1}{1260}u^{\alpha+1} + u^\alpha \mathbb{S}\Big[\int_0^1 xt\sum_{n=0}^\infty A_{n-1}(t)dx\Big],$$

where the first few Adomian polynomials are given by $A_0(t) = u_0^4(t)$, $A_1(t) = 4u_0^3(t)u_1(t)$, $A_2(t) = 6u_0^2(t)u_1^2(t) + 4u_0^3(t)u_2(t)$. The modified decomposition technique introduces the use of the recursive relation

$$\mathbb{S}[u_0(x)] = 2u^{\alpha+\frac{3}{2}} - 2u^{\alpha+\frac{1}{2}}, \qquad (13)$$

$$\mathbb{S}[u_1(t)] = -\frac{1}{1260}u^{\alpha+1} + u^\alpha \mathbb{S}\Big[\int_0^1 xtA_0(t)dx\Big] \qquad (14)$$

and

$$\mathbb{S}[u_2(t)] = u^\alpha \mathbb{S}\Big[\int_0^1 xtA_1(t)dx\Big]. \qquad (15)$$

In general, we take the n-th term to be

$$\mathbb{S}[u_n(t)] = u^\alpha \mathbb{S}\Big[\int_0^1 xtA_{n-1}(t)dx\Big], n \ge 3. \qquad (16)$$

Taking the inverse Sumudu transform of both sides of $\mathbb{S}[u_0(t)]$ yields

$$u_0(t) = \frac{2}{\Gamma[\alpha + \frac{3}{2}]}\Big[\frac{t^{\alpha + \frac{3}{2}}}{\alpha + \frac{3}{2}} - t^{\alpha + \frac{1}{2}}\Big].$$

So, we can simplify $\mathbb{S}[u_1(t)]$ appeared in equation (14) as

$$
\begin{aligned}
\mathbb{S}[u_1(t)] &= -\frac{1}{1260}u^{\alpha+1} + u^\alpha\mathbb{S}\Big[\int_0^1 xtA_0(t)dx\Big] \\
&= -\frac{1}{1260}u^{\alpha+1} + u^\alpha\mathbb{S}\Big[\frac{t^{3+4\alpha}(3 - 2t + 2\alpha)^4}{2(\Gamma[\alpha + \frac{5}{2}])^4}\Big]
\end{aligned}
$$

or

$$
\begin{aligned}
u_1(t,\alpha) &= \frac{8\alpha^4\Gamma(4\alpha + 4)t^{5\alpha+3}}{\Gamma\left(\alpha + \frac{5}{2}\right)^4\Gamma(5\alpha + 4)} + \frac{48\alpha^3\Gamma(4\alpha + 4)t^{5\alpha+3}}{\Gamma\left(\alpha + \frac{5}{2}\right)^4\Gamma(5\alpha + 4)} - \frac{64\alpha^3\Gamma(4\alpha + 5)t^{5\alpha+4}}{\Gamma\left(\alpha + \frac{5}{2}\right)^4\Gamma(5\alpha + 5)} \\
&+ \frac{108\alpha^2\Gamma(4\alpha + 4)t^{5\alpha+3}}{\Gamma\left(\alpha + \frac{5}{2}\right)^4\Gamma(5\alpha + 4)} - \frac{288\alpha^2\Gamma(4\alpha + 5)t^{5\alpha+4}}{\Gamma\left(\alpha + \frac{5}{2}\right)^4\Gamma(5\alpha + 5)} + \frac{192\alpha^2\Gamma(4\alpha + 6)t^{5\alpha+5}}{\Gamma\left(\alpha + \frac{5}{2}\right)^4\Gamma(5\alpha + 6)} \\
&- \frac{t^{\alpha+1}}{1260\Gamma(\alpha + 2)} + \frac{108\alpha\Gamma(4\alpha + 4)t^{5\alpha+3}}{\Gamma\left(\alpha + \frac{5}{2}\right)^4\Gamma(5\alpha + 4)} + \frac{81\Gamma(4\alpha + 4)t^{5\alpha+3}}{2\Gamma\left(\alpha + \frac{5}{2}\right)^4\Gamma(5\alpha + 4)} \\
&- \frac{216\Gamma(4\alpha + 5)t^{5\alpha+4}}{\Gamma\left(\alpha + \frac{5}{2}\right)^4\Gamma(5\alpha + 5)} + \frac{576\alpha\Gamma(4\alpha + 6)t^{5\alpha+5}}{\Gamma\left(\alpha + \frac{5}{2}\right)^4\Gamma(5\alpha + 6)} + \frac{432\Gamma(4\alpha + 6)t^{5\alpha+5}}{\Gamma\left(\alpha + \frac{5}{2}\right)^4\Gamma(5\alpha + 6)} \\
&- \frac{256\alpha\Gamma(4\alpha + 7)t^{5\alpha+6}}{\Gamma\left(\alpha + \frac{5}{2}\right)^4\Gamma(5\alpha + 7)} - \frac{384\Gamma(4\alpha + 7)t^{5\alpha+6}}{\Gamma\left(\alpha + \frac{5}{2}\right)^4\Gamma(5\alpha + 7)} + \frac{128\Gamma(4\alpha + 8)t^{5\alpha+7}}{\Gamma\left(\alpha + \frac{5}{2}\right)^4\Gamma(5\alpha + 8)} \\
&- \frac{432\alpha\Gamma(4\alpha + 5)t^{5\alpha+4}}{\Gamma\left(\alpha + \frac{5}{2}\right)^4\Gamma(5\alpha + 5)}.
\end{aligned}
$$

To obtain the inverse Sumudu transform of $\mathbb{S}[u_2(t)]$ from (15), we use *mathematica* to avoid lengthy calculations. The approximate solution is given by $u_a(t) = u_0(t) + u_1(t) + u_2(t)$. When $\alpha = 0.5$, then $u_a(t) = t^2 - t$ which is the exact solution. The value of $\alpha = 0.5$ is the only case for which we know the exact solution, and our approximate solution is in excellent agreement with the exact values as shown in Figure 2.

Example 4.2 Consider the following nonlinear fourth-order fractional integro-differential equation [8, 17]

$$D^\alpha u(x) = 1 + \int_0^x e^{-t}u^2(t))dt, \ 0 \le x \le 1, \ \ 3 < \alpha \le 4, \tag{17}$$

subject to the boundary conditions $u(0) = u'(0) = 1$, $u(1) = u'(1) = e$. Since $3 < \alpha \le 4$, in equation (7), we take $n = 4$. Applying the Sumudu transform to both sides of equation (17), we get

$$\mathbb{S}[D^\alpha u(x)] = \mathbb{S}[1] + \mathbb{S}\Big[\int_0^x e^{-t}u^2(t))dt\Big].$$
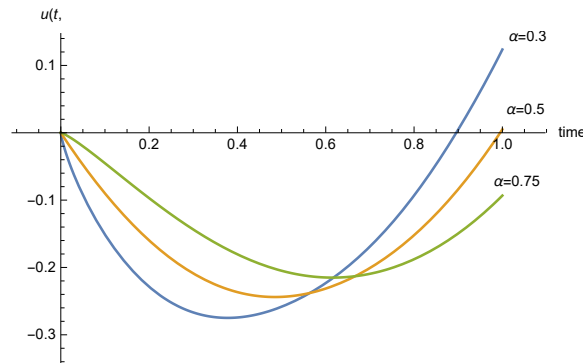
Figure 1: The approximate solution when $0 < t < 1$, for Example 4.1 for different values of α.
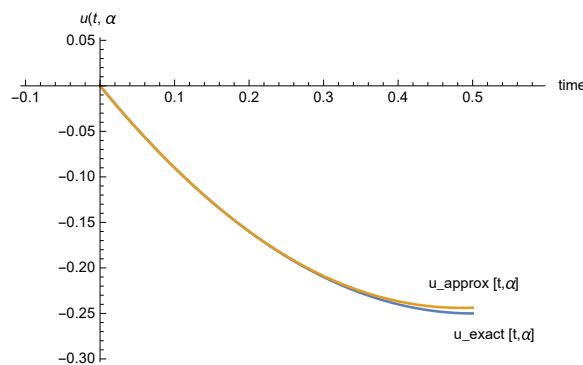
Figure 2: Comparison between the approximate solution when $\alpha = 0.5$ and the exact solution when $0 < t < 0.5$, for Example 4.1.

Use the initial conditions together with equation (7) to obtain

$$\frac{\mathbb{S}[u(x)]}{u^{\alpha}} - \frac{1}{u^{\alpha}} - \frac{1}{u^{\alpha-1}} - \frac{A}{u^{\alpha-2}} - \frac{B}{u^{\alpha-3}} = 1 + \mathbb{S}\Big[\int_0^x e^{-t} u^2(t)]dt\Big], \tag{18}$$

where the constants $A = u''(0)$ and $B = u'''(0)$ are to be determined by imposing the other two boundary conditions $u(1) = u'(1) = e$ on the obtained approximate solution. Simplify equation (18), we get

$$\mathbb{S}[u(x)] = 1 + u + Au^2 + Bu^3 + u^{\alpha} + u^{\alpha}\mathbb{S}\Big[\int_0^x e^{-t} u^2(t)]dt\Big]. \tag{19}$$

Substituting the decomposition series (8) for $u(x)$, and the series $\sum_{n=0}^{\infty} A_n(t)$ for the nonlinear term $u^2(t)$, we have

$$\mathbb{S}[\sum_{n=0}^{\infty} u_n(x)] = 1 + u + Au^2 + Bu^3 + u^{\alpha} + u^{\alpha}\mathbb{S}\Big[\int_0^x e^{-t} \sum_{n=0}^{\infty} A_n(t))dt\Big], \tag{20}$$

where the first two Adomian polynomials are given by $A_0(t) = u_0^2(t)$, $A_1(t) = 2u_0(t)u_1(t)$. The modified decomposition technique introduces the use of the recursive

Sumudu-Adomian decomposition algorithm as

$$\mathbb{S}[u_0(x)] = 1 + u + u^\alpha, \tag{21}$$

and

$$\mathbb{S}[u_1(x)] = Au^2 + Bu^3 + u^\alpha \mathbb{S}\left[\int_0^x e^{-t} A_0(t) dt\right]. \tag{22}$$

The $2-$term approximation is given by

$$\phi_2(x, A; B) = u_0(x) + u_1(x), \tag{23}$$

where the constants A and B can be determined using the remaining boundary conditions. Table 1 shows some numerical values for different values of α. The exact solution of the problem in equation (17) is $u(x) = e^x$, and the values in Table 1 corresponding to $\alpha = 4$ are in an excellent agreement with the exact values. Table 2 shows some numerical values for different values of α. In the theory of fractional calculus, it is obvious that when the fractional derivative α $(m - 1 < \alpha \leq m)$ tends to positive integer m, then the approximate solution *continuously* tends to the exact solution of the problem with derivative m. A closer look at the values obtained by our method in Table 1 do have this characteristic. In Table 2, we compare the approximate solution for problem (17) obtained by the proposed method for different values of α with those obtained by the Adomian method [8], and the Legendre collocation method [17]. In Table 2, our results for $\alpha = 4$, which is the only case where we know the exact solution, are in better agreement than those obtained by the methods described in [8] and [17].
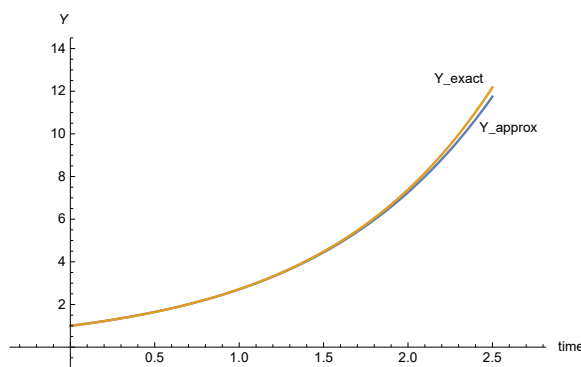
Figure 3: The approximate solution for $0 < t < 2.5$, when $\alpha = 4$, compared to the exact solution for Example 4.2.

5   Conclusion

The fundamental goal of this paper is to propose an efficient algorithm for the solution of fractional integro-differential equations. This goal has been achieved by using the Sumudu-Adomian decomposition method. The validity and accuracy of our approach is examined by solving two examples found in [15, 17]. In order to illustrate the technique, plots of the behavior of the approximate solutions are provided which ensure that the

α (A, B)	3.10 $(1.005, 0.163)$	3.90 $(1.0055, 0.9351)$	3.99 $(0.9974, 1.0056)$	4.00 $(0.996, 1.01)$	$Exact$ e^x
$x = 0.1$	1.10517	1.10519	1.10516	1.10516	1.10517
$x = 0.2$	1.22137	1.22145	1.22136	1.22135	1.22140
$x = 0.3$	1.34974	1.34993	1.34978	1.34976	1.34986
$x = 0.4$	1.49161	1.49189	1.49170	1.49168	1.49182
$x = 0.5$	1.64842	1.64877	1.64857	1.64855	1.64872
$x = 0.6$	1.82177	1.82214	1.82197	1.82195	1.82212
$x = 0.7$	2.01344	2.01375	2.01362	2.01361	2.01375
$x = 0.8$	2.22533	2.22552	2.22546	2.22545	2.22554
$x = 0.9$	2.45957	2.45959	2.45957	2.45957	2.45960
$x = 1.0$	2.71828	2.71828	2.71828	2.71828	2.71828

Table 1: Numerical values for Example 4.2 with different values of the order α.

x_i	$\alpha = 3.25$			$\alpha = 3.5$		
	Results [15]	Results [17]	Our Method	Results [15]	Results [17]	Our Method
0.1	1.10101	1.10655	1.10517	1.10675	1.10679	1.10516
0.2	1.21402	1.22393	1.22137	1.22432	1.22441	1.22136
0.3	1.34119	1.35320	1.34974	1.35375	1.35388	1.34978
0.4	1.48170	1.49560	1.49161	1.49627	1.49642	1.49170
0.5	1.63876	1.65255	1.64842	1.65327	1.65343	1.64857
0.6	1.81365	1.82565	1.82177	1.82635	1.82651	1.82197
0.7	2.00662	2.01668	2.01344	2.01729	2.01744	2.01362
0.8	2.22023	2.22763	2.22533	2.22808	2.22819	2.22546
0.9	2.45691	2.46069	2.45953	2.46093	2.46099	2.45957
1.0	2.71828	2.71828	2.71828	2.71828	2.71828	2.71828

Table 2: Comparison of the methods for solving equation (17) for $\alpha = 3.25, 3.5$.

Sumudu decomposition method is a very helpful and efficient method to produce the approximate solutions. Finally, we would like to claim that the method presented in this work for solving nonlinear fractional integro-differential equation is an excellent one in terms of its simplicity, implementation and high accuracy. Also, we conclude that it can be applied to several sophisticated linear and nonlinear equations.

As future work, we aim to apply alternative methods based on different versions of the fractional power series technique [26–31] to solve different types of fractional integro-differential problems and other fractional problems arising in engineering and science applications.

References

[1] K. Al-Khaled and F. Allan. Decomposition method for solving nonlinear integro-differential equations. *J. Appl. Math. and Computing* **19** (1-2) (2005) 415–425.

[2] K. Al-Khaled and E. Az-Zobi. A new convergence proof of the Adomian decomposition method for a mixed hyperbolic elliptic system of conservation laws. *Appl. Math. and Comput.* **217** (8) 4248–4256.

[3] A.M. Nagy and N.H. Sweilam. An efficient method for solving fractional Hodgkin-Huxley model. *Phy. Lett. A* **378** (2014) 1980–1984.

[4] K.B. Oldham and J. Spanier. *The Fractional Calculus.* Academic Press. New York, 1974.

[5] I. Podlubny. *Fractional Differential Equations.* Academic Press. New York, 1999.

[6] I. Podlubny. What Euler could further write, or the unnoticed "big bang" of the fractional calculus. *Frac. Calc. Appl. Anal.* **16** (2013) 501–506.

[7] K.S. Miller. and B. Ross. An Introduction to the Fractional Calculus and Fractional Differential Equations. John Wiley and Sons Inc. New York, 1993.

[8] S. Momani and Z. OdibatZ. Numerical methods for nonlinear paartial differential equations of fractional order. *Appl. Math. Modeling* **32** (2008) 28–39.

[9] I. Podlubny. Gemmetric and physical interpretaion of fractional integration and fractional differentaition. *Frac. Calc. Appl. Anal.* **5** (2002) 367–386.

[10] G.K. Watuagala. Sumudu transform: a new integral transform to solve differential equations in control engineering problems. *Mathematical Engineering in Industry* **6**(4) (1998) 319–329.

[11] G.K. Watuagala. Sumudu transform: an integral transform to solve differential equation and control engineering problems. *Int. J. Math. Educ. Sci. and Technol.* **24**(1) (1993) 35-42.

[12] K. Abdolamir, M.M. Mohammad and H.M. Hamed. Exact Solution of Time-Fractional Partial Differential Equations Using Sumudu Transform. *WSEAS Trans. Math.* **13** (2014) 142–151.

[13] Q. Katatbeh and F. Belgacem. Applications of the Sumudu transform to fractional differential equations. *Nonlinear Studies* **18** (1) (2011) 99–112.

[14] F. Jarad, K. Bayram, T. Abdeljawad and D. Baleanu. On the disrete Sumudu transform. *Romanian Reports in Phys.* **64**(2) (2012) 356–356.

[15] K. Al-Khaled, M. Alquran., A. Al-Saidi, G.M. NGuerekata and J. Chattopadhyay. Numerical Methods for Solving Nonlinear Fractional Integro-Differential Equations. *Nonlinear Studies* **22** (4) (2015) 647–657.

[16] M. Alquran, I. Jaradat and S. Sivasundaram. Elegant scheme for solving Caputo-time-fractional integro-differential equations. *Nonlinear Studies* **25** (2) (2018) 385–393.

[17] A. Saadatmandi and M. Dehghan. A Legendre collocation method for fractional integro-differential equations. *J. of Vibration and Control* **17** (13) (2011) 2050–2058.

[18] A. Ahmed, K.P. Ghadle and S.M. Atshan. The approximate solutions of fractional integro-differential equations by using modified Adomian decomposition method. *Khayyam J. Math.* **5** (1) (2019) 21–39.

[19] C. Yang and J. Hou. Numerical solution of integro-differential equations of fractional order by Laplace decomposition method. *J. Wseas Transactions on Mathematics* **12** (12) (2013) 1173–2880.

[20] K. Al-Khaled. Numerical solution of time-fractional partial differential equations using Sumudu decomposition method. *Rom. J. of Phy.* **60** (1-2) (2015) 99–110.

[21] M. Caputo. Linear models of dissipation whose Q is almost frequency independent-II. *Geophys. J. R. Astron. Soc.* **13** (1967) 529–539.

[22] F. Belgacem and A.A. KaraballiA. Sumudu transform fundamental properties investigations and applications. *International J. Appl. Math. Stoch. (2005) 1–23*, DOI 10.1155/JAMSA/2006/91083.

[23] G. Adomian. A review of the decomposition method in applied mathematics. *J. Math. Anal. Appl.* **135** (1988) 501–544.

[24] G. Adomian. *Solving Frontier Problems of Physics: The Decompsition Method.* Kluwer Academic Publishers. Boston, 1994.

[25] A.M. Wazwaz. A new algorithm for calculating Adomian polynomials for nonlinear operators, *Applied Mathematics and Computation* **111** (2000) 53–69.

[26] M. Alquran, K. Al-Khaled, S. Sivasundaram and H.M. JaradatM. Mathematical and numerical study of existence of bifurcations of the generalized fractional Burgers-Huxley equation. *Nonlinear Studies* **24** (1) (2017) 235–244.

[27] I. Jaradat, M. Alquran and K. Al-Khaled. An analytical study of physical models with inherited temporal and spatial memory. *Eur. Phys. J. Plus.* (2018) 133: 162.

[28] I. Jaradat, M. Al-Dolat, K. Al-Zoubi and M. Alquran. Theory and applications of a more general form for fractional power series expansion. *Chaos Solitons Fract.* **108** (2018) 107–110.

[29] I. Jaradat, M. Alquran and M. Al-Dolat. Analytic solution of homogeneous time-invariant fractional IVP. *Adv. Differ. Equ.* (2018) 2018: 143.

[30] I. Jaradat, M. Alquran and R. Abdel-Muhsen. An analytical framework of 2D diffusion, wave-like, telegraph, and Burgers' models with twofold Caputo derivatives ordering. *Nonlinear Dynamics* **93** (4) (2018) 1911–1922.

[31] H.M. Jaradat, I. Jaradat, M. Alquran, M.M.M. Jaradat, Z. Mustafa, K. Abohassan and Abdelkarim R. Approximate solutions to the generalized time-fractional Ito system. *Italian journal of pure and applied mathematics* **37** (2017) 699–710.

[32] M. Alquran and I. Jaradat. A novel scheme for solving Caputo time-fractional nonlinear equations: theory and application. *Nonlinear Dynamics* **91** (4) (2018) 2389–2395.

Analysis of the Model Reduction Using Singular Perturbation Approximation on Unstable and Non-Minimal Discrete-Time Linear Systems and Its Applications

D. K. Arif [1*], Fatmawati [2], D. Adzkiya [1], Mardlijah [1], H. N. Fadhilah [1] and P. Aditya [1]

[1] *Department of Mathematics, Sepuluh Nopember Institute of Technology, Sukolilo ITS Campus-Surabaya 60111, Indonesia*
[2] *Department of Mathematics, Airlangga University, Surabaya 60115, Indonesia*

Abstract: In the natural phenomena, many systems are unstable and non-minimal. Moreover, the systems in the universe often have large order. Therefore, we need to simplify the order of the system without any significant errors. Simplification of this system can be done using the reduction of the model. Model reduction can only be done on the stable and minimal system. Thus, we need a model reduction for unstable and non-minimal systems. There are many model reduction methods in the literature, for example, a balanced truncation method and a singular perturbation approximation. In this work, we propose a method to reduce unstable and non-minimal systems by using the singular perturbation approximation (SPA). First, we decompose the unstable system into a stable subsystem and an unstable subsystem. Then, if the stable subsystem is non-minimal, we apply the minimization process to obtain a stable subsystem that is minimal. Next, we apply the singular perturbation approximation to the stable and minimal subsystem to obtain a reduced subsystem. Finally, we obtain a total reduced model by combining the unstable subsystem and the reduced subsystem. Then we apply the method to shallow water equations. Based on the simulation results, frequency response of the original system and the reduced minimal system using the SPA method has similarity in low frequency, but in high frequency the value tends to be different. Furthermore, the error bound of the SPA and the balanced truncation method is almost the same.

Keywords: *model reduction; singular perturbation approximation; unstable systems; non-minimal systems.*

Mathematics Subject Classification (2010): 78M34.

---

* Corresponding author: `mailto:didik@matematika.its.ac.id`

1   Introduction

Mathematics has an important role in solving the existing problems. One of them is using mathematical modeling. Mathematical modeling is used to represent the problem to be solved. The problems taken often adopt real natural phenomena. If we construct a model of the real natural phenomena as a mathematical model, it will contain many state variables. On the other hand, due to the huge number of variables in the system, the computational time to simulate the model is longer and it is not efficient. Not only that, the system that has larger order is more complicated than the system that has small order. Therefore, it should be simplified to smaller order without significant errors. Those simplifications of the system are called a model reduction [4].

The model reduction can be used if the system is stable and minimal. For an unstable system, we need to decompose the unstable system so that we obtain a stable subsystem that can be reduced. Then, we investigate whether the system is minimal. A system is called minimal if the system is controllable and observable. If we have an uncontrollable or unobservable system (commonly called a non-minimal system), we have to find the minimal representation of the system by applying the minimization process. After the decomposition process (for unstable systems) and minimization (for uncontrollable or unobservable systems) of the system, we obtain a system that is suitable for model reduction [2, 11].

There are many methods in the literature for the model order reduction, such as a balanced truncation, model analysis, Krylov method, Hankel norm approximation, singular value decomposition [6–8, 13, 14]. Ayadi and Benhadj Braiek [5] discuss a new method to reduce LTI and LTV systems by using orthogonal functions. Solikhatun et al. [16] discuss a procedure to choose the reduced order of bilinear time-invariant systems. Aleksandrov et al. [1] discuss the stability problem by using a nonlinear approach. Martynyuk [9] discusses a new approach for the stability analysis of dynamical systems defined over metric spaces. In this paper, we discuss a model reduction procedure for non-minimal systems by using a singular perturbation approximation (SPA) method. The procedure to reduce unstable and non-minimal systems using the singular perturbation approximation is as follows. First, we decompose the unstable system into a stable subsystem and an unstable subsystem. Then, for the stable subsystem, if the system is non-minimal, we apply the minimization process to obtain a stable subsystem that is minimal. Next, we apply the singular perturbation approximation to the stable and minimal subsystem to obtain a reduced subsystem. The total reduced system is obtained by combining the unstable subsystem and the reduced subsystem. Then, we apply the model reduction of non-minimal systems to shallow water equations. Shallow water equations are a system that may become stable, unstable or non-minimal system. Furthermore, shallow water equations can produce a high-order system. Thus, we are interested to apply the technique to this system. In the simulation, we compare the frequency response and infinity-norm error of the singular perturbation approximation method and the balanced truncation method.

2   Linear Systems

Give an nth order discrete-time linear system as follows [12]:

$$\begin{cases} x(k+1) &= Ax(k) + Bu(k), \\ y(k) &= Cx(k) + Du(k). \end{cases} \tag{1}$$

Next, we refer to the system (1) as the original system. The system can be rewritten as

$$G = \left[\begin{array}{c|c} A & B \\ \hline C & D \end{array} \right].$$

The transfer function of the system (A, B, C, D) is denoted as $G(z)$ and is defined as follows [12]:

$$G(z) = C(zI - A)^{-1}B + D. \tag{2}$$

We can analyze the properties of the system (1). We focus on the following properties: stability, controllability, and observability. To analyze the stability, we look at the eigenvalues (λ) [12]. If $|\lambda| < 1$, then the system is asymptotically stable. Otherwise, if the eigenvalue $|\lambda| > 1$, the system is unstable. To analyze the controllability of the system, we can use the controllability matrix M_c. If the controllability matrix has the rank equal to n, then the system is controllable. To analyze the observability of the system, we can use the observability matrix M_o. If the observability matrix has the rank equal to n, then the system is observable.

The relationship between stability, controllability, and observability of systems with the controllability Gramian W and the observability Gramian M is described by the following theorem.

Theorem 2.1 *Given a system (A, B, C, D) that is stable, controllable, and observable, the controllability Gramian W and the observability Gramian M, each is a single and positive definite solution from the Lyapunov equation [18]*

$$AWA^T + BB^T - W = 0, \tag{3}$$

$$A^T M A + C^T C - M = 0. \tag{4}$$

The model reduction can only be done on the stable and minimal system. If the system is unstable, we need to decompose the system into a stable subsystem and an unstable subsystem. In other words, the decomposition of unstable systems is a separation between the stable subsystem and the unstable subsystem. If the system is non-minimal, we apply the minimization process to the system to obtain minimal systems.

3   Decomposition Process of Unstable Systems

The decomposition process of unstable systems has two transformation steps. First, we apply a real Schur block transformation using the unitary matrix U_d in the Schur upper triangular form. Second, we solve the Lyapunov equation for transformation to obtain stable and unstable subsystems. We denote $(A_{ss}, B_{ss}, C_{ss}, D_{ss})$ for the stable subsystem and $(A_{us}, B_{us}, C_{us}, D_{us})$ for the unstable subsystem.

$$G_d = \left[\begin{array}{c|c} A_{ss} & B_{ss} \\ \hline C_{ss} & D_{ss} \end{array} \right] + \left[\begin{array}{c|c} A_{us} & B_{us} \\ \hline C_{us} & 0 \end{array} \right]$$

with

$$stable\ subsystem = \left[\begin{array}{c|c} A_{ss} & B_{ss} \\ \hline C_{ss} & D_{ss} \end{array} \right]$$

and

$$unstable\ subsystem = \left[\begin{array}{c|c} A_{us} & B_{us} \\ \hline C_{us} & 0 \end{array} \right].$$

So from (1), we obtain a stable subsystem as follows:

$$\begin{cases} x_{ss}(k+1) &= A_{ss}x_{ss}(k) + B_{ss}u_{ss}(k), \\ y_{ss}(k) &= C_{ss}x_{ss}(k) + D_{ss}u_{ss}(k). \end{cases} \tag{5}$$

4   Minimization Process of Non-Minimal Systems

If the system (5) is non-minimal, we can minimize the system to obtain a minimal system. The minimization process is done by removing the uncontrollable and unobservable states in the state-space model. After the minimization process is finished, we obtain a minimal system (observable and controllable) as follows:

$$\begin{cases} x_m(k+1) &= A_m x_m(k) + B_m u_m(k), \\ y_m(k) &= C_m x_m(k) + D_m u_m(k). \end{cases} \tag{6}$$

The transfer function of the minimal system is

$$G_m = \left[\begin{array}{c|c} A_m & B_m \\ \hline C_m & D_m \end{array} \right].$$

Because the model reduction needs a stable and minimal system, then we define a stable and minimal discrete-time linear system as follows:

$$\begin{cases} x_{sm}(k+1) &= A_{sm}x_{sm}(k) + B_{sm}u_{sm}(k), \\ y_{sm}(k) &= C_{sm}x_{sm}(k) + D_{sm}u_{sm}(k). \end{cases} \tag{7}$$

5   Balanced Systems

In order to use the SPA method, first the system has to be balanced. The balanced system is a system such that the controllability Gramian is the same as the observability Gramian. Thus, in a balanced system, the state variables are ordered based on their influence on the system. In general, the controllability Gramian and the observability Gramian are not the same. To construct a balanced system, we transform the original system using the transformation matrix T so that we obtain a balanced system.

The algorithm to compute matrix T is described as follows:

1 Find a matrix ϕ that satisfies $W = \phi^T \phi$.

2 Construct a matrix $\phi M \phi^T$ and diagonalize $\phi M \phi^T$ so that $\phi M \phi^T = U\Sigma^2 U^T$.

3 The non-singular transformation matrix T is $T = \phi^T U \Sigma^{-\frac{1}{2}}$.

So we obtain a balanced system $(\tilde{A}, \tilde{B}, \tilde{C}, \tilde{D})$, where

$$\tilde{A} = T^{-1}AT, \tilde{B} = T^{-1}B, \tilde{C} = CT, \tilde{D} = D.$$

The balanced system has the controllability Gramian $\tilde{W}$ and the observability Gramian $\tilde{M}$ that is a single solution from the Lyapunov equation:

$$\tilde{W} = T^{-1}WT^{-T} \tag{8}$$

and

$$\tilde{M} = T^T MT \tag{9}$$

such that

$$\tilde{W} = \tilde{M} = \sum = diag(\sigma_1, \sigma_2, \cdots, \sigma_r),\ \sigma_1 \geq \cdots \geq \sigma_r \geq \cdots \geq \sigma_n > 0,$$

where σ_i is the Hankel singular value from the balanced system that is defined as

$$\sigma_i = \sqrt{\lambda_i(WM)}, \quad i = 1, 2, ..., n,$$

where λ_i is the eigenvalue from the multiplication of the controllability Gramian W and the observability Gramian M.

6   Model Reduction Using Singular Perturbation Approximation

The singular perturbation approximation (SPA) method can be applied to stable and minimal systems. The reduction process in the SPA method is almost the same as in the balanced truncation (BT) method. In the BT method, the model reduction is performed by cutting the state variables that correspond to small Hankel singular values. In the reduced model using the SPA method, all state variables of the balanced system are partitioned into the fast and slow modes. The variable circumstances corresponding to the small Hankel singular value are defined as a fast mode, while the variable circumstances corresponding to the larger Hankel singular value are defined as a slow mode. Furthermore, the reduced model is obtained by assuming the speed of the fast mode equal to zero [3].

7   Model Reduction Procedure for Unstable and Non-Minimal Systems Using Singular Perturbation Approximation

In this section, we describe the procedure to reduce unstable and non-minimal systems using the singular perturbation approximation. The steps are as follows:

1. We apply the decomposition process to produce a stable and an unstable subsystem (see Section 3).

2. Because the system is non-minimal, then the stable subsystem is also non-minimal. Then we apply the minimization process to the stable subsystem to obtain a minimal stable subsystem (controllable and observable) (see Section 4).

   After step 1 and 2, we will obtain a stable and minimal subsystem.

3. The next step is applying the SPA method to the stable and minimal subsystem (see Section 6) to obtain a reduced stable subsystem.

4. We combine the reduced stable subsystem (from Step 3) and the unstable subsystem (from Step 1) to obtain a total reduced system.

5. The last step is to check or re-analyze the properties of the total reduced system. The properties are stability, controllability and observability.

8   Numerical Example

In this section, we introduce a numerical example as an application of the model reduction using the SPA to the shallow water equation. In the simulation results, we compare the errors of the SPA method and the BT method.

8.1   Shallow water equations

We discuss the shallow water equation that describes the flow of water in rivers [17]:

$$\frac{\partial h}{\partial t} + D\frac{\partial v}{\partial x} = 0, \tag{10}$$

$$\frac{\partial v}{\partial t} + g\frac{\partial h}{\partial x} + C_f u = 0, \tag{11}$$

with the initial and boundary conditions

$$h(x,0) = 1, v(x,0) = 0, h(0,t) = \psi_b(t), v(L,t) = v_N(t), \tag{12}$$

where $h(x,t)$ is the water level above the reference plane at position x and time t, $v(x,t)$ is the average current velocity at position x and time t, t is the time variable, x is the position along the river, D is the water depth, g is the gravitational acceleration and c is a friction constant.

Using the initial and boundary conditions (12) for $i = 14$ to $n = 30$, then, the following values for the parameters are assumed:

$$D = 10m, C_f = 0.0002, \Delta x = 60000/N\Delta t = 360, g = 9.8m/s^2.$$

Thus, we can write the equations (10) and (11) in matrix notation as follows:

$$A_1 x(k+1) = A_2 x(k) + Bu(k), \tag{13}$$

$$x(k+1) = A_1^{-1} A_2 x(k) + A_1^{-1} B_1 u(k). \tag{14}$$

The above system is a discrete-time linear-time-invariant system

$$x(k+1) = Ax(k) + Bu(k),$$

where $A = A_1^{-1} A_2$ and $B = A_1^{-1} B_1$. By using the parameters described above, those matrices are given by

$$
A =
\left(
\begin{array}{ccccccccc}
0 & 0 & 0 & 0 & 0 & 0 & 0 & 0 & \cdots \\
0.3468 & 0.6851 & -0.6054 & 0.2142 & -0.0770 & 0.0272 & -0.0098 & 0.0035 & \cdots \\
0.1271 & 0.6178 & 0.5238 & -0.5392 & 0.1937 & -0.0686 & 0.0246 & -0.0087 & \cdots \\
0.0441 & 0.2142 & 0.5284 & 0.4981 & -0.5382 & 0.1905 & -0.0684 & 0.0242 & \cdots \\
0.0162 & 0.0785 & 0.1937 & 0.5492 & 0.5484 & -0.5479 & 0.1969 & -0.0697 & \cdots \\
0.0056 & 0.0272 & 0.0672 & 0.1905 & 0.5370 & 0.4951 & -0.5371 & 0.1901 & \cdots \\
0.0021 & 0.0100 & 0.0246 & 0.0698 & 0.1969 & 0.5481 & 0.5488 & -0.5481 & \cdots \\
\vdots & \vdots & \vdots & \vdots & \vdots & \vdots & \vdots & \ddots \\
0.0000 & 0.0000 & 0.0000 & 0.0000 & 0.0000 & 0.0000 & 0.0000 & 0.0000 & \cdots \\
0.0000 & 0.0000 & 0.0000 & 0.0000 & 0.0000 & 0.0000 & 0.0000 & 0.0000 & \cdots \\
0.0000 & 0.0000 & 0.0000 & 0.0000 & 0.0000 & 0.0000 & 0.0000 & 0.0000 & \cdots \\
0.0000 & 0.0000 & 0.0000 & 0.0000 & 0.0000 & 0.0000 & 0.0000 & 0.0000 & \cdots \\
0.0000 & 0.0000 & 0.0000 & 0.0000 & 0.0000 & 0.0000 & 0.0000 & 0.0000 & \cdots \\
0.0000 & 0.0000 & 0.0000 & 0.0000 & 0.0000 & 0.0000 & 0.0000 & 0.0000 & \cdots \\
0 & 0 & 0 & 0 & 0 & 0 & 0 & 0 & \cdots \\
\end{array}
\right.
$$

$$
\left.
\begin{array}{ccccc}
\cdots & 0 & 0 & 0 & 0 \\
\cdots & -0.0000 & 0.0000 & -0.0000 & 0.0000 \\
\cdots & 0.0000 & -0.0000 & 0.0000 & -0.0000 \\
\cdots & -0.0000 & 0.0000 & -0.0000 & 0.0000 \\
\cdots & 0.0000 & -0.0000 & 0.0000 & -0.0000 \\
\cdots & -0.0000 & 0.0000 & -0.0000 & 0.0000 \\
\cdots & 0.0000 & -0.0000 & 0.0000 & -0.0000 \\
\ddots & \vdots & \vdots & \vdots & \vdots \\
\cdots & -0.0684 & 0.0238 & -0.0098 & 0.0021 \\
\cdots & 0.1973 & -0.0686 & 0.0282 & -0.0059 \\
\cdots & -0.5382 & 0.1870 & -0.0770 & 0.0162 \\
\cdots & 0.5520 & -0.5392 & 0.2219 & -0.0466 \\
\cdots & 0.5284 & 0.4708 & -0.6054 & 0.1271 \\
\cdots & 0.2219 & 0.6178 & 0.7457 & -0.3666 \\
\cdots & 0 & 0 & 0 & 0 \\
\end{array}
\right), \tag{15}
$$

$$
B = \begin{pmatrix} 1.0000 \\ 0.3468 \\ 0.1271 \\ 0.0441 \\ 0.0162 \\ 0.0056 \\ 0.0021 \\ 0.0007 \\ \vdots \\ 0.0000 \\ 0.0000 \\ 0.0000 \\ 0.0000 \\ 0.0000 \\ 0 \end{pmatrix}, \quad
x_{k+1} = \begin{pmatrix} h_0^{k+1} \\ u_1^{k+1} \\ h_1^{k+1} \\ u_2^{k+1} \\ h_2^{k+1} \\ u_3^{k+1} \\ h_3^{k+1} \\ u_4^{k+1} \\ \vdots \\ h_N^{k+1} \\ u_{N+\frac{1}{2}}^{k+1} \\ h_{N+1}^{k+1} \\ u_{N+1}^{k+1} \\ h_{N+2}^{k+1} \\ u_{N+\frac{3}{2}}^{k+1} \end{pmatrix}, \quad
x_k = \begin{pmatrix} h_0^{k} \\ u_{\frac{1}{2}}^{k} \\ h_1^{k} \\ u_{\frac{3}{2}}^{k} \\ h_2^{k} \\ u_{\frac{5}{2}}^{k} \\ h_3^{k} \\ u_{\frac{7}{2}}^{k} \\ \vdots \\ h_{N-1}^{k} \\ u_{N-\frac{1}{2}}^{k} \\ h_N^{k} \\ u_{N+\frac{1}{2}}^{k} \\ h_{N+1}^{k} \\ u_{N+1}^{k} \end{pmatrix}, \quad
u_k = \begin{pmatrix} 1 \\ 0 \\ 0 \\ 0 \\ 0 \\ 0 \\ 0 \\ 0 \\ \vdots \\ 0 \\ 0 \\ 0 \\ 0 \\ 0 \\ 0 \end{pmatrix}, \tag{16}
$$

then, we construct a measurement equation at time k as follows:

$$
y(k) = Cx(k) + Du(k), \tag{17}
$$

where

$$
C = \begin{pmatrix} 0 & 0 & 0 & 0 & 0 & 0 & 0 & 0 & 0 & 0 & 0 & 0 & 0 & 0 & 1 & \cdots & 0 \end{pmatrix}, \quad D = 0. \tag{18}
$$

Based on the eigenvalues of the original system (A, B, C, D), the system is asymptotically stable, while based on the rank of the controllability and observability matrix, the system is uncontrollable (rank=29) and unobservable (rank=29). Thus, the original system is non-minimal.

Because the original system is asymptotically stable and non-minimal, then we go to step 2 (minimization, see Section 4). To produce a minimal system, we use command "minreal.m" in MATLAB [10]. The order of minimal system G_m is 29. By using the parameters defined in this section, the asymptotically stable and minimal system (controllable and observable) is given by

$$
G_m = \left(\begin{array}{ccccccc}
0.9614 & -0.1228 & -0.0598 & -0.0799 & -0.0213 & \cdots \\
0.0515 & 0.9614 & 0.0318 & 0.1105 & -0.0233 & \cdots \\
0 & 0 & 0.9315 & -0.3160 & 0.0245 & \cdots \\
0 & 0 & 0.2025 & 0.9315 & 0.0656 & \cdots \\
0 & 0 & 0 & 0 & 0.8756 & \cdots \\
0 & 0 & 0 & 0 & 0.3766 & \cdots \\
0 & 0 & 0 & 0 & 0 & \cdots \\
\vdots & \vdots & \vdots & \vdots & \vdots & \ddots \\
0 & 0 & 0 & 0 & 0 & \cdots \\
0 & 0 & 0 & 0 & 0 & \cdots \\
0 & 0 & 0 & 0 & 0 & \cdots \\
0 & 0 & 0 & 0 & 0 & \cdots \\
0 & 0 & 0 & 0 & 0 & \cdots \\
0 & 0 & 0 & 0 & 0 & \cdots \\
0 & 0 & 0 & 0 & 0 & \cdots \\
\hline
-0.2529 & 0.3194 & -0.1701 & 0.0569 & 0.3133 & \cdots
\end{array}\right.
$$

$$
\left.\begin{array}{ccccc|c}
\cdots & -0.0476 & 0.0975 & 0.2965 & 0.0000 & 0.1482 \\
\cdots & 0.0671 & 0.0223 & 0.2424 & -0.0000 & 0.1212 \\
\cdots & 0.0520 & 0.0104 & 0.1117 & -0.0000 & 0.0559 \\
\cdots & 0.1113 & 0.1192 & 0.3712 & 0.0000 & 0.1856 \\
\cdots & 0.2364 & -0.0964 & 0.1617 & 0.0000 & 0.0809 \\
\cdots & -0.1058 & 0.1330 & 0.2081 & -0.0000 & 0.1041 \\
\cdots & -0.0591 & -0.0082 & 0.1998 & -0.0000 & 0.0999 \\
\ddots & \vdots & \vdots & \vdots & \vdots & \vdots \\
\cdots & -0.0042 & -0.0460 & 0.0093 & -0.0000 & 0.0047 \\
\cdots & -0.0274 & -0.1478 & 0.0198 & 0.0000 & 0.0099 \\
\cdots & 0.1931 & -0.0271 & -0.0212 & 0.0000 & -0.0106 \\
\cdots & 0.2287 & -0.8517 & -0.0339 & 0.0000 & -0.0169 \\
\cdots & 1.0617 & 0.2287 & -0.0240 & -0.0000 & -0.0120 \\
\cdots & 0 & 0 & 0 & 0 & 0.5000 \\
\hline
\cdots & 0.0223 & 0.2130 & 0 & 0 & 0
\end{array}\right). \tag{19}
$$

Then we construct a balanced system of shallow water equations. In our case, the balanced system $(\tilde{A}, \tilde{B}, \tilde{C}, \tilde{D})$ has the Hankel singular value shown in Figure 1.
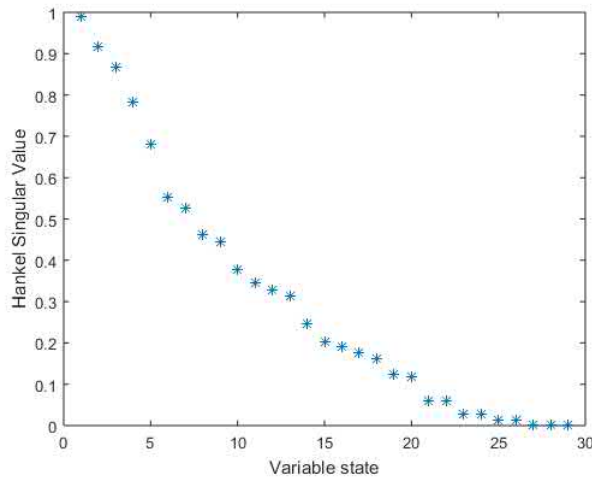
Figure 1: The Hankel singular value of shallow water equation.

After we get a balanced system, we go to the model reduction process. In this case, we reduce the model from order 29 to order 15 $(\tilde{A}_r, \tilde{B}_r, \tilde{C}_r, \tilde{D}_r)$ by using the SPA. Based on the eigenvalues of the reduced system, we conclude that the reduced system is asymptotically stable, while based on the rank of the controllability matrix M_c and the observability matrix M_o, the system is controllable (rank=15) and observable (rank=15). Thus, the reduced system is minimal.

After that we compare the frequency response of the total reduced model of order 15 and the original system (minimal system) of order 29 to the original system in Figure 2 as follows. Here, we also show the model reduction using the balanced truncation (BT).

From Figure 2, we can analyze the frequency response of the original system and the total reduced system of order 15 using the SPA method. We can see that the frequency response has similarity in low frequency, but in high frequency, the frequency response tends to be different. Furthermore, we can see that by using the BT method, the frequency response has similarity in high frequency, but in low frequency, the frequency response tends to be different. Thus, the SPA method is better in low frequency, whereas the BT is better in high frequency.

From Figure 2, we can also determine the infinity norm of the error. The results are given in Table 1. Based on Table 1, we know that both model reduction methods (SPA and BT) have the same error bound.

9   Conclusions

The model reduction of unstable and non-minimal systems is conducted by applying the decomposition and minimization to the system. From the results of analysis, the properties of the reduced system are the same as the properties of the original system. From the simulation results, we obtained that the SPA method is better in low frequency
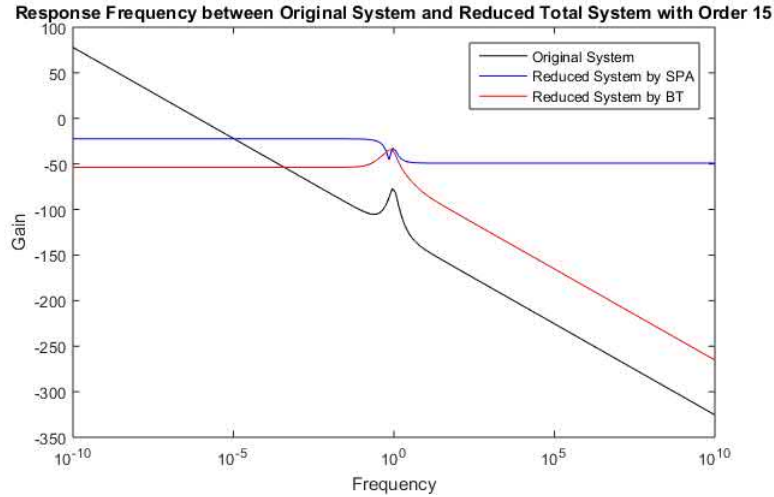
Figure 2: Frequency response of the reduced system with order 15 using SPA and BT to the original system.

Order of Result Reduced Model (r)	$\parallel G - G_r \parallel_\infty$ by SPA	$\parallel G - G_r \parallel_\infty$ by BT
6	1.0199	1.0644
9	0.7101	1.1475
15	0.4047	0.2775
18	0.0443	0.0405
24	0.0061	0.0038
27	8.7333×10^{-4}	8.5926×10^{-4}

Table 1: The ∞ norm of $(G - G_r)$ and the error bound.

and the BT method is better in high frequency. In terms of the error bound, the SPA method and the BT method are almost the same.

Acknowledgment

References

[1] A. Yu. Aleksandrov, A. A. Martynyuk and A. P. Zhabko. The problem of stability by non-linear approximation. *Nonlinear Dynamics and Systems Theory* **15** (3) (2015) 221–230.

[2] D. K. Arif, D. Adzkiya, E. Apriliani, and I. N. Khasanah. Model Reduction of Non-minimal Discrete-Time Linear-Time-Invariant Systems. *Malaysian Journal of Mathematical Science* **11**(3) (2017) 377–391.

[3] D. K. Arif, H. N. Fadhilah, D. Adzkiya, L. N. Rochmah, N. A. W. Yoga, H. Setiawan, R. Kamilah, and R. R. N. Cahyani. Accelerating simulation time of unstable discrete-time systems using Singular Perturbation Approximation. In: *Proc. International Conf. on Instrumentation, Control, and Automation* Yogyakarta, Indonesia, 2017, 7–12.

[4] D. K. Arif, Widodo, Salmah, and E. Apriliani. Construction of the Kalman Filter Algorithm on the Model Reduction. *International Journal of Control and Automation* **7**(9) (2014) 257–270.

[5] B. Ayadi, and N. Benhadj Braiek. Orthogonal Functions Approach for Model Order Reduction of LTI and LTV Systems. *Nonlinear Dynamics and Systems Theory* **13**(2) (2013) 115-134.

[6] S. D. Djukić, and A. T. Sarić. Dynamic model reduction: An overview of available techniques with application to power systems. *Serbian journal of electrical engineering* **9**(2) (2012) 131–169.

[7] Fatmawati, R. Saragih, R. Bambang, and Y. Soeharyadi. Balanced truncation for unstable infinite dimensional systems via reciprocal transformation. *International Journal of Control, Automation, and Systems* **9**(2) (2011) 249–257.

[8] D. A. Kartika, D. K. Arif, E. Apriliani and D. Adzkiya. A study on model order reduction of stable continuous-time linear-time-invariant systems using balanced truncation methods. *Journal of Physics: Conference Series* **1867**(1) (2017) 020050.

[9] A. A. Martynyuk. Stability of dynamical systems in metric space. *Nonlinear Dynamics and Systems Theory* **5**(2) (2005) 157–167.

[10] MATLAB Release 2010a, The MathWorks, Inc., Natick, Massachusetts, United States.

[11] K. Mustaqim, D. K. Arif, E. Apriliani, and D. Adzkiya. Model reduction of unstable systems using balanced truncation method and its application to shallow water equations. *Journal of Physics: Conference Series* **855**(1) (2017) 012029.

[12] K. Ogata. *Discrete-time Control Systems*. Prentice-Hall International, Inc., Canada, 1995.

[13] R. Saragih, and Fatmawati. Singular perturbation approximation of balanced infinite-dimensional systems. *International Journal of Control and Automation* **6**(5) (2013) 409–420.

[14] Y. I. Sari, D. K. Arif, E. Apriliani, and D. Adzkiya. A study on model order reduction of stable discrete-time linear-time-invariant systems using balanced truncation methods. *Journal of Physics: Conference Series* **1867**(1) (2017) 020049.

[15] S. Skogestad and I. Postlethwaite. *Multivariable Feedback Control Analysis and Design*. John Wiley and Sons, Chichester, 2001.

[16] Solikhatun, R. Saragih, and E. Joelianto. Reduced Order Bilinear Time Invariant System by Means of Error Transfer Function Least Upper Bounds. *Nonlinear Dynamics and Systems Theory* **16**(2) (2016) 206–220.

[17] M. Verlaan. *Efficient Kalman Filtering Algorithms for Hydrodynamic Models.* PhD Thesis, Delft University of Technology, The Netherlands, 1998.

[18] L. Zhang, J. Lam, and Q. Zhang. Lyapunov and Riccati equations of discrete-time descriptor systems. *IEEE Transactions On Automatic Control* **44**(11) (1999) 2134–2139.

Stability Analysis for Stochastic Neural Networks with Markovian Switching and Infinite Delay in a Phase Space

B. Benaid [*], H. Bouzahir, C. Imzegouan and F. El Guezar

ISTI Lab, (1)ENSA PO Box 1136 and (2)FS PO Box 8106, Ibn Zohr University,
Agadir, Morocco

Abstract: This paper focuses on global stochastic (asymptotic) stability for a kind of stochastic neutral networks with infinite delay and Markovian switching in a fading memory phase space. Our approach is based on the Lyapunov method, stochastic analysis technique and M-matrix theory. The results complete some existing ones. Two examples are illustrated for demonstration of applicability and effectiveness of the proved theoretical theorems.

Keywords: *Markov chain; stochastic stability; neural networks; infinite delay; Lyapunov function.*

Mathematics Subject Classification (2010): 37Hxx, 37B25, 37C75.

1 Introduction

Recently, some interesting studies in the literature have been reported, such as stability of dynamical systems, especially stability of neural networks with Markovian switching and time delay [1–3, 6, 11, 18].

Thanks to the advantages given by neural networks (NNs) they have attracted much attention in these few recent years, and we have noted that the number of studies in that field has rised. NNs systems have witnessed successful applications in many areas such as securing communication systems, pattern recognition, signal processing, population dynamics systems, chemical process control and especially, in processing static images and combinatorial optimization [4]. All these applications are mainly related to the

---

* Corresponding author: `mailto:brahim.benaid@gmail.com`

dynamical behaviors of the considered systems and their NNs equilibrium points [5, 6, 12, 14].

Since time-delay assignment in neural networks can cause oscillation and instability behavior, so many researchers have been interested in the study of delay neural networks [15–17].

It is worth noting that NNs are often perturbed by various kinds of environmental noises, under which some properties of NNs may change. As mentioned in [12], environmental noises can turn a given stable system into an unstable, that is why, one can find many works that deal with stability of NNs disturbed by white noise. For example, in [25], the authors have discussed the exponential stability of a kind of NNs with white noise. They have set the sufficient conditions to guarantee stability of the considered system. Also, in [27], the authors have studied a stochastic NNs system with infinite delay, by means of Lyapunov method and It's formula. They have derived some sufficient conditions to ensure three types of stability. They have also shown that stochastic stability of the considered system with small noise is maintained if the NNs with infinite delay, is stable under some conditions. Recently, NNs with Markovian switching have been considered, because NNs with Markovian switching comprise general NNs as a special case [20–24]. For example, in [20], the authors have studied stability of a class of delayed NNs with Markovian switching in which the jumping parameters are determined by a continuous-time, and under some conditions, the *pth* moment exponential stability is ensured. They have provided a numerical example to validate the theoretical results. On the other hand, the work in [22] has dealt with stability of delayed stochastic NNs with Markovian switching. The authors have shown stability of the considered system and they have verified the founded results on three numerical examples.

To our best of knowledge, stability of stochastic Markovian switched NNs with infinite delay in a fading memory phase space is not fully investigated in the literature, which is the subject of our article.

Stimulated by the discussion of the studies mentioned above, our aim in this paper is to study a kind of stochastic Markovian switched NNs system with infinite delay in a fading memory phase space, considering white noise, infinite delay, and Markovian switching in such model. Firstly, the existence and uniqueness of solutions are shown. Secondly, by defining a Lyapunov Krasovskii functional, and using stochastic analysis technique and M-matrix theory, we give sufficient conditions to ensure three easily verified kinds of stochastic stability. These conditions are in terms of the coefficients of the system. Finally, two numerical examples are provided to test the proposed conditions and results.

This paper is organized as follows: we start by this introduction, then, in Section 2, we give the used notations in this paper and we define the model to study. After that, we introduce the definitions of three types of stochastic stability. In Section 3, existence and uniqueness of solutions for the studied system are established. Then, the three types of stochastic stability are discussed after styding existence and uniqueness. In Section 4, two numerical examples are given.

2 Preliminaries

For the sake of simplicity, we give the following notations of this paper. Write $\mathbb{R}$ for the set of real numbers and $\mathbb{R}^n$ for n dimensional Euclidean space. Denote $a \wedge b$ $(a \vee b)$ be the minimum (maximum) for $(a, b) \in \mathbb{R}^2$. For matrix A, its trace norm is defined

by $|A| = \left(Trace(A^T A)\right)^{\frac{1}{2}}$, with A^T its transpose. Let $C^\mu = \left\{\phi \in C((-\infty, 0]; \mathbb{R}^n) : \lim\limits_{\theta \to -\infty} e^{\mu\theta}\phi(\theta) \text{ exists in } \mathbb{R}^n\right\}$, with $\mu > 0$, denote the family of continuous functions ϕ defined on $(-\infty, 0]$ with norm $|\phi|_\mu = \sup\limits_{\theta \leq 0} e^{\mu\theta}|\phi(\theta)|$.

The process $x_t : (-\infty, 0] \longrightarrow \mathbb{R}^n; \theta \longmapsto x_t(\theta) = x(t + \theta); -\infty < \theta \leq 0$ can be regarded as a C^μ-value stochastic process, where $x_t(\theta) = (x_t^1(\theta), x_t^2(\theta), ..., x_t^n(\theta))^T$. The initial data of the stochastic process is defined on $(-\infty, 0]$. That is, the initial value is $x_0(\theta) = \xi(\theta)$ for $-\infty < \theta \leq 0$.

We define $C_\alpha^\mu \triangleq \{\phi \in C^\mu; |\phi|_\mu < \alpha\}$. Let G be a vector or matrix. By $G \geq 0$ we mean each element of G is non-negative. By $G > 0$ we mean $G \geq 0$ and at least one element of G is positive. By $G \gg 0$ we mean all elements of G are positive.

Let $(\Omega, \mathcal{F}, \mathfrak{F}, P)$ be a complete probability space with a filtration $\mathfrak{F} = \{\mathcal{F}_t\}_{t \geq 0}$ satisfying the usual conditions, and $W(.)$ be a Brownian motion defined on the space. The mathematical expectation with respect to the given probability measure P is denoted by $E(.)$. Let $r(t)$ be a right-continuous Markov chain on the probability space taking values in a finite state space $\mathcal{M} = \{1, 2, ..., N\}$ with the generator $\Gamma = (\gamma_{k\ell})_{N \times N}$ given by

$$P(r(t + \Delta t) = \ell/r(t) = k) = \begin{cases} \gamma_{k\ell}\Delta t + o(\Delta t), & k \neq \ell \\ 1 + \gamma_{kk}\Delta t + o(\Delta t), & \text{otherwise,} \end{cases}$$

where $\Delta t > 0$ and $\gamma_{k\ell} > 0$ is the transition rate from k to ℓ. If $k = \ell$, it follows $\gamma_{kk} = -\sum\limits_{\ell=1,\ell \neq k}^{N} \gamma_{k\ell}$. We also assume that Markov chain $r(t)$ is independent of Brownian motion $W(t)$, and it is irreducible in the sense that the system of equations

$$\begin{cases} \pi\Gamma = 0, \\ \pi\mathbb{1} = 1, \end{cases} \tag{1}$$

has a unique positive solution, where $\mathbb{1}$ is a column vector with all component being 1. The positive solution is termed a stationary distribution.

For any $M > 0$, define two random variables τ_M^y and τ_y^M as follows:

$$\tau_M^y = \inf\{t \geq t_0 : |y(t)| \geq M, |\xi|_\mu < M, a.s.\},$$

$$\tau_y^M = \inf\{t \geq t_0 : |y(t)| \leq M, |\xi|_\mu > M, a.s.\},$$

where $y : [0, +\infty) \times \Omega \longrightarrow \mathbb{R}$ is a continuous stochastic process. The general NNs with infinite delay can be described as Volterra integro-differential equations as follows:

$$\dot{u}(t) = -Du(t) + Ag(u(t)) + \int_{-\infty}^{t} CK^T(t - s)g(u(s))ds + J, \tag{2}$$

$$\dot{u}_i(t) = -d_i u_i(t) + \sum_{j=1}^{n} a_{ij}g_j(u_j(t)) + \sum_{j=1}^{n} c_{ij} \int_{-\infty}^{t} K_{ij}(t-s)g_j(u_j(s))ds + J_i, \quad i = 1, 2, ..., n, \tag{3}$$

where $u(t) = (u_1(t), u_2(t), ..., u_n(t))^T \in \mathbb{R}^n$ is the state vector associated with the neurons, $D = diag(d_1, d_2, ..., d_n) \gg 0$ is the firing rate of the neurons, $A = (a_{ij})_{n \times n}$ and $C = (c_{ij})_{n \times n}$ are connection weight matrices $J = (J_1, J_2, ..., J_n)^T$ is the constant external input vector, $g(u) = (g_1(u_1), g_2(u_2), ..., g_n(u_n))^T$ is the neuron activation function vector,

and $K_{ij} : [0, +\infty) \longrightarrow [0, +\infty)$ $(i, j = 1, 2, ..., n)$ are piecewise continuous on $[0, +\infty)$ satisfying

$$\int_0^{+\infty} K_{ij}(s)e^{\mu s}ds = \bar{K}. \qquad i, j = 1, 2, ..., n. \tag{4}$$

where $\bar{K}$ is a positive constant depending on μ.

As mentioned in Section 1, it is assumed that system (2) has an equilibrium point $u^* = (u_1^*, u_2^*, ..., u_n^*)$. The conditions, which guarantee that system (2) has a unique equilibrium point, can be found in [26]. By making a transformation $x(t) = u(t) - u^*$, system (2) can be rewritten as

$$\dot{x}(t) = -Dx(t) + AF(x(t)) + \int_{-\infty}^t CK^T(t-s)F(x(s))ds, \tag{5}$$

where $F(x(t)) = \left(g_1(x_1(t) + u_1^*), g_2(x_2(t) + u_2^*), ..., g_n(x_n(t) + u_n^*)\right)^T \triangleq \left(f_1(x_1(t)), f_2(x_2(t)), ..., f_n(x_n(t))\right)^t$. The main purpose of this paper is to study system (5) disturbed by white noise and Markovian switching, which, naturally, could be generalized into stochastic NNs with infinite delay and Markovian switching as follows:

$$dx(t) = \left[-Dx(t) + A(r(t))F(x(t)) + \int_{-\infty}^t C(r(t))K^T(t-s)F(x(s))ds\right]dt$$
$$+ B(r(t))Q(x(t))dW(t), \tag{6}$$

where $A(r(t)) = \left(a_{ij}(r(t))\right)_{n\times n}$, $C(r(t)) = \left(c_{ij}(r(t))\right)_{n\times n}$, $B(r(t)) = \left(b_{ij}(r(t))\right)_{n\times n}$ and $Q(x) = \left(q_1(x_1(t)), q_2(x_2(t)), ..., q_n(x_n(t))\right)^T$ represents the disturbance intensity of white noise satisfying $Q(0) = 0$.

For any $k \in \mathcal{M}$, system (6) can be regarded as the result of the n stochastic NNs with infinite delay

$$dx(t) = \left[-Dx(t) + A(k)F(x(t)) + \int_{-\infty}^t C(k)K^T(t-s)F(x(s))ds\right]dt + B(k)Q(x(t))dW(t), \tag{7}$$

switching from one to the others according to the movement of the Markov chain.

For any $(\phi, k) \in C^\mu \times \mathcal{M}$, we denote

$$\begin{cases} \mathbb{E}(\phi, k) = -D\phi(0) + A(k)F(\phi(0)) + \int_{-\infty}^t C(k)K^T(t-s)F(\phi(s-t))ds, \\ \mathbb{H}(\phi, k) = B(k)Q(\phi(0)). \end{cases}$$

Let $\mathcal{C}^{2,1}\left(\mathbb{R}^n \times \mathbb{R}_+ \times \mathcal{M}; \mathbb{R}_+\right)$ denote the family of all nonnegative functions $V(x, t, k)$ on $\mathbb{R}^n \times \mathbb{R}_+ \times \mathcal{M}$ which are continuously twice differentiable in x and one differentiable in t. If $V \in \mathcal{C}^{2,1}\left(\mathbb{R}^n \times \mathbb{R}_+ \times \mathcal{M}; \mathbb{R}_+\right)$, define an operator $\mathcal{L}V$ from $\mathbb{R}^n \times \mathbb{R}_+ \times \mathcal{M}$ to $\mathbb{R}$ by

$$\mathcal{L}V(x, t, k) = V_t(x, t, k) + V_x(x, t, k)\mathbb{E}(x_t, k) + \frac{1}{2}Trace\left[\mathbb{H}^T(x_t, k)V_{xx}(x, t, k)\mathbb{H}(x_t, k)\right]$$
$$+ \sum_{\ell=1}^N \gamma_{k\ell}V(x, t, \ell),$$

where

$$V_t(x, t, k) = \frac{\partial V(x, t, k)}{\partial t}, \quad V_x(x, t, k) = \left(\frac{\partial V(x, t, k)}{\partial x_1}, ..., \frac{\partial V(x, t, k)}{\partial x_n}\right)$$

and

$$V_{xx}(x,t,k) = \left(\frac{\partial^2 V(x,t,k)}{\partial x_i \partial x_j}\right)_{n \times n}.$$

In the sequel, we introduce the following concepts of stochastic stability.

Definition 2.1 [24]. The trivial solution of system (6) with initial data $x_{t_0} = \xi$ is said to be stochastically stable if for every pair $\varepsilon \in (0,1)$ and $\alpha > 0$, there exists a $\delta = \delta(\varepsilon, \alpha) > 0$ such that

$$P\big\{|x(t,t_0,\xi)| < \alpha, t \geq t_0\big\} \geq 1 - \varepsilon,$$

whenever $(\xi, k) \in C_\delta^\mu \times \mathcal{M}$.

Definition 2.2 [24]. The trivial solution of system (6) with initial data $x_{t_0} = \xi$ is said to be stochastically asymptotically stable if it is stochastically stable and, moreover, for every $\varepsilon \in (0,1)$, there exist $\delta_0 = \delta_0(\varepsilon) > 0$ such that

$$P\big\{\lim_{t\to\infty} x(t,t_0,\xi) = 0\big\} \geq 1 - \varepsilon,$$

whenever $(\xi, k) \in C_{\delta_0}^\mu \times \mathcal{M}$.

Definition 2.3 [24]. The trivial solution of system (6) with initial data $x_{t_0} = \xi$ is said to be globally stochastically asymptotically stable if it is stochastically stable and, moreover, for any $(\xi, k) \in C^\mu \times \mathcal{M}$,

$$P\big\{\lim_{t\to\infty} x(t,t_0,\xi) = 0\big\} = 1.$$

3   Main Results

In this section, we derive the criteria which are concerned with the three kinds of stochastic stability defined in Section 2 for the solution to system (6). The proof is based on the Lyapunov method, generalized It's formula, some inequalities, and M-matrix technique. Let us introduce first the following assumption.

Assumption 3.1 For each $j \in \{1, 2, ..., n\}$, functions $g_j : \mathbb{R} \longrightarrow \mathbb{R}$ and $q_j : \mathbb{R} \longrightarrow \mathbb{R}$ satisfy global Lipschitz conditions

$$|g_j(x) - g_j(y)| \vee |q_j(x) - q_j(y)| \leq L_j|x - y|, \quad \text{for} \quad x, y \in \mathbb{R}, \tag{8}$$

that is,

$$|F(x)| \vee |Q(x)| \leq L|x|, \tag{9}$$

where $L = \max\{L_1, L_2, ..., L_n\}$. In addition, the initial data $x_{t_0} = \xi$ satisfies $|\xi| := \sup_{\theta \leq 0} |\xi(\theta)| < \infty$.

Let us denote

$$\beta_k := -d + L|A(k)| + \frac{1}{2}L^2|B(k)|^2 + n^2\bar{K}L|C(k)|, \quad k \in \mathcal{M},$$

and $\mathcal{A} := -diag(2\beta_1, 2\beta_2, ..., 2\beta_n) - \Gamma$, where $d = \min\{d_1, d_2, ..., d_n\}$.

Now, we introduce an existence and uniqueness result for the solution of system (6). The steps of proof for this result are similar to the proof of Theorem 1 in [13].

Theorem 3.1 *Suppose that Assumption 3.1 holds. Then system (6) has a unique global solution on $(-\infty, \infty)$ with initial data $\xi \in C^\mu$ and $r(t_0) = r_0$.*

Proof. By definition of the right continuous Markov jump $r(.)$, there is a sequence $\{\tau_k\}_{k \geq 0}$ of stoping times such that $r(.)$ is a random constant on every interval $[\tau_k, \tau_{k+1})$, that is $r(t) = r(\tau_k)$ on $\tau_k \leq t < \tau_{k+1}$, for any $k \geq 0$. We proceed by induction. We consider first system (6) for $t \in [\tau_0, \tau_1)$

$$
\begin{aligned}
dx(t) &= \left[-Dx(t) + A(r_0)F(x(t)) + \int_{-\infty}^{t} C(r_0)K^T(t-s)F(x(s))ds \right]dt \\
&\quad + B(r_0)Q(x(t))dW(t) \\
&= \left[-Dx_t(0) + A(r_0)F(x_t(0)) + \int_{-\infty}^{t} C(r_0)K^T(t-s)F(x_t(s-t))ds \right]dt \\
&\quad + B(r_0)Q(x_t(0))dW(t).
\end{aligned}
\tag{10}
$$

By change of variable $v = t - s$, we get

$$
\begin{aligned}
dx(t) =& \left[-Dx_t(0) + A(r_0)F(x_t(0)) + \int_{0}^{+\infty} C(r_0)K^T(v)F(x_t(-v))dv \right]dt \\
&+ B(r_0)Q(x_t(0))dW(t).
\end{aligned}
$$

For any $\xi \in C^\mu$, let

$$
\begin{cases}
\mathbb{E}(\xi, r_0) = -D\xi(0) + A(r_0)F(\xi(0)) + \int_0^{+\infty} C(r_0)K^T(v)F(\xi(-v))dv, \\
\mathbb{H}(\xi, r_0) = B(r_0)Q(\xi(0)),
\end{cases}
\tag{11}
$$

then system (10) for $t \in [\tau_0, \tau_1)$ can be rewrite as

$$
dx(t) = \mathbb{E}(x_t, r_0)dt + \mathbb{H}(x_t, r_0)dW(t).
\tag{12}
$$

From (4), (9) and (11), we have

$$
\begin{aligned}
|\mathbb{E}(\xi, r_0) - \mathbb{E}(\zeta, r_0)| &\leq |D||\xi(0) - \zeta(0)| + |A(r_0)||F(\xi(0)) - F(\zeta(0))| \\
&\quad + \int_0^{+\infty} |C(r_0)K^T(v)||F(\xi(-v)) - F(\zeta(-v))|dv \\
&\leq |D||\xi(0) - \zeta(0)| + L|A(r_0)||\xi(0) - \zeta(0)| \\
&\quad + L\int_0^{+\infty} |C(r_0)||K^T(v)||\xi(-v) - \zeta(-v)|dv \\
&\leq |D||\xi(0) - \zeta(0)| + L|A(r_0)||\xi(0) - \zeta(0)| \\
&\quad + L\int_0^{+\infty} |C(r_0)||K^T(v)|e^{\mu v}e^{-\mu v}|\xi(-v) - \zeta(-v)|dv \\
&\leq \left(|D| + L|A(r_0)| + n^2 L|C(r_0)|\bar{K} \right)|\xi - \zeta|_\mu
\end{aligned}
$$

and

$$
|\mathbb{H}(\xi, r_0) - \mathbb{H}(\zeta, r_0)| \leq L|B(r_0)||\xi - \zeta|_\mu.
$$

By the main theorem in [7], system (10) with initial condition $\xi \in C^\mu$ and $r(t_0) = r_0$ has a unique solution on $[\tau_0, \tau_1)$.

If we consider system (10) for $t \in [\tau_1, \tau_2)$, then, (12) becomes

$$dx(t) = \mathbb{E}(x_t, r_1)dt + \mathbb{H}(x_t, r_1)dW(t). \tag{13}$$

By the same argument of existence and uniqueness as the first step above, system (6) with initial condition $x_{\tau_1} \in C^\mu$ and $r(\tau_1) = r_1$ has a unique solution on $[\tau_1, \tau_2)$.

By induction, system (6) with initial condition $\xi \in C^\mu$ and $r(0) = r_0$ has a unique solution on $(-\infty, \infty)$. Next, to show stochastic stability, we need to following assumption.

Assumption 3.2 There is a $\lambda = (\lambda_1, \lambda_2, ..., \lambda_N)^T \geq 0$ in $\mathbb{R}^N$ such that $P = \mathcal{A}\lambda \geq 0$.

Theorem 3.2 *Suppose that Assumptions 3.1 and 3.2 hold. Then the trivial solution to system (6) is stochastically stable.*

Proof. For any $\varepsilon \in (0,1)$ and $\alpha > 0$, we choose a sufficiently small $\delta = \delta(\varepsilon, \alpha) < \alpha$, such that for any $\xi \in C^\mu_{\delta(\varepsilon,\alpha)}$,

$$\lambda_k |\xi|^2_\mu + 2n^2 \bar{K} L |\xi|_\mu < \lambda_k \varepsilon \alpha^2 \text{ for any } k \in \mathcal{M}.$$

The choice of δ above is guaranteed by taking

$$\lambda_k \delta^2 + 2n^2 \bar{K} L \delta < \lambda_k \varepsilon \alpha^2 \text{ for any } k \in \mathcal{M}.$$

Fix any $\xi \in C^\mu_\delta$ and write $x(t) \triangleq x(t, t_0, \xi)$. For $t \geq t_0, \quad k = 1, 2, ..., N$, let

$$V(x, t, k) = \frac{1}{2} \lambda_k |x|^2 + \int_t^{+\infty} \sum_{i=1}^n \sum_{j=1}^n K_{ij}(s-t) |f_j(x_j(2t-s))| ds. \tag{14}$$

From Assumptions 3.1 and 3.2, we infer

$$\mathcal{L}V(x(t), t, k) \triangleq V_x(x, t, k) \Big[-Dx(t) + A(k)F(x(t)) + \int_{-\infty}^t C(k)K^T(t-s)F(x(s))ds \Big]$$

$$+ V_t(x, t, k) + \frac{1}{2} Trace \Big[(B(k)Q(x(t)))^T V_{xx}(x, t, k) (B(k)Q(x(t))) \Big]$$

$$+ \sum_{\ell=1}^N \gamma_{k\ell} V(x(t), t, \ell)$$

$$= \lambda_k x^T(t) \Big[-Dx(t) + A(k)F(x(t)) + \int_{-\infty}^t C(k)K^T(t-s)F(x(s))ds \Big]$$

$$- \sum_{i=1}^n \sum_{j=1}^n K_{ij}(0) |f_j(x_j(t))| + \frac{\lambda_k}{2} Trace \Big[(B(k)Q(x(t)))^T (B(k)Q(x(t))) \Big]$$

$$+ \sum_{\ell=1}^N \gamma_{k\ell} \Big[\frac{\lambda_\ell}{2} |x(t)|^2 + \int_t^{+\infty} \sum_{i=1}^n \sum_{j=1}^n K_{ij}(s-t) |f_j(x_j(2t-s))| ds \Big]$$

$$= -\lambda_k \sum_{i=1}^n d_i x_i^2(t) + \lambda_k \sum_{i=1}^n x_i(t) \sum_{j=1}^n a_{ij}(k) f_j(x_j(t))$$

$$+ \lambda_k \int_{-\infty}^{t} \sum_{i=1}^{n} x_i(t) \sum_{j=1}^{n} \sum_{\ell=1}^{n} c_{i\ell}(k) K_{\ell j}(t-s) f_j(x_j(s)) ds$$

$$- \sum_{i=1}^{n} \sum_{j=1}^{n} K_{ij}(0) |f_j(x_j(t))| + \frac{\lambda_k}{2} \sum_{i=1}^{n} \Big(\sum_{j=1}^{n} b_{ij}(k) q_j(x_j(t)) \Big)^2$$

$$+ \sum_{\ell=1}^{N} \gamma_{k\ell} \frac{\lambda_\ell}{2} |x(t)|^2$$

$$\leq -\lambda_k \sum_{i=1}^{n} d_i x_i^2(t) + \lambda_k \sum_{i=1}^{n} |x_i(t)| \sum_{j=1}^{n} L_j |a_{ij}(k)||x_j(t)|$$

$$+ \frac{\lambda_k}{2} \Big(\sum_{i=1}^{n} \sum_{j=1}^{n} b_{ij}^2(k) \Big) \sum_{j=1}^{n} q_j^2(x_j(t))$$

$$+ \lambda_k \int_{-\infty}^{t} \sum_{i=1}^{n} |x_i(t)| \sum_{j=1}^{n} \sum_{\ell=1}^{n} L_j K_{ij}(t-s) |c_{i\ell}(k)||x_j(s)| ds + \sum_{\ell=1}^{N} \gamma_{k\ell} \frac{\lambda_\ell}{2} |x(t)|^2.$$

By using the fact that $x(t) = x(t+0) = x_t(0)$ and the transformation $v = t - s$, one has

$$\mathcal{L}V(x(t), t, k) \leq -\lambda_k \sum_{i=1}^{n} d_i x_i^2(t) + \lambda_k L \Big(\sum_{i=1}^{n} \sum_{j=1}^{n} a_{ij}^2(k) \Big)^{\frac{1}{2}} \sum_{i=1}^{n} x_i^2(t)$$

$$+ \frac{\lambda_k}{2} L^2 \Big(\sum_{i=1}^{n} \sum_{j=1}^{n} b_{ij}^2(k) \Big) \sum_{i=1}^{n} x_i^2(t)$$

$$+ \lambda_k \int_{0}^{+\infty} \sum_{i=1}^{n} |x_t^i(0)| \sum_{j=1}^{n} \sum_{\ell=1}^{n} L_j K_{ij}(v) |c_{i\ell}(k)||x_t^j(-v)| dv + \sum_{\ell=1}^{N} \gamma_{k\ell} \frac{\lambda_\ell}{2} |x(t)|^2$$

$$\leq \lambda_k \Big[- \sum_{i=1}^{n} d_i |x_t^i(0)|^2 + L \Big(\sum_{i=1}^{n} \sum_{j=1}^{n} a_{ij}^2(k) \Big)^{\frac{1}{2}} \sum_{i=1}^{n} |x_t^i(0)|^2$$

$$+ \frac{L^2}{2} \Big(\sum_{i=1}^{n} \sum_{j=1}^{n} b_{ij}^2(k) \Big) \sum_{i=1}^{n} |x_t^i(0)|^2$$

$$+ |x_t|_\mu |C(k)| L \int_{0}^{+\infty} \sum_{i=1}^{n} \sum_{j=1}^{n} K_{ij}(v) e^{\mu v} e^{-\mu v} |x_t^j(-v)| dv \Big] + \sum_{\ell=1}^{N} \gamma_{k\ell} \frac{\lambda_\ell}{2} |x_t(0)|^2$$

$$\leq \lambda_k \Big[- d + L|A(k)| + \frac{1}{2} L^2 |B(k)|^2 + n^2 \bar{K} L |C(k)| \Big] |x_t|_\mu^2 + \sum_{\ell=1}^{N} \gamma_{k\ell} \frac{\lambda_\ell}{2} |x_t|_\mu^2$$

$$\leq \frac{1}{2} \Big(2\lambda_k \beta_k + \sum_{\ell=1}^{N} \gamma_{k\ell} \lambda_\ell \Big) |x_t|_\mu^2$$

$$\leq -\frac{1}{2} p_k |x_t|_\mu^2.$$

Thus, by use of It's generalized formula, for any $t \geq t_0$,

$$EV(x(t \wedge \tau_x^\alpha), t \wedge \tau_x^\alpha, k) = EV(x(t_0), t_0, k) + E \int_{t_0}^{t \wedge \tau_x^\alpha} \mathcal{L}V(x(s), s, r(s)) ds$$

$$= EV(\xi(0), t_0, k) + E \int_{t_0}^{t \wedge \tau_x^\alpha} \mathcal{L}V(x(s), s, r(s))ds$$

$$\leq EV(\xi(0), t_0, k).$$

Besides, by use of Assumption 3.1 and Eq. (4) we obtain

$$EV(x(t_0), t_0, k) = E\Big(\frac{\lambda_k}{2} \sum_{i=1}^{n} x_i^2(t_0)\Big) + E\Big(\int_{t_0}^{+\infty} \sum_{i=1}^{n} \sum_{j=1}^{n} K_{ij}(s - t_0)|f_j(x_j(2t_0 - s))|ds\Big)$$

$$\leq \frac{\lambda_k}{2} E|\xi|_\mu^2 + E \int_0^{+\infty} \sum_{i=1}^{n} \sum_{j=1}^{n} K_{ij}(v)|f_j(x_{t_0 j}(-v))|dv$$

$$\leq \frac{\lambda_k}{2} E|\xi|_\mu^2 + n^2 \bar{K} L E|\xi|_\mu.$$

We also have

$$V(x(t \wedge \tau_x^\alpha), t \wedge \tau_x^\alpha, k) \geq \frac{\lambda_k}{2}|x(t \wedge \tau_x^\alpha)|^2$$

$$E\big[\mathbb{1}_{\{\tau_x^\alpha < t\}} V(x(t \wedge \tau_x^\alpha), t \wedge \tau_x^\alpha, k)\big] \geq E\big[\mathbb{1}_{\{\tau_x^\alpha < t\}} V(x(\tau_x^\alpha), \tau_x^\alpha, k)\big]$$

$$\geq \frac{\lambda_k}{2} E\big[\mathbb{1}_{\{\tau_x^\alpha < t\}} |x(\tau_x^\alpha)|^2\big]$$

$$\geq \frac{\lambda_k}{2}\alpha^2 E\big[\mathbb{1}_{\{\tau_x^\alpha < t\}}\big] = \frac{\lambda_k}{2}\alpha^2 P(\tau_x^\alpha < t).$$

Consequently,

$$\frac{\lambda_k \alpha^2}{2} P\{\tau_x^\alpha < t\} \leq E\big(\mathbb{1}_{\{\tau_x^\alpha < t\}} V(x(\tau_x^\alpha), \tau_x^\alpha, k)\big)$$

$$\leq EV(x(t \wedge \tau_x^\alpha), t \wedge \tau_x^\alpha, k)$$

$$\leq \frac{\lambda_k}{2}|\xi|_\mu^2 + n^2 \bar{K} L|\xi|_\mu$$

$$< \frac{\lambda_k}{2}\varepsilon\alpha^2,$$

gives

$$P\{\tau_x^\alpha < t\} < \varepsilon.$$

Letting $t \longrightarrow \infty$ we have $P\{\tau_x^\alpha < \infty\} < \varepsilon$, which is equivalent to

$$P\{|x(t, t_0, \xi)| \leq \alpha, t \geq t_0\} \geq 1 - \varepsilon. \tag{15}$$

This completes the proof.

For stochastic asymptotic stability and global stochastic asymptotic stability, we add the following assumption.

Assumption 3.3 If $\mathcal{A}$ is a nonsingular M-matrix, there is a $\lambda = (\lambda_1, \lambda_2, ..., \lambda_N)^T \gg$ 0 in $\mathbb{R}^N$ such that $P = \mathcal{A}\lambda \gg 0$.

For further properties on M-matrices, we refer the readers to Chapter 2 of [24].

Theorem 3.3 *Suppose that Assumptions 3.1 and 3.3 hold. Then the trivial solution of system (6) is stochastically asymptotically stable.*

Idea of proof:
The proof is similar to the one in [13]. The only differences are

- Inequality (17) in [13] becomes: For δ_1 and any $\varepsilon_1 \in (0,1)$, there exists a $H(\varepsilon_1, \delta)$ sufficiently large such that

$$P\{|x(t, \theta^*, \xi_{\theta^*})| \leq H, t \geq \theta^*\} \geq 1 - \frac{\varepsilon_1}{4}, \quad \text{and} \quad P\{|x_{\theta^*}|_\mu < H, \theta^* \leq t\} = 1.$$

- Inequality before (20) in [13] becomes

$$\bar{K} < \frac{(\lambda_k \alpha)^2}{2n^2 LH}.$$

- In a slightly different way as in [13], we define the Lyapunov function by

$$V(x, t, k) = \frac{\lambda_k}{2} \sum_{i=1}^{n} x_i^2 + \int_t^{+\infty} \sum_{i=1}^{n} \sum_{j=1}^{n} K_{ij}(s-t)|f_j(x_j(2t-s))|ds.$$

Theorem 3.4 *Suppose that Assumptions 3.1 and 3.3 hold. Then the trivial solution of system (6) is globally stochastically asymptotically stable.*

We omit this proof because it is very similar to the equivalent one in [13].

4   Applications

Two examples are given. In the first example, we consider system (6) on $\mathbb{R}^3$ and the Markov process $r(t)$ is switching between two subsystems. In the second example, we define system (6) on $\mathbb{R}^2$ and the Markov process $r(t)$ switches between tree subsystems.

Example 4.1 Let $r(t)$ be a right-continuous Markovian chain taking values in $\mathcal{M} = \{1, 2\}$ with generator

$$\Gamma = (\gamma_{ij})_{2 \times 2} = \begin{pmatrix} -1 & 1 \\ 3 & -3 \end{pmatrix}.$$

Consider a three dimensional system of type (6) with the following specifications

$$D = \begin{pmatrix} 12 & 0 & 0 \\ 0 & 12 & 0 \\ 0 & 0 & 12 \end{pmatrix}, \quad A(1) = \begin{pmatrix} 1.5 & 0.5 & 0.5 \\ 0.5 & 0.5 & 0.25 \\ 0.5 & 0.5 & 0.5 \end{pmatrix},$$

$$B(1) = \begin{pmatrix} 1 & 0 & 0 \\ 0 & 1 & 0 \\ 0 & 0 & 1 \end{pmatrix}, \quad C(1) = \begin{pmatrix} 0.25 & 0 & 0 \\ 0 & 0.3 & 0 \\ 0 & 0 & 0.2 \end{pmatrix},$$

$$A(2) = \begin{pmatrix} 0.5 & 0.5 & 0.5 \\ 0.8 & 0.5 & 0.5 \\ 0.25 & 0.25 & 0.5 \end{pmatrix}, \quad B(2) = \begin{pmatrix} 1 & 0 & 0 \\ 0 & 1 & 0 \\ 0 & 0 & 1 \end{pmatrix}, \quad C(2) = \begin{pmatrix} 0.2 & 0 & 0 \\ 0 & 0.2 & 0 \\ 0 & 0 & 0.4 \end{pmatrix}.$$

We rewrite System (6) in the following detailed form

$$
\begin{cases}
dx(t) &= \big[-12x(t) + a_{11}(r(t))f(x(t)) + a_{12}(r(t))f(y(t)) + a_{13}(r(t))f(z(t)) \\
& \quad + \int_{-\infty}^{t} c_{11}(r(t))e^{s-t}(f(x(s)) + f(y(s)) + f(z(s)))ds \big]dt + b_{11}(r(t))\sin x(t)dW(t), \\
dy(t) &= big\big[-12y(t) + a_{21}(r(t))f(x(t)) + a_{22}(r(t))f(y(t)) + a_{23}(r(t))f(z(t)) \\
& \quad + \int_{-\infty}^{t} c_{22}(r(t))e^{s-2t}(f(x(s)) + f(y(s)) + f(z(s)))ds \big]dt + b_{22}(r(t))\sin y(t)dW(t), \\
dz(t) &= \big[-12z(t) + a_{31}(r(t))f(x(t)) + a_{32}(r(t))f(y(t)) + a_{33}(r(t))f(z(t)) \\
& \quad + \int_{-\infty}^{t} c_{33}(r(t))e^{s-t}(f(x(s)) + f(y(s)) + f(z(s)))ds \big]dt + b_{33}(r(t))\sin z(t)dW(t),
\end{cases}
\tag{16}
$$

where $f(x)$ satisfies a global Lipschitz condition with a Lipschitz constant $L = 1$. We choose $f(x) = x$.

In order to get the conditions of Theorem 3.4

a) We take $q_j(x) = \sin x, j = 1, 2, 3$. Then Assumption 3.1 holds.

b) We choose $K(t - s) = e^{s-t}$. Then, $\bar{K} = \frac{1}{1-\mu}$ for $0 < \mu < 1$.

c) For $\mu = 0.5$, we can see that $\beta_1 = -0.5870$ and $\beta_2 = -0.1768$, so $\mathcal{A} = \begin{pmatrix} 2.1739 & -1.000 \\ -3.000 & 3.3537 \end{pmatrix}$,

which implies immediately that Assumption 3.3 is satisfied. By Theorem 3.4, the trivial solution to System (16) is globally stochastically asymptotically stable.

Figure 1 shows the way of randomly switching between the two subsystems with initial condition $r(0) = 1$. Figure 2 shows trajectory of the stochastic approximate solution for system (16) with initial condition $x(t) = \sin^2(t), y(t) = 0.5\cos^2(t), z(t) = 0$.
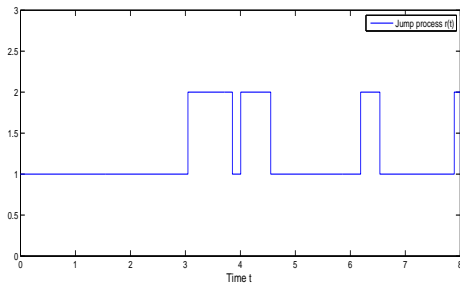
Figure 1: Jump process r(t) with initial condition r(0)=1.
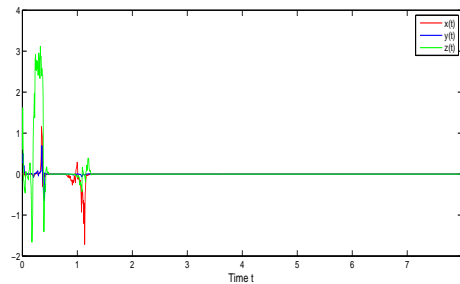
Figure 2: Approximate solution of system (16).

Example 4.2 Let $r(t)$ be a right-continuous Markovian chain taking values in $\mathcal{M} = \{1, 2, 3\}$ with generator

$$
\Gamma = (\gamma_{ij})_{3\times 3} = \begin{pmatrix} -2 & 1 & 1 \\ 2 & -4 & 2 \\ 3 & 2 & -5 \end{pmatrix}.
$$

Consider a two-dimensional System (6) with the following specification

$$
D = \begin{pmatrix} 15 & 0 \\ 0 & 15 \end{pmatrix}, \quad A(1) = \begin{pmatrix} 2 & 1 \\ 1 & 1.5 \end{pmatrix}, \quad B(1) = \begin{pmatrix} 1 & 0 \\ 0 & 1 \end{pmatrix} \quad C(1) = \begin{pmatrix} 0.5 & 0 \\ 0 & \sqrt{2,} \end{pmatrix},
$$

$$A(2) = \begin{pmatrix} 2 & 0.5 \\ 0.3 & 0.8 \end{pmatrix} \quad B(2) = \begin{pmatrix} \sqrt{0.2} & 0 \\ 0 & \sqrt{0.2} \end{pmatrix}, \quad C(2) = \begin{pmatrix} 1 & 0 \\ 0 & \sqrt{2}\sqrt{2} \end{pmatrix}.$$

$$A(3) = \begin{pmatrix} 2 & 0.25 \\ 0.25 & 0.5 \end{pmatrix}, \quad B(3) = \begin{pmatrix} 1 & 0 \\ 0 & 1 \end{pmatrix}, \quad C(3) = \begin{pmatrix} 0.3 & 0 \\ 0 & 0.5, \end{pmatrix}.$$

We rewrite system (6) in the following detailed form

$$\begin{cases} dx(t) &= \big[-15x(t) + a_{11}(r(t))h(x(t)) + a_{12}(r(t))y(t) \\ &\quad + \int_{-\infty}^{t} c_{11}(r(t))e^{s-t}(h(x(s)) + h(y(s)))ds \big]dt + b_{11}(r(t))q_1(x(t))dW(t), \\ dy(t) &= \big[-15x(t) + a_{21}(r(t))h(x(t)) + a_{22}(r(t))y(t) \\ &\quad + \int_{-\infty}^{t} c_{22}(r(t))e^{s-t}(h(x(s)) + h(y(s)))ds \big]dt + b_{22}(r(t))q_2(x(t))dW(t), \end{cases} \quad (17)$$

where $q_1(x) = q_2(x) = \sin x$ satisfy a global Lipschitz condition with Lipschitz constant $L = 1, h(x) = \sin x$. This means that Assumption 3.1 is verified. To assure Assumption 3.3, let $\mu = 0.4$. Then, we can see that $\beta_1 = -1.1277, \beta_2 = -1.0214$ and $\beta_3 = -8.0210$. So

$$\mathcal{A} = \begin{pmatrix} +4.2554 & -1.000 & -1.0000 \\ -2.0000 & +6.0428 & -2.0000 \\ -3.0000 & -2.0000 & 21.0421 \end{pmatrix}.$$

Hence, it is guaranteed that $\mathcal{A}$ is a nonsingular M-matrix. By Theorem 3.4, System (17) is globally asymptotically stochastic stable.

Figure 3 shows a way of random switching between the three subsystems with initial condition $r(0) = 1$. Figure 4 depicts the stochastic approximate solution for System (17) with initial condition $x(t) = \sin^2(t), y(t) = 0.6$.
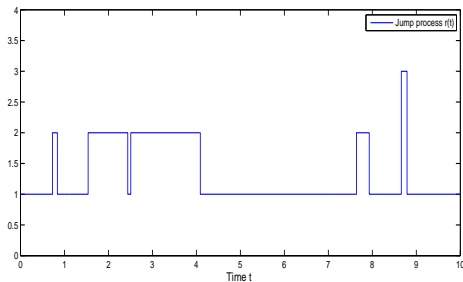
Figure 3: Jump process r(t) with initial condition r(0)=1.
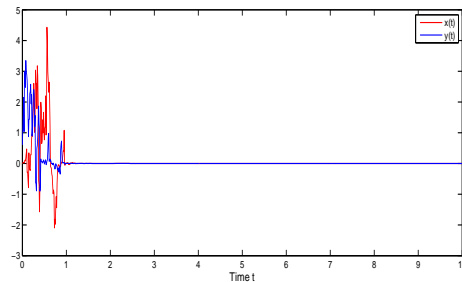

Figure 4: Approximate solution of System (17).

5   Conclusion

We have provided the existence and uniqueness of solutions for a kind of NNs with Markovian switching. Basing on the Lyapunov method and stochastic analysis and M-matrix theory, we have given the new conditions that ensure stochastic stability, stochastic asymptotic stability and global stochastic asymptotic stability of neural networks with Markovian switching and infinite time delay in a phase space. Two simulated numerical examples under Matlab have been presented to validate the proposed conditions.

We notice that the stability of the system depends also on the positive number μ associated to the phase space. Also the theoretical outcome in this paper can be applied to many complex systems and other NNs, such as the processing of motion related phenomena.

References

[1] A. Yu. Aleksandrov, E. B. Aleksandrova, P. A. Lakrisenko, A. V. Platonov and Y. Chen. Asymptotic stability conditions for some classes of mechanical systems with switched nonlinear force fields. *Nonlinear Dynamics and Systems Theory* **15** (2) (2015) 127–140.

[2] A. Yu. Aleksandrov, A. A. Martynyuk and A. V. Platonov. Dwell time stability analysis for nonlinear switched difference systems. *Nonlinear Dynamics and Systems Theory* **16** (3) (2016) 221–234.

[3] A. Yu. Aleksandrov, E. B. Aleksandrova, A. V. Platonov and M. V. Voloshin. On the global asymptotic stability of a class of nonlinear switched systems. *Nonlinear Dynamics and Systems Theory* **17** (2) (2017) 107–120.

[4] J.J. Hopfield. Neural networks and physical systems with emergent collect computational abilities. *Proc. Natl. Acad. Sci. USA* **79** (2) (1982) 2554–2558.

[5] S. Arik, V. Tavsanoglu. Absolute stability of nonsymmetric neural networks. *IEEE Trans. Circuits Syst.* **3** (3) (1996) 441–444.

[6] S. Arik, V. Tavsanoglu, Equilibrium analysis of delayed CNNs. *IEEE Trans. Circuits Syst.* **45** (2) (1998) 168–171.

[7] H. Bouzahir, B. Benaid and C. Imzegouan. Some stochastic functional differential equations with infinite delay: A result on existence and uniqueness of solutions in a concrete fading memory space. *Chin. J. Math.* (2017).

[8] H. Bouzahir, H. You, R. Yuan. Global attractor for some partial functional differential equations with infinite delay. *Funkcialaj Ekvacioj.* **54** (1) (1989) 139–156.

[9] F. El Guezar, H. Bouzahir, D. Fournier-Prunaret. Event detection occurrence for planar piece-wise affine hybrid systems. *Nonlinear Anal. Hybrid Syst.* **5** 4 (2011) 626–638.

[10] C. Imzegouan, H. Bouzahir, B. Benaid and F. El Guezar. A note on Exponential Stochastic Stability of Markovian Switching Systems. *International Journal of Evolution Equations.* **10** (2) (2016) 189–198.

[11] C. Imzegouan. Stochastic stablity in terms of an associated transfer function matrix for some hybrid systems with Markovian switching. *Commun. Fac. Sci. Univ. Ank. Series A1* **67** (1) (2018) 198–210.

[12] C. Imzegouan. Stability for Markovian switching stochastic neural networks with infinite delay driven by Lvy noise. *International Journal of Dynamics and Control* **6** (2018) 1–10.

[13] Y. Guo, H. Su, X. Ding and K. Wang. Global stochastic stability analysis for stochastic neural networks with infinite delay and Markovian switching. *Applied Mathematics and Computation.* **245** (2014) 53–65.

[14] Ju H. Park. A new stability analysis of delayed cellular neural networks. *Appl. Math. Comput.* **181** (2006) 200–205.

[15] C. M. Marcus, R. M. Westervelt. Stability of analog neural networks with delays. *Phys. Rev. A* **39** (1) (1989) 347–359.

[16] Z. Wang, H. Shu, J. Fang, X. Liu. Robust stability for stochastic Hopfield neural networks with time delays. *Nonlinear Anal. Real World Appl.* **7** (2006) 1119–1128.

[17] S. Arik. An analysis of exponential stability of delayed neural networks with time varying delays. *Neural Networks* **17** (2004) 1027–1031.

[18] Q. Song, Design of controller on synchronization of chaotic neural networks with mixed time-varying delays. *Neurocomputing* **72** (2009) 3288–3295.

[19] F. Wei, K. Wang. The existence and uniqueness of the solution for stochastic functional differential equations with infinite delay. *J. Math. Anal. Appl.* **331** (2007) 516–531.

[20] Q. Zhu, J. Cao, pth moment exponential synchronization for stochastic delayed Cohen-Grossberg neural networks with Markovian switching. *Nonlinear Dyn.* **67** (2012) 829–845.

[21] H. Huang, D.W.C. Ho, Y. Qu. Robust stability of stochastic delayed additive neural networks with Markovian switching. *Neural Networks* **20** (2007) 799–809.

[22] H. Huang, T. Huang, X. Chen. Global exponential estimates of delayed stochastic neural networks with Markovian switching. *Neural Networks* **36** (2012) 136–145.

[23] S. Zhu, Y. Shen. Robustness analysis of global exponential stability of neural networks with Markovian switching in the presence of time-varying delays or noises. *Neural Comput. Appl.* **23** (2013) 1563–1571.

[24] X. Mao, C. Yuan. *Stochastic Differential Equations with Markovian Switching.* Imperial College Press, London, 2006.

[25] X. Li, J. Cao. Exponential stability of stochastic CohenGrossberg neural networks with time-varying delays. In: *Second International Symposium on Neural Networks* **1** (1), (2005) 162–167.

[26] Z. Zhang, X. Jin, W. Zhang, Global stability analysis in dynamical neural networks with distributed time delays. *IEEE, Circuits and Systems and West Sino Exposition Proceedings* **2** (2), 2002, pp. 1662–1665.

[27] H. Su, W. Li, K. Wang, X. Ding. Stability analysis for stochastic neural network with infinite delay. *Neurocomputing* **74** (2011) 1535–1540.

Exact Solutions of a Klein-Gordon System by (G'/G)-Expansion Method and Weierstrass Elliptic Function Method

M. Al Ghabshi [1], E.V. Krishnan [2*] and M. Alquran [3]

[1] *Visiting Consultant, Department of Mathematics, Sultan Qaboos University,*
PO Box 36, Al Khod 123, Muscat, Sultanate of Oman
[2] *Department of Mathematics, Sultan Qaboos University,*
PO Box 36, Al Khod 123, Muscat, Sultanate of Oman
[3] *Department of Mathematics and Statistics, Jordan University of Science and Technology,*
P.O. Box (3030), Irbid (22110), Jordan

Abstract: This paper deals with the exact solutions of a Klein-Gordon system of equations. The (G'/G)-expansion method has been employed to derive kink solutions, solitary wave solutions and singular solutions. Solitary wave solutions have also been derived for the Klein-Gordon system using the Weierstrass elliptic function method.

Keywords: (G'/G)-expansion method; Klein-Gordon equation; solitary wave solutions; Weierstrass elliptic function.

Mathematics Subject Classification (2010): 74J35, 34G20, 93C10.

1 Introduction

The nonlinear evolution equations (NLEEs) are the most important fields of research in applied mathematics and theoretical physics. There are several forms of NLEEs that arise in various branches of science and engineering [1–5]. Exact solutions of NLEEs play an important role as they provide a better insight into the various aspects of the problem which leads to significant applications. Several methods such as the tanh method [6–11], exponential function method [12], Jacobi elliptic function (JEF) method [13–15], mapping methods [16–21] have been applied in the last few decades and the results have been reported. Also, many physical phenomena have been governed by systems of

---

* Corresponding author: `mailto:drkrish52@gmail.com`

partial differential equations (PDEs) and there have been significant contributions in this area [22, 23].

In this paper, we use the (G'/G)-expansion method [24–28] to find some exact solutions for a coupled Klein-Gordon equation [29]. The paper is organized as follows. In Section 2, we give a mathematical analysis of the (G'/G)-expansion method, in Section 3, we derive solitary wave solutions (SWSs) and kink solutions to the nonlinear Klein-Gordon system, in Section 4, we use the Weierstrass elliptic function (WEF) method [30] to derive SWSs of the Klein-Gordon system of equations, in Section 5 we write down the conclusion.

2 (G'/G)-Expansion Method

Consider the nonlinear partial differential equation (PDE)

$$P(u, u_t, u_x, u_{tt}, u_{xt}, u_{xx}, ...) = 0, \tag{1}$$

where $u(x,t)$ is an unknown function, P is a polynomial in $u = u(x,t)$ and its various partial derivatives. The traveling wave variable $\xi = x - ct$ reduces the PDE (1) to the ordinary differential equation (ODE)

$$P(u, -cu', u', -c^2u'', -cu'', u'', ...) = o, \tag{2}$$

where $u = u(\xi)$ and $'$ denotes differentiation with respect to ξ.

We suppose that the solution of equation (2) can be expressed by a polynomial in $\left(\dfrac{G'}{G}\right)$ as follows:

$$u(\xi) = \sum_{i=0}^{m} a_i \left(\frac{G'}{G}\right)^i, \ a_m \neq 0, \tag{3}$$

where $a_i (i = 0, 1, 2, ..)$ are constants. Here, G satisfies the second order linear ODE

$$G''(\xi) + \lambda G'(\xi) + \mu G(\xi) = 0 \tag{4}$$

with λ and μ being constants. The positive integer m can be determined by a balance between the highest order derivative term and the nonlinear term appearing in equation (2). By substituting equation (3) into equation (2) and using equation (4), we get a polynomial in G'/G. The coefficients of various powers of G'/G give rise to a set of algebraic equations for a_i $(i = 0, 1, 2, ..., m)$, λ and μ.

The general solution of equation (4) is a linear combination of sinh and cosh or of sine and cosine functions if $\Delta = \lambda^2 - 4\mu > 0$ or $\Delta = \lambda^2 - 4\mu < 0$, respectively. In this paper we consider only the first case and so,

$$G(\xi) = e^{-\lambda\xi/2}\left(C_1 \sinh(\frac{\sqrt{\lambda^2-4\mu}}{2}\xi) + C_2 \cosh(\frac{\sqrt{\lambda^2-4\mu}}{2}\xi)\right), \tag{5}$$

where C_1 and C_2 are arbitrary constants.

3 Klein-Gordon System of Equations

Consider the Klein-Gordon system of equations

$$u_{xx} - u_{tt} - u - 2u^3 - 2uv = 0, \tag{6}$$

$$v_x - v_t - 4uu_t = 0. \tag{7}$$

We seek TWSs of equations (6) and (7) in the form $u = u(\xi), \quad v = v(\xi), \quad \xi = x - ct.$
Then equations (6) and (7) give

$$(1 - c^2)u'' - u - 2u^3 - 2uv = 0, \tag{8}$$

$$v' + cv' + 4cuu' = 0. \tag{9}$$

Integrating equation (9) with respect to ξ and using the solitary wave boundary conditions, we get

$$v = -\frac{2c}{1 + c}u^2. \tag{10}$$

Substituting for v into equation (8), we obtain

$$(1 - c)(1 + c)^2 u'' - (1 + c)u - 2(1 - c)u^3 = 0. \tag{11}$$

Assuming the expansion $u(\xi) = \sum_{i=0}^{m} a_i \left(\frac{G'}{G}\right)^i, \; a_m \neq 0$ in equation (11) and balancing
the nonlinear term and the derivative term, we get $m + 2 = 3m$ so that $m = 1$.

So, we assume a solution of equation (11) in the form

$$u(\xi) = a_0 + a_1 \left(\frac{G'}{G}\right), \; a_1 \neq 0. \tag{12}$$

So, we can obtain

$$u'(\xi) = -a_1 \left(\frac{G'}{G}\right)^2 - \lambda a_1 \left(\frac{G'}{G}\right) - \mu a_1, \tag{13}$$

$$u''(\xi) = 2a_1 \left(\frac{G'}{G}\right)^3 + 3a_1\lambda \left(\frac{G'}{G}\right)^2 + (a_1\lambda^2 + 2a_1\mu) \left(\frac{G'}{G}\right) + a_1\lambda\mu, \tag{14}$$

$$u^3(\xi) = a_1^3 \left(\frac{G'}{G}\right)^3 + 3a_0 a_1^2 \left(\frac{G'}{G}\right)^2 + 3a_0^2 a_1 \left(\frac{G'}{G}\right) + a_0^3. \tag{15}$$

Now, substituting equations (12), (14) and (15) into equation (11) and collecting the
coefficients of $\left(\frac{G'}{G}\right)^i, i = 0, 1, 2, 3$, we get

$$(1 - c)(1 + c)^2 a_1\lambda\mu - (1 + c)a_0 - 2(1 - c)a_0^3 = 0, \tag{16}$$

$$a_1(1-c)(1+c)^2(\lambda^2 + 2\mu) - (1+c)a_1 - 6(1-c)a_0^2 a_1 = 0, \tag{17}$$

$$3a_1\lambda(1-c)(1+c)^2 - 6a_0 a_1^2(1-c) = 0, \tag{18}$$

$$2(1-c)(1+c)^2 a_1 - 2(1-c)a_1^3 = 0. \tag{19}$$

From equation (19), we get

$$a_1 = \pm(1+c). \tag{20}$$

Equation (18) leads us to

$$a_0 = \pm\frac{\lambda}{2}(1+c) = \frac{\lambda}{2}a_1. \tag{21}$$

When $\mu = 0$ in equation (17), we get $\lambda = \pm\sqrt{\dfrac{2}{c^2-1}}$ and when $\lambda = 0$, we get $\mu = \dfrac{1}{2(1-c^2)}$. In both cases, $\Delta = \lambda^2 - 4\mu = \dfrac{2}{c^2-1}$.

Equation (17) is identically satisfied in both cases without any constraints on the coefficients of the governing equation.

Case 1: $\mu = 0$, $\lambda = \sqrt{\dfrac{2}{c^2-1}}$,

$$u_1(x,t) = \pm\sqrt{-\frac{1+c}{2(1-c)}}\left(1 + \frac{(C_1 - C_2)(1 - \tanh\frac{1}{2}\sqrt{\frac{2}{c^2-1}}(x-ct))}{C_1\tanh\frac{1}{2}\sqrt{\frac{2}{c^2-1}}(x-ct) + C_2}\right), \tag{22}$$

$$v_1(x,t) = \frac{c}{1-c}\left(1 + \frac{(C_1 - C_2)(1 - \tanh\frac{1}{2}\sqrt{\frac{2}{c^2-1}}(x-ct))}{C_1\tanh\frac{1}{2}\sqrt{\frac{2}{c^2-1}}(x-ct) + C_2}\right)^2. \tag{23}$$

Here, $C_1 \neq \pm C_2$ and $c > 1$.

Figure 1 and Figure 2 represent the solutions given by equations (22) and (23), respectively.

Case 2: $\mu = 0$, $\lambda = -\sqrt{\dfrac{2}{c^2-1}}$,

$$u_2(x,t) = \pm\sqrt{-\frac{1+c}{2(1-c)}}\left(1 + \frac{(C_1 + C_2)(1 - \tanh\frac{1}{2}\sqrt{\frac{2}{c^2-1}}(x-ct))}{C_2 - C_1\tanh\frac{1}{2}\sqrt{\frac{2}{c^2-1}}(x-ct)}\right), \tag{24}$$

$$v_2(x,t) = \frac{c}{1-c}\left(1 + \frac{(C_1 + C_2)(1 - \tanh\frac{1}{2}\sqrt{\frac{2}{c^2-1}}(x-ct))}{C_2 - C_1\tanh\frac{1}{2}\sqrt{\frac{2}{c^2-1}}(x-ct)}\right)^2. \tag{25}$$
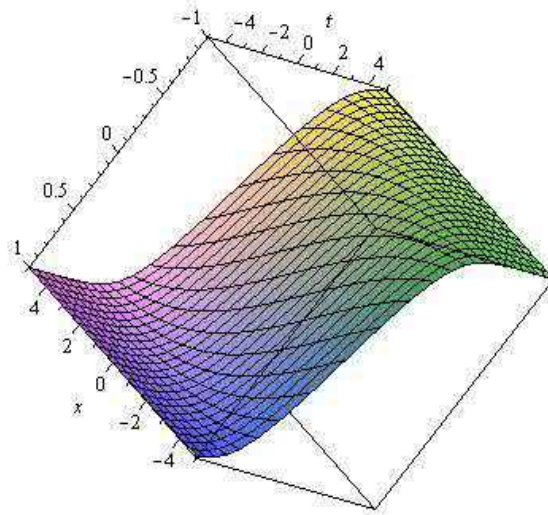
Figure 1: The solution for $u_1(x,t)$, $c = 3, C_1 = 0, C_2 = 1$.
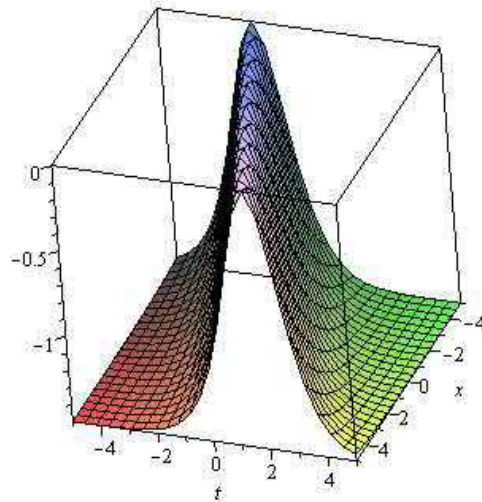
Figure 2: The solution for $v_1(x,t)$, $c = 3, C_1 = 0, C_2 = 1$.

Here also, $C_1 \neq \pm C_2$ and $c > 1$.

Case 3: $\lambda = 0$, $\mu = \dfrac{1}{2(1 - c^2)}$,

$$u_3(x, t) = \pm \sqrt{-\frac{1 + c}{2(1 - c)}} \left(\frac{C_1 + C_2 \tanh \frac{1}{2} \sqrt{\frac{2}{c^2 - 1}} \xi}{C_1 \tanh \frac{1}{2} \sqrt{\frac{2}{c^2 - 1}} \xi + C_2} \right), \tag{26}$$

$$v_3(x, t) = \frac{c}{1 - c} \left(\frac{C_1 + C_2 \tanh \frac{1}{2} \sqrt{\frac{2}{c^2 - 1}} \xi}{C_1 \tanh \frac{1}{2} \sqrt{\frac{2}{c^2 - 1}} \xi + C_2} \right)^2. \tag{27}$$

In this case also, we have the same restrictions on c, C_1 and C_2.

4   Weierstrass Elliptic Function Solutions of Klein-Gordon Equation

The Weierstrass elliptic function (WEF) $\wp(\xi; g_2, g_3)$ with invariants g_2 and g_3 satisfy

$$\wp'^2 = 4\wp^3 - g_2 \wp - g_3, \tag{28}$$

where g_2 and g_3 are related by the inequality

$$g_2^3 - 27 g_3^2 > 0. \tag{29}$$

The WEF $\wp(\xi)$ is related to the JEFs by the following relations:

$$\mathrm{sn}(\xi) = [\wp(\xi) - e_3]^{-1/2}, \tag{30}$$

$$\mathrm{cn}(\xi) = \left[\frac{\wp(\xi) - e_1}{\wp(\xi) - e_3} \right]^{1/2}, \tag{31}$$

$$\mathrm{dn}(\xi) = \left[\frac{\wp(\xi) - e_2}{\wp(\xi) - e_3} \right]^{1/2}, \tag{32}$$

where e_1, e_2, e_3 satisfy

$$4z^3 - g_2 z - g_3 = 0 \tag{33}$$

with

$$e_1 = \frac{1}{3}(2 - m^2), \ \ e_2 = \frac{1}{3}(2m^2 - 1), \ \ e_3 = -\frac{1}{3}(1 + m^2). \tag{34}$$

From equation (34), one can see that the modulus m of the JEF and the $e's$ of the WEF are related by

$$m^2 = \frac{e_2 - e_3}{e_1 - e_3}. \tag{35}$$

We consider the ODE of order $2k$ given by

$$\frac{d^{2k}\phi}{d\xi^{2k}} = f(\phi; r+1),$$ (36)

where $f(\phi; r+1)$ is an $(r+1)$ degree polynomial in ϕ. We assume that

$$\phi = \gamma Q^{2s}(\xi) + \mu$$ (37)

is a solution of equation (36), where γ and μ are arbitrary constants and $Q^{(2s)}(\xi)$ is the $(2s)^{\text{th}}$ derivative of the reciprocal Weierstrass elliptic function (RWEF) $Q(\xi) = \dfrac{1}{\wp(\xi)}, \wp(\xi)$ being the WEF.

It can be shown that the $(2s)^{\text{th}}$ derivative of the RWEF $Q(\xi)$ is a $(2s+1)$ degree polynomial in $Q(\xi)$ itself. Therefore, for ϕ to be a solution of equation (36), we should have the relation

$$2k - r = 2rs.$$ (38)

So, it is necessary that $2k \geq r$ for us to assume a solution in the form of equation (37). But this is in no way a sufficient condition for the existence of the PWS in the form of equation (37).

Now, we shall search for the WEF solutions of equation (11). For a solution in the form of equation (37), we should have $r = 2$ and $k = 1$ so that $s = 0$. So, our solution will be

$$u(\xi) = \frac{\gamma}{\wp(\xi)} + \mu.$$ (39)

Substituting equation (39) into equation (11) and equating the coefficients of like powers of $\wp(\xi)$ to zero, we obtain

$$\wp^3(\xi): \quad 2\gamma(1-c)(1+c)^2 - \mu(1+c) - 2\mu^3(1-c) = 0,$$ (40)

$$\wp^2(\xi): \quad -\gamma(1+c) - 6\gamma\mu^2(1-c) = 0,$$ (41)

$$\wp(\xi): \quad -\frac{3}{2}\gamma g_2(1-c)(1+c)^2 - 6\gamma^2\mu(1-c) = 0,$$ (42)

$$\wp^0(\xi): \quad -2\gamma g_3(1-c)(1+c)^2 - 2\gamma^3(1-c) = 0.$$ (43)

From equations (40)-(43), it can be found that

$$\gamma = \pm(1+c)\sqrt{-g_3},$$ (44)

$$\mu = \pm\sqrt{-\frac{1+c}{6(1-c)}},$$ (45)

$$g_2 = -\frac{4\gamma\mu}{(1+c)^2}. \tag{46}$$

From equations (44), (45) and (46), one can infer that $g_3 < 0$, $|c|$ should be greater than 1 and γ and μ are of opposite signs as g_2 should always be positive. Equation (40) leads us to the value of g_3 given by

$$g_3 = \frac{1}{54(1-c)^3(1+c)^3}, \tag{47}$$

which clearly indicates that $g_3 < 0$ when $|c| > 1$. The condition $g_2^3 - 27g_3^2 > 0$ gives the constraint relation

$$\gamma\mu < -\frac{1}{12(4)^{1/3}(1-c)^2}. \tag{48}$$

One may observe that both sides of the inequality (48) are always negative as γ and μ are of opposite signs.

The equations (30)–(32) will give rise to the same PWS of equation (11) which can be obtained using equation (39) with the help of equation (34). Thus, the PWS of equation (11) in terms of JEFs can be written as

$$u(\xi) = \frac{\gamma\mathrm{sn}^2(\xi)}{1 - \frac{1}{3}(1+m^2)\mathrm{sn}^2(\xi)} + \mu. \tag{49}$$

As $m \to 1$, the SWS of the Klein-Gordon system given by equations (6) and (7) are

$$u(x,t) = \frac{\gamma\tanh^2(x-ct)}{1 - \frac{2}{3}\tanh^2(x-ct)} + \mu \tag{50}$$

and

$$v(x,t) = -\frac{2c}{1+c}\left[\frac{\gamma\tanh^2(x-ct)}{1 - \frac{2}{3}\tanh^2(x-ct)} + \mu\right]^2, \tag{51}$$

where γ and μ are given by equations (44) and (45).

5   Conclusions

The (G'/G)-expansion method has been applied to a Klein-Gordon system of equations. The kink wave solutions and SWSs have been graphically illustrated. It was found that there are no restrictions on the coefficients in the governing equation for the solutions in terms of hyperbolic functions to exist. The WEF method has also been applied to the Klein-Gordon system to derive SWSs. We intend to apply the method for higher order and higher dimensional PDEs of physical interest.

References

[1] A. Biswas. Solitary wave solution for KdV equation with power law nonlinearity and time-dependent coefficients. *Nonlinear Dynamics* **58** (2009) 345–348.

[2] A. Biswas. Solitary waves for power-law regularized long wave equation and $R(m, n)$ equation.*Nonlinear Dynamics* **59** (2010) 423–426.

[3] R. Sassaman and A. Biswas. Topological and non-topological solitons of the Klein-Gordon equations in $(1 + 2)$-dimensions. *Nonlinear Dynamics* **61** (2010) 23–28.

[4] A. Biswas, A.B. Kara, A.H. Bokhari and F.D. Zaman. Solitons and conservation laws of Klein-Gordon equation with power law and log law nonlinearities. *Nonlinear Dynamics* **73** (2013) 2191–2196.

[5] M. Mirzazadeh, M. Eslami, E. Zerrad, M.F. Mahmood, A. Biswas and M. Belic. Optical solitons in nonlinear directional couplers by sine-cosine function method and Bernoulli's equation approach. *Nonlinear Dynamics* **81** (2015) 1933–1949.

[6] W. Malfliet. The tanh method: Exact solutions of nonlinear evolution and wave equations. *Physica Scripta* **54** (1996) 563–568.

[7] M. Alquran and K. Al-Khaled. Sinc and Solitary Wave Solutions to the Generalized Benjamin-Bona-Mahony-Burgers Equations. *Physica Scripta* **83** (2011) 065010, 6 pp.

[8] M. Alquran and K. Al-Khaled. The tanh and sine-cosine methods for higher order equations of Korteweg-de Vries type. *Physica Scripta* **84** (2011) 025010, 4 pp.

[9] S. Shukri and K. Al-Khaled. The Extended Tanh Method For Solving Systems of Nonlinear Wave Equations. *Applied Mathematics and Computation* **217** (2010) 1997–2006.

[10] M. Alquran, H.M. Jaradat and M. Syam. A modified approach for a reliable study of new nonlinear equation: two-mode Korteweg-de Vries-Burgers equation. *Nonlinear Dynamics* **91**(3) (2018) 1619–1626.

[11] A. Jaradat, M. S. M. Noorani, M. Alquran and H. M. Jaradat. A Variety of New Solitary-Solutions for the Two-mode Modified Korteweg-de Vries Equation. *Nonlinear Dynamics and Systems Theory* **19**(1) (2019) 88–96.

[12] J. H. He and X. H. Wu. Exp-function method for nonlinear wave equations. *Chaos Solitons and Fractals* **30** (2006) 700–708.

[13] J. Liu, L. Yang and K. Yang. Jacobi elliptic function solutions of some nonlinear PDEs. *Physics Letters A* **325** (2004) 268-275.

[14] M. Alquran and A. Jarrah. Jacobi elliptic function solutions for a two-mode KdV equation. *Journal of King Saud University-Science* (2017).
https://doi.org/10.1016/j.jksus.2017.06.010.

[15] M. Alquran, A. Jarrah and E.V. Krishnan. Solitary wave solutions of the phi-four equation and the breaking soliton system by means of Jacobi elliptic sine-cosine expansion method. *Nonlinear Dynamics and Systems Theory* **18**(3) (2018) 233–240.

[16] Y. Peng. Exact periodic wave solutions to a new Hamiltonian amplitude equation. *J of the Phys Soc of Japan,* **72** (2003) 1356–1359.

[17] Y. Peng. New Exact solutions to a new Hamiltonian amplitude equation. *J. of the Phys. Soc. of Japan* **72** (2003) 1889–1890.

[18] Y. Peng. New Exact solutions to a new Hamiltonian amplitude equation II. *J. of the Phys. Soc. of Japan* **73** (2004) 1156–1158.

[19] E. V. Krishnan and Y. Peng. A new solitary wave solution for the new Hamiltonian amplitude equation. *Journal of the Physical Society of Japan* **74** (2005) 896-897.

[20] J. F. Alzaidy. Extended mapping method and its applications to nonlinear evolution equations. *Journal of Applied Mathematics* **2012** (2012) Article ID 597983, 14 pages.

[21] M. Al Ghabshi, E.V. Krishnan, K. Al-Khaled and M. Alquran. Exact and Approximate Solutions of a System of Partial Differential Equations. *International Journal of Nonlinear Science* **23** (2017) 11–21.

[22] R. Hirota and J. Satsuma. Soliton solutions of a coupled Korteweg-de Vries equation. *Physics Letters A* **85** (1981) 407–408.

[23] R. Dodd and A.P. Fordy. On the integrability of a system of coupled KdV equations. *Physics Letters A* **89** (1982) 168–170.

[24] Gao H. and Zhao R.X., New application of the (G'/G)-expansion method to high-order nonlinear equations. *Appl Math Computation* **215** (2009) 2781–2786.

[25] F. Chand and A.K. Malik. Exact traveling wave solutions of some nonlinear equations using (G'/G)-expansion method. *International Journal of Nonlinear Science* **14** (2012) 416–424.

[26] M. Alquran and A. Qawasmeh. Soliton solutions of shallow water wave equations by means of (G'/G)-expansion method. *Journal of Applied Analysis and Computation* **4** (2014) 221–229.

[27] O. Yassin and M. Alquran. Constructing New Solutions for Some Types of Two-Mode Nonlinear Equations. *Applied Mathematics and Information Sciences* **12**(2) (2018) 361–367.

[28] M. Alquran and O. Yassin. Dynamism of two-mode's parameters on the field function for third-order dispersive Fisher: Application for fibre optics. *Optical and Quantum Electronics* **50**(9) (2018) 354.

[29] R. Hirota and Y. Ohta. Hierarchies of coupled soliton equations I. *J. of the Phys. Soc. of Japan* **60** (1991) 798–809.

[30] D. W. Lawden. *Elliptic Functions and Applications*. Springer Verlag, Berlin, 1989.

Extensions of Schauder's and Darbo's Fixed Point Theorems

Zhaocai Hao [1,2], Martin Bohner [1*] and Junjun Wang [2]

[1] *Missouri S&T, Rolla, MO 65409, USA*
[2] *Qufu Normal University, Qufu 273165, Shandong, China*

Abstract: In this paper, some new extensions of Schauder's and Darbo's fixed point theorems are given. As applications of the main results, the existence of global solutions for first-order nonlinear integro-differential equations of mixed type in a real Banach space is investigated.

1 Introduction

It is well known that the following two fixed points are very important.

Theorem 1.1 (Schauder's fixed point theorem) *Let Ω be a nonempty, bounded, closed, and convex subset of a Banach space E. Then each continuous and compact map $T : \Omega \to \Omega$ has at least one fixed point in Ω.*

The Schauder fixed point theorem plays an important role in nonlinear analysis. In 1955, Darbo [9] proved a fixed point property for set-contraction on a closed, bounded and convex subset of Banach spaces in terms of the measure of noncompactness, which was first defined by Kuratowski [17].

---

* Corresponding author: `mailto:bohner@mst.edu`

Theorem 1.2 (Darbo's fixed point theorem) *Let $\Omega \neq \emptyset$ be a bounded, closed, and convex subset of a Banach space E and let $T : \Omega \to \Omega$ be a continuous mapping. Assume that there exists a constant $k \in [0,1)$ such that*

$$\alpha(TX) \leq k\alpha(X) \tag{1}$$

for any nonempty subset $X \subset \Omega$, where α is a measure of noncompactness defined in E. Then T has a fixed point in Ω.

Darbo's fixed point theorem is a significant extension of the Schauder fixed point theorem, and it also plays a key role in nonlinear analysis, especially in proving the existence of solutions for many classes of nonlinear equations. Since then, some generalizations of Darbo's fixed point theorem have appeared. For example, we refer the reader to [1–3, 6, 13, 23] and the references therein.

Recently, the authors of [21] established the following new fixed point theorem, which is a generalization of Darbo's fixed point theorem.

Theorem 1.3 (See [21, Lemma 2.4]) *Let F be a closed and convex subset of a real Banach space E, $A : F \to F$ be a continuous operator, and $A(F)$ be bounded. For any bounded subset $B \subset F$, put*

$$\widetilde{A}^1(B) = A(B) \quad and \quad \widetilde{A}^{n+1}(B) = A(\overline{\mathrm{co}}(\widetilde{A}^n(B))), \quad n \in \mathbb{N}.$$

If there exist a constant $0 \leq k < 1$ and $n_0 \in \mathbb{N}$ such that for any bounded subset $B \subset F$,

$$\alpha(\widetilde{A}^{n_0}(B)) \leq k\alpha(B), \tag{2}$$

then A has a fixed point in F.

As an application of their result, the authors in [21] investigated the existence of global solutions of the Volterra type integral equation

$$u(t) = h(t) + \int_0^t G(t,s)f(s,u(s),(Tu)(s),(Su)(s))\mathrm{d}s, t \in J, \tag{3}$$

where $J = [0,a]$, $a > 0$, $f \in \mathrm{C}(J \times E \times E \times E, E)$,

$$(Tu)(t) = \int_0^t k(t,s)u(s)\mathrm{d}s, \quad (Su)(t) = \int_0^a h(t,s)u(s)\mathrm{d}s, \quad t \in J,$$

$k \in \mathrm{C}(D,\mathbb{R})$, $h \in \mathrm{C}(D_0,\mathbb{R})$,

$$D = \{(t,s) \in \mathbb{R}^2 : \ 0 \leq s \leq t \leq a\}, \quad D_0 = \{(t,s) \in \mathbb{R}^2 : \ 0 \leq t,s \leq a\},$$

and $\mathbb{R}$ denotes the set of real numbers. The main results of [21] extend and improve related results in [11, 12, 20–22]. For other results concerning integro-differential equations, we refer to [4, 5, 7, 8, 10, 14–16].

Motivated by the above works, in this paper, we first establish a new fixed point theorem (Theorem 2.1), which is an extension of Schauder's fixed point theorem. Then, by using this extended Schauder fixed point theorem, we get a new extension of Darbo's fixed point theorem (Theorem 2.2). As an application of the new extended Darbo fixed point theorem, we obtain the existence of global solutions of (3). The existence result (Theorem 3.1) includes and extends and improves related results in [11, 12, 20–22].

This paper is organized as follows. In Section 2, we present our main results, the extensions of Schauder's and Darbo's fixed point theorems. In Section 3, in order to demonstrate the applicability of our main results, we obtain the existence of global solutions of (3).

2 Main Results

Throughout this paper, let $C(J, E)$ denote the Banach space of all continuous mappings $u : J \to E$ with norm $\|u\|_c = \max_{t \in J} \|u(t)\|$, while $C^1(J, E)$ denotes the Banach space of all $u \in C(J, E)$ such that u' is continuous on J with norm $\|u\|_{c^1} = \max\{\|u\|_c, \|u'\|_c\}$. Let α denote the Kuratowski measure of noncompactness in E and $C(J, E)$. Please, see [18] for more details on the Kuratowski measure of noncompactness. For any $B \in C(J, E)$, $t \in J$, let

$$B(t) = \{u(t) : u \in B\} \subset E,$$

$$(TB)(t) = \left\{\int_0^t k(t, s)u(s)\mathrm{d}s : u \in B\right\},$$

$$(SB)(t) = \left\{\int_0^a h(t, s)u(s)\mathrm{d}s : u \in B\right\}.$$

For any $R > 0$, let

$$T_R = \{x \in E : \|x\| \leq R\} \quad \text{and} \quad B_R = \{u \in C(J, E) : \|u\|_c \leq R\}.$$

Lemma 2.1 (See [12]) *If $B \subset C(J, E)$ is bounded and equicontinuous, then $\overline{\mathrm{co}}(B) \subset C(J, E)$ is also bounded and equicontinuous.*

Lemma 2.2 (See [12]) *If $B \subset C(J, E)$ is bounded and equicontinuous, then $\alpha(B(t))$ is continuous on J and*

$$\alpha\left(\int_J B(s)\mathrm{d}s\right) \leq \int_J \alpha(B(s))\mathrm{d}s.$$

Lemma 2.3 (See [19]) *If f is bounded and uniformly continuous on $J \times T_R \times T_R \times T_R$ for all $R > 0$ and $B \subset C(J, E)$ is bounded and equicontinuous, then $\{f(t, u(t), (Tu)(t), (Su)(t)) : u \in B\}$ is bounded and equicontinuous in $C(J, E)$.*

First, we give the extension of Schauder's fixed point theorem.

Theorem 2.1 *Let D be a closed and convex subset of a real Banach space E. Suppose that the operator $A : D \to D$ is continuous. If there exists $n_0 \in \mathbb{N}$ such that $\widetilde{A}^{n_0 - 1}(D)$ is bounded and $\alpha(\widetilde{A}^{n_0}(D)) = 0$, where*

$$\widetilde{A}^0(D) = D \quad \text{and} \quad \widetilde{A}^n(D) = \overline{\mathrm{co}}(A(\widetilde{A}^{n-1}(D))), \quad n \in \mathbb{N},$$

then A has a fixed point in D.

Proof. Since $A(D) \subset D$ and D is a closed convex subset, we have

$$\widetilde{A}^1(D) = \overline{\mathrm{co}}(A(D)) \subset \overline{\mathrm{co}}(D) = D = \widetilde{A}^0(D).$$

Hence,

$$\widetilde{A}^2(D) = \overline{\mathrm{co}}(A(\widetilde{A}^1(D))) \subset \overline{\mathrm{co}}(A(D)) = \widetilde{A}^1(D).$$

By the method of mathematical induction, we can deduce that

$$\widetilde{A}^n(D) \subset \widetilde{A}^{n-1}(D), \quad n \in \mathbb{N}.$$

Thus,

$$A(\widetilde{A}^{n_0-1}(D)) \subset \overline{\mathrm{co}}(A(\widetilde{A}^{n_0-1}(D))) = \widetilde{A}^{n_0}(D) \subset \widetilde{A}^{n_0-1}(D).$$

Consequently, $A : \widetilde{A}^{n_0-1}(D) \to \widetilde{A}^{n_0-1}(D)$ is continuous. Moreover, for any bounded subset $S \subset \widetilde{A}^{n_0-1}(D)$, we get

$$A(S) \subset A(\widetilde{A}^{n_0-1}(D)) \subset \widetilde{A}^{n_0}(D),$$

and hence,

$$\alpha(A(S)) \leq \alpha(\widetilde{A}^{n_0}(D)) = 0.$$

Noting that $\widetilde{A}^{n_0-1}(D)$ is a closed bounded convex subset of E, we know from Schauder's fixed point theorem that A has a fixed point in $\widetilde{A}^{n_0-1}(D) \subset D$.

Remark 2.1 The well-known Schauder fixed point theorem is the special case $n_0 = 1$ of Theorem 2.1.

By using Theorem 2.1, we now present a new extension of Darbo's fixed point theorem.

Theorem 2.2 *Let D be a closed and convex subset of a real Banach space E. Suppose that the operator $A : D \to D$ is continuous. For any bounded subset $B \subset E$, put*

$$\widetilde{A}^0(B) = B \quad and \quad \widetilde{A}^n(B) = A(\overline{\mathrm{co}}(\widetilde{A}^{n-1}(B))), \quad n \in \mathbb{N}. \tag{4}$$

If there exists $n_0 \in \mathbb{N}$ such that $\widetilde{A}^{n_0-1}(D)$ is bounded and for any decreasing sequence of sets $\{B_n\} \subset D$, $n \in \mathbb{N}$,

$$\alpha\left(\widetilde{A}^{n_0}\left(\bigcap_{n=1}^{\infty} B_n\right)\right) = 0, \tag{5}$$

then A has a fixed point in D.

Proof. Let

$$B_0 = D \quad and \quad B_n = \overline{\mathrm{co}}(\widetilde{A}^{n_0}(B_{n-1})), \quad n \in \mathbb{N}. \tag{6}$$

Then (6) and $A : D \to D$ imply that

$$B_1 = \overline{\mathrm{co}}(\widetilde{A}^{n_0}(B_0)) \subset D = B_0.$$

Hence, $\widetilde{A}^{n_0}(B_1) \subset \widetilde{A}^{n_0}(B_0)$. Therefore,

$$B_2 = \overline{\mathrm{co}}(\widetilde{A}^{n_0}(B_1)) \subset \overline{\mathrm{co}}(\widetilde{A}^{n_0}(B_0)) = B_1.$$

By the method of mathematical induction, we can prove

$$B_n \subset B_{n-1}, \quad n \in \mathbb{N}. \tag{7}$$

If we set

$$\widehat{B} = \bigcap_{n=0}^{\infty} B_n, \tag{8}$$

where $\{B_n\}$ is defined as in (6), then $\widehat{B}$ is a nonempty and convex subset in D. Hence, (5), (7), and (8) imply

$$\alpha(\widetilde{A}^{n_0}(\widehat{B})) = 0. \tag{9}$$

Since $\widetilde{A}^{n_0-1}(D)$ is bounded, we get that

$$\widetilde{A}^{n_0-1}(\widehat{B}) \text{ is bounded.} \tag{10}$$

Next, we shall prove

$$A(\widehat{B}) \subset \widehat{B}. \tag{11}$$

In fact, from $B_1 \subset \overline{\mathrm{co}}(\widetilde{A}^{n_0-1}(B_0))$, we have

$$A(B_1) \subset A(\overline{\mathrm{co}}(\widetilde{A}^{n_0-1}(B_0))) = \widetilde{A}^{n_0}(B_0) \subset \overline{\mathrm{co}}(\widetilde{A}^{n_0}(B_0)) = B_1.$$

By the same method, we can prove $A(B_n) \subset B_n$, $n \in \mathbb{N}$. Hence, we get

$$A(\widehat{B}) = \bigcap_{n=0}^{\infty} A(B_n) \subset \bigcap_{n=0}^{\infty} B_n = \widehat{B}.$$

Then (11) holds. From (9), (10), (11), and Theorem 2.1, we deduce that A has a fixed point in $\widehat{B} \subset D$.

Remark 2.2 When

$$B_n \equiv D, \quad n \in \mathbb{N}$$

in Theorem 2.2, then Theorem 2.1 is obtained.

Remark 2.3 When

$$n_0 = 1, \quad B_n \equiv D, \quad n \in \mathbb{N}$$

in Theorem 2.2, then Theorem 1.2, i.e., Darbo's fixed point theorem is obtained. So Theorem 2.2 includes and extends Darbo's fixed point theorem.

Remark 2.4 Comparing with [21, Lemma 2.4], i.e., Theorem 1.3, the conclusion of Theorem 2.2 is the same. But the conditions are different. First, the assumption that $\widetilde{A}^{n_0-1}(D)$ is bounded is weaker than that $A(D)$ is bounded in [21, Lemma 2.4]. After that, we only need to consider the decreasing sequences without the boundedness $\{B_n\} \subset D$ in (5), while [21, Lemma 2.4] needs to consider all bounded sets $B \subset F$ in (2). Finally, (5) and (2) cannot be deduced from each other. Above all, Theorem 2.2 is a good supplement to the extension of Darbo's fixed point theorem.

3 Applications

Now, as an application of Theorem 2.2, we give an existence theorem for global solutions of (3).

Theorem 3.1 *Let E be a real Banach space. Assume*

(H_1) *For any $R > 0$, f is bounded and uniformly continuous on $J \times T_R \times T_R \times T_R$, and*

$$\limsup_{R \to \infty} \frac{M(R)}{R} < \frac{1}{aa_0 b}, \tag{12}$$

where

$$a_0 = \max\{1, ak_0, ah_0\}, \quad k_0 = \max\{|k(t,s)| : (t,s) \in D\},$$
$$h_0 = \max\{|h(t,s)| : (t,s) \in D_0\}, \quad b = \max\{G(t,s) : (t,s) \in D\},$$
$$M(R) = \sup\{\|f(t,x,y,z)\| : (t,x,y,z) \in J \times T_R \times T_R \times T_R, t \in J\}.$$

(H_2) *There exist nonnegative Lebesgue integrable functions $L_i \in \mathrm{L}(J, R^+)$ such that for any decreasing sequences of bounded sets $\{D_{in}\} \subset E$, $\alpha(D_{in}) \to 0$, $n \to \infty$, $i = 1, 2, 3$ and $t \in J$,*

$$\alpha(f(t, D_{1n}, D_{2n}, D_{3n})) \leq \sum_{i=1}^{3} L_i(t)\alpha(D_{in}). \tag{13}$$

Then (3) *has at least one global solution in* $\mathrm{C}^1(J, E)$.

Proof. First, we define an operator $A : \mathrm{C}(J, E) \to \mathrm{C}(J, E)$ by

$$(Au)(t) = h(t) + \int_0^t G(t, s)f(s, u(s), (Tu)(s), (Su)(s))\mathrm{d}s, \quad u \in \mathrm{C}(J, E). \tag{14}$$

Note that since $u \in \mathrm{C}^1(J, E)$ is a solution of (3) if and only if $u \in \mathrm{C}(J, E)$ is a solution of the integral equation

$$u(t) = (Au)(t), \quad t \in J,$$

we only need to prove that A has a fixed point. Since f is uniformly continuous on $J \times T_R \times T_R \times T_R$, we can easily see that $A : \mathrm{C}(J, E) \to \mathrm{C}(J, E)$ is continuous and bounded. On account of (12), there exist $0 < r < (aa_0b)^{-1}$ and $R_0 > 0$ such that for any $R \geq a_0R_0$,

$$\frac{M(R)}{R} < r. \tag{15}$$

Let

$$R^* = \max\left\{R_0, \|h\|_c\,(1 - aa_0b)^{-1}\right\}. \tag{16}$$

Then, by using (14) and (15), it is not difficult to verify that $A(B_{R^*}) \subset \mathrm{C}(J, E)$ is equicontinuous and bounded, and $A : B_{R^*} \to B_{R^*}$ is bounded and continuous. Set $D = \overline{\mathrm{co}}(A(B_{R^*}))$. Then, from Lemma 2.1, we get that $D \subset B_{R^*}$ is bounded and equicontinuous and

$$A : D \to D \text{ is continuous and bounded.} \tag{17}$$

For any decreasing sequence of bounded sets $\{B_m\} \subset D$, $m \in \mathbb{N}$, by (H_1) and (14), we have that $A(B_m)$ is bounded and equicontinuous. Hence, from Lemma 2.1, Lemma 2.3, and (4), we get for any $n \in \mathbb{N}$ that $\widetilde{A}^n(B_m)$ is bounded and equicontinuous on J, and so

$$\alpha(\widetilde{A}^n(B_m)) = \max_{t \in J} \alpha((\widetilde{A}^n(B_m))(t)), \quad m \in \mathbb{N}.$$

Next, we show that for any $n_0 \in \mathbb{N}$, we have

$$\widetilde{A}^{n_0-1}(D) \text{ is bounded,} \tag{18}$$

and for any decreasing sequence of sets $\{B_m\} \subset D$, $\alpha(B_m) \to 0$, $m \in \mathbb{N}$,

$$\alpha\left(\widetilde{A}^{n_0}\left(\bigcap_{m=1}^{\infty} B_m\right)\right) = 0. \tag{19}$$

Indeed, (18) follows from the fact that $D \subset B_{R^*}$ is bounded. Furthermore, from (13), (14), and (15), we get

$$
\begin{aligned}
&\alpha((\widetilde{A}^1(B_m))(t)) \\
&\quad = \alpha\left(\int_0^t G(t,s)f(s,(\overline{\mathrm{co}}B_m)(s),(T(\overline{\mathrm{co}}B_m))(s),(S(\overline{\mathrm{co}}B_m))(s))\mathrm{d}s\right) \\
&\quad \leq b\int_0^t [L_1(s)\alpha((\overline{\mathrm{co}}B_m)(s)) + L_2(s)\alpha((T(\overline{\mathrm{co}}B_m))(s)) + L_3(s)\alpha((S(\overline{\mathrm{co}}B_m))(s))]\mathrm{d}s \\
&\quad \leq b\int_0^t [L_1(s)\alpha((\overline{\mathrm{co}}B_m)(s)) + L_2(s)k_0\alpha((\overline{\mathrm{co}}B_m)(s)) + L_3(s)h_0\alpha((\overline{\mathrm{co}}B_m)(s))]\mathrm{d}s \\
&\quad = b\int_0^t [L_1(s)\alpha((B_m(s)) + L_2(s)k_0\alpha(B_m(s)) + L_3(s)h_0\alpha(B_m(s))]\mathrm{d}s \\
&\quad \to 0, \quad m \to \infty.
\end{aligned}
$$

Assume

$$\alpha((\widetilde{A}^k(B_m))(t)) \to 0, \quad m \to \infty, \quad k \in \mathbb{N} \setminus \{1\}.$$

Then

$$
\begin{aligned}
&\alpha((\widetilde{A}^{k+1}(B_m))(t)) \\
&\quad = \alpha\left(\int_0^t G(t,s)f(s,(\overline{\mathrm{co}}\widetilde{A}^k(B_m))(s),T(\overline{\mathrm{co}}\widetilde{A}^k(B_m))(s),S(\overline{\mathrm{co}}\widetilde{A}^k(B_m))(s))\mathrm{d}s\right) \\
&\quad \leq b\int_0^t \Big[L_1(s)\alpha((\overline{\mathrm{co}}\widetilde{A}^k(B_m))(s)) + L_2(s)\alpha(T(\overline{\mathrm{co}}\widetilde{A}^k(B_m))(s)) \\
&\qquad\qquad + L_3(s)\alpha(S(\overline{\mathrm{co}}\widetilde{A}^k(B_m)(s)))\Big]\mathrm{d}s \\
&\quad \leq b\int_0^t \Big[L_1(s)\alpha((\overline{\mathrm{co}}\widetilde{A}^k(B_m))(s)) + L_2(s)k_0\alpha((\overline{\mathrm{co}}\widetilde{A}^k(B_m))(s)) \\
&\qquad\qquad + L_3(s)h_0\alpha((\overline{\mathrm{co}}\widetilde{A}^k(B_m))(s))\Big]\mathrm{d}s \\
&\quad = b\int_0^t \Big[L_1(s)\alpha((\widetilde{A}^k(B_m))(s)) + L_2(s)k_0\alpha((\widetilde{A}^k(B_m))(s)) \\
&\qquad\qquad + L_3(s)h_0\alpha((\widetilde{A}^k(B_m))(s))\Big]\mathrm{d}s \\
&\quad \to 0, \quad m \to \infty.
\end{aligned}
$$

Consequently,

$$\alpha(\widetilde{A}^n(B_m)) \to 0, \quad m \to \infty, \quad n \in \mathbb{N},$$

and so $\alpha(\widetilde{A}^{n_0}(B_m)) \to 0$, $m \to \infty$. Thus, we have

$$\alpha\left(\widetilde{A}^{n_0}\left(\bigcap_{m=1}^\infty B_m\right)\right) \leq \alpha(\widetilde{A}^{n_0}(B_m)) \to 0, \quad m \to \infty.$$

Hence, (19) holds. It follows from Theorem 2.2, (17), (18), and (19) that A has a fixed point in D. Thus, (3) has at least one global solution in $\mathrm{C}^1(J,E)$.

Remark 3.1 The main result of [21], i.e., [21, Theorem 3.1] is as follows: *Let E be a real Banach space. Assume*

(H_3) *For any $R > 0$, f is bounded and uniformly continuous on $J \times T_R \times T_R \times T_R$, and*

$$\limsup_{R \to \infty} \frac{M(R)}{R} < \frac{1}{aa_0 b},$$

where

$$a_0 = \max\{1, ak_0, ah_0\}, \quad b = \max\{G(t,s) : (t,s) \in D\},$$
$$M(R) = \sup\{\|f(t,x,y,z)\| : (t,x,y,z) \in J \times T_R \times T_R \times T_R, t \in J\}.$$

(H_4) *There exist nonnegative Lebesgue integrable functions $L_i \in \mathrm{L}(J, \mathbb{R}^+)$ such that for any bounded sets $\{D_i\} \subset E$ and $t \in J$,*

$$\alpha(f(t, D_1, D_2, D_3)) \leq \sum_{i=1}^{3} L_i(t)\alpha(D_i). \tag{20}$$

Then (3) has at least one global solution in $\mathrm{C}^1(J, E)$. Comparing [21, Theorem 3.1] with Theorem 3.1 above, we can see that the only difference is between (13) and (20). For all bounded sets $\{D_i\} \subset E$, (20) should hold. For only those bounded and decreasing sequences $\{D_{in}\} \subset E$, $\alpha(D_{in}) \to 0$, $i = 1, 2, 3$, we need that (13) holds. So (13) is weaker than (20). Moreover, (20) is a special case of (13) when $D_{in} \equiv D_i$, $i = 1, 2, 3$, $n \in \mathbb{N}$. Thus, Theorem 3.1 includes and extends [21, Theorem 3.1], which extended and improved the main results of [11, 12, 20, 22]. Consequently, Theorem 3.1 in this paper extends and improves not only the main results of [21], but also related results of [11, 12, 20, 22].

Acknowledgements

References

[1] Asadollah Aghajani and M. Aliaskari. Commuting mappings and generalization of darbo's fixed point theorem. *Math. Sci. Lett.* **4** (2) (2015) 187–190.

[2] Asadollah Aghajani, Reza Allahyari, and Mohammad Mursaleen. A generalization of Darbo's theorem with application to the solvability of systems of integral equations. *J. Comput. Appl. Math.* **260** (2014) 68–77.

[3] Asadollah Aghajani, Józef Banaś, and Navid Sabzali. Some generalizations of Darbo fixed point theorem and applications. *Bull. Belg. Math. Soc. Simon Stevin* **20** (2) (2013) 345–358.

[4] Theodore A. Burton. Existence and uniqueness results by progressive contractions for integro-differential equations. *Nonlinear Dyn. Syst. Theory* **16** (4) (2016) 366–371.

[5] Theodore A. Burton. Integro-differential equations, compact maps, positive kernels, and Schaefer's fixed point theorem. *Nonlinear Dyn. Syst. Theory* **17** (1) (2017) 19–28.

[6] Longsheng Cai and Jin Liang. New generalizations of Darbo's fixed point theorem. *Fixed Point Theory Appl.* **156** (2015) 8 pages.

[7] Alka Chadha. Mild solution for impulsive neutral integro-differential equation of Sobolev type with infinite delay. *Nonlinear Dyn. Syst. Theory* **15** (3) (2015) 272–289.

[8] Jaydev Dabas. Existence and uniqueness of solutions to quasilinear integro-differential equations by the method of lines. *Nonlinear Dyn. Syst. Theory* **11** (4) (2011) 397–410.

[9] Gabriele Darbo. Punti uniti in trasformazioni a codominio non compatto. *Rend. Sem. Mat. Univ. Padova* **24** (1955) 84–92.

[10] Zachary Denton and J. Diego Ramírez. Monotone method for finite systems of nonlinear Riemann-Liouville fractional integro-differential equations. *Nonlinear Dyn. Syst. Theory* **18** (2) (2018) 130–143.

[11] Dajun Guo. Solutions of nonlinear integrodifferential equations of mixed type in Banach spaces. *J. Appl. Math. Simulation* **2** (1) (1989) 1–11.

[12] Dajun Guo, V. Lakshmikantham, and Xinzhi Liu. *Nonlinear Integral Equations in Abstract Spaces*, vol. 373 of *Mathematics and its Applications*. Kluwer Academic Publishers Group, Dordrecht, 1996.

[13] Ahmed Hajji. A generalization of Darbo's fixed point and common solutions of equations in Banach spaces. *Fixed Point Theory Appl.* **62** (2013) 9 pages.

[14] Hossein Jafari and A. Azad. A computational method for solving a system of Volterra integro-differential equations. *Nonlinear Dyn. Syst. Theory* **12** (4) (2012) 389–396.

[15] Pradeep Kumar. On the new concepts of solutions and existence results for impulsive integro-differential equations with a deviating argument. *Nonlinear Dyn. Syst. Theory* **14** (1) (2014) 58–75.

[16] Pradeep Kumar, Rajib Haloi, Dhirendra Bahuguna, and Dwijendra N. Pandey. Existence of solutions to a new class of abstract non-instantaneous impulsive fractional integro-differential equations. *Nonlinear Dyn. Syst. Theory* **16** (1) (2016) 73–85.

[17] Kazimierz Kuratowski. Sur les espaces complets. *Fund. Math.* **15** (1) (1930) 301–309.

[18] V. Lakshmikantham. Some problems in integro-differential equations of Volterra type. *J. Integral Equations* **10** (1-3, suppl.) (1985) 137–146. Integro-differential evolution equations and applications (Trento, 1984).

[19] Lishan Liu. Iterative method for solutions and coupled quasi-solutions of nonlinear Fredholm integral equations in ordered Banach spaces. *Indian J. Pure Appl. Math.* **27** (10) (1996) 959–972.

[20] Lishan Liu. Existence of global solutions of initial value problems for nonlinear integro-differential equations of mixed type in Banach spaces. *J. Systems Sci. Math. Sci.* **20** (1) (2000) 112–116.

[21] Lishan Liu, Fei Guo, Congxin Wu, and Yonghong Wu. Existence theorems of global solutions for nonlinear Volterra type integral equations in Banach spaces. *J. Math. Anal. Appl.* **309** (2) (2005) 638–649.

[22] Lishan Liu, Congxin Wu, and Fei Guo. Existence theorems of global solutions of initial value problems for nonlinear integrodifferential equations of mixed type in Banach spaces and applications. *Comput. Math. Appl.* **47** (1) (2004) 13–22.

[23] Ayub Samadi and Mohammad B. Ghaemi. An extension of Darbo's theorem and its application. *Abstr. Appl. Anal.* (2014), Art. ID 852324, 11 pages.

State Estimation of Rotary Inverted Pendulum Using HOSM Observers: Experimental Results

F. A. Haouari [1], Q. V. Dang [2], J.-Y. Jun [3], M. Djemai [2*] and B. Cherki [1]

[1] *Department of Electrical Engineering and Electronics, Tlemcen University, Algeria*
[2] *LAMIH, UMR CNRS 8201; UVHC, 59313 Valenciennes, France*
[3] *Sorbonne University, UPMC Univ Paris 06, UMR 7222, ISIR, F-75005, Paris, France*

Abstract: This paper presents the observer design for the state estimation of the rotary inverted pendulum (RIP) system. A Takagi-Sugeno (T-S) fuzzy descriptor approach is used for modeling the nonlinear dynamic system. Two higher-order sliding mode (HOSM) observers, based on the super-twisting algorithm, are proposed and applied to the RIP with real-time implementation. The experimental results illustrate the finite-time convergence and accuracy of the state estimates of the designed observers.

Keywords: *rotary inverted pendulum; T-S fuzzy descriptor model; super-twisting algorithm; higher-order sliding mode observer.*

Mathematics Subject Classification (2010): 93B07, 93C10, 93C42, 93C85.

1 Introduction

Recently, sliding mode techniques have been widely used for the problems of dynamic systems control and observation due to their finite-time convergence and robustness against various kinds of uncertainties such as parameter perturbations and external disturbances [1]. In particular, higher-order sliding mode (HOSM) based observers can be considered as a successful technique for the state observation of perturbed systems, due to their high precision and robust behavior with respect to parametric uncertainties [13]. In [7], the step-by-step first-order sliding mode observers are designed for a class of systems in triangular input form. Nevertheless, the realization of first-order sliding mode implies the undesirable chattering phenomena.

Many observers, based on the high-order sliding mode technique, have been developed

---

* Corresponding author: `mailto:mohamed.djemai@univ-valenciennes.fr`

recently for a class of nonlinear systems. The high-order sliding mode is used to over-come the chattering phenomena occurring. In [2]- [6], the HOSM observers based on an exact and robust sliding mode differentiator of order 2 (a super-twisting algorithm) have been proposed. The super-twisting algorithm (STA) is one of the most popular second-order sliding mode algorithms which offer a finite-time and exact convergence and it has been widely used for control and observation [13]. The robustess, better accuracy and finite-time convergence of these observers can be used for the state estimation and fault diagnosis of uncertain nonlinear dynamics systems.

In this paper, the synthesis of an iterative sliding mode observer for the state estimation of the RIP system using the super-twisting algorithm is presented, when the angular velocities are not measured directly. As an underactuated and unstable system, the rotary inverted pendulum system has been regarded as an attractive test platform for linear and nonlinear control law verification since Katsuhisa Furuta, Professor at the Tokyo Institute of Technology, introduced it to the feedback control community in 1992 [11]. Also, it has some significant real-life applications such as the position control, aerospace vehicles control, and robotics [14]. Here, the modeling of the RIP system is based on T-S fuzzy descriptor systems [9]. The T-S fuzzy systems have been proven to be a powerful tool for modeling and controlling complex systems [8]. Recently, the fuzzy T-S representation in a descriptor form has generated a great interest in control systems design. The descriptor system describes a wider class of systems including physical models and nondynamic constraints [9] and using the fuzzy descriptor system can reduce the number of LMI conditions for controller design [10].

This paper is structured as follows. In Section 2, the description and T-S fuzzy descriptor model of the RIP system are given. Section 3 presents the design procedure and convergence analysis of the proposed HOSM observers. Section 4 provides experimental results. The final Section 5 concludes this paper.

2   Rotary Inverted Pendulum System

2.1   Mathematical model

A schematic of the rotary inverted pendulum is represented in Fig. 1 [12]. The system consists of a servo-motor which runs a gear to rotate a pendulum arm of radius r which in turn affects the motion of a pendulum rod of length l and mass m. The plane of the pendulum is orthogonal to the radial arm. Let ϕ be the angle of the pendulum rod from the upright position about the x_1-axis and θ be the rotational angle of the pendulum arm about the vertical axis z.

The mathematical model of the RIP is derived from the Euler-Lagrange equations which are obtained from an energy analysis of the system [12]. The nonlinear model is represented by a set of dynamical equations given as follows:

$$\begin{cases} \frac{4}{3}c_1\ddot{\phi} + c_2\ddot{\theta}cos\phi - c_1\dot{\theta}^2 sin\phi\,cos\phi + c_3\dot{\phi} - c_4 sin\phi = 0 \\ c_2\ddot{\phi}cos\phi + (c_5 + c_1 sin^2\phi)\ddot{\theta} - c_2\dot{\phi}^2 sin\phi + c_6\dot{\theta} + 2c_1\dot{\phi}\dot{\theta}sin\phi\,cos\phi = c_7V_m \end{cases} \tag{1}$$

where

$$c_1 = \frac{ml^2}{4} \quad c_2 = \frac{mlr}{2} \quad c_3 = B_r \quad c_5 = J_{eq} + mr^2 + \eta_g K_g^2 J_m$$
$$c_4 = \frac{mgl}{2} \quad c_7 = \frac{\eta_m\eta_g K_t K_g}{R} \quad c_6 = B_a + \frac{\eta_m\eta_g K_t K_v K_g^2}{R}$$

V_m is the control input voltage applied on the motor. For the definition of notations used for the constants, see Table 2.
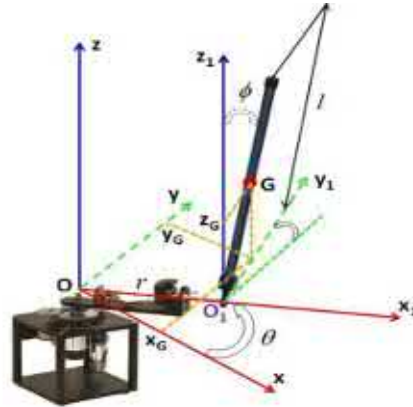
Figure 1: Schematic of the rotary inverted pendulum (upright position).

2.2 Descriptor T-S model

Introducing the variables $x_1 = \phi$, $x_2 = \theta$, $x_3 = \dot{\phi}$, $x_4 = \dot{\theta}$, the input $u = V_m$ and the measured output $y = [\phi \ \theta]^T$, the pendulum model (1) can be written in a regular descriptor form

$$\begin{cases} E(x)\dot{x}(t) = A(x)x(t) + Bu(t) \\ y(t) = Cx(t) \end{cases} \tag{2}$$

where $x = [x_1 x_2 x_3 x_4]^T$ is the state vector,

$$E(x) = \begin{bmatrix} 1 & 0 & 0 & 0 \\ 0 & 1 & 0 & 0 \\ 0 & 0 & \frac{4}{3}c_1 & c_2 cos\phi \\ 0 & 0 & c_2 cos\phi & c_5 + c_1 sin^2\phi \end{bmatrix} \quad B = \begin{bmatrix} 0 \\ 0 \\ 0 \\ c_7 \end{bmatrix}$$

$$A(x) = \begin{bmatrix} 0 & 0 & 1 & 0 \\ 0 & 0 & 0 & 1 \\ c_4 \frac{sin\phi}{\phi} & 0 & -c_3 & \alpha \\ 0 & 0 & \beta & -c_6 \end{bmatrix} \quad C = \begin{bmatrix} 1 & 0 & 0 & 0 \\ 0 & 1 & 0 & 0 \end{bmatrix}$$

with $\alpha = c_1 \dot{\theta} sin\phi cos\phi$ and $\beta = c_2 \dot{\phi} sin\phi - 2c_1 \dot{\theta} sin\phi cos\phi$.

Consider n_e and n_a being the numbers of nonlinear terms contained in the matrices $E(x)$ and $A(x)$, respectively. Then, the descriptor T-S fuzzy model is described by a set of $r_e \times r_a = 2^{n_e} \times 2^{n_a} = 32$ linear models, with $n_e = 2$ and $n_a = 3$. In order to simplify the model, the nonlinearities α and β are taken into account as bounded uncertainties. This allows reducing the number of linear models from 32 to 8.

Thus 3 nonlinearities are under consideration and specify a state dependent premise vector, $z(t)$. The premise variables $z_j(t) \ \ j = 1 \quad 3$, are given by

$$z_1 = c_2 cos(\phi) \quad z_2 = c_5 + c_1 sin^2\phi \quad z_3 = c_4 \frac{sin(\phi)}{\phi} \tag{3}$$

Therefore, through the local sector nonlinearities approach [9], the nonlinear dynamics model of the RIP can be approximated by the following fuzzy T-S representation in a

descriptor form

$$\begin{cases} \sum_{k=1}^{r_e} v_k(z(t))E_k\dot{x}(t) = \sum_{i=1}^{r_a} w_i(z(t))(A_ix(t) + Bu(t)) \\ y(t) = Cx(t) \end{cases} \tag{4}$$

where $r_e = 4$, $r_a = 2$, and both nonlinear functions $v_k(z(t)) \geq 0$, $k \in \{1 \quad r_e\}$, $w_i(z(t)) \geq 0$, $i \in \{1 \quad r_a\}$ satisfy the convex sum property, i.e. $\sum_{k=1}^{r_e} v_k(z(t)) = 1$ and $\sum_{i=1}^{r_a} w_i(z(t)) = 1$.

Consider $\overline{z_j}$ (resp. $\underline{z_j}$) being the maximum (resp. minimum) of z_j, the premise variables $z_j(t)$, $j = 1 \quad 3$, can be written as

$$z_j(t) = M_{j1}(z_j(t))\overline{z_j} + M_{j2}(z_j(t))\underline{z_j} \tag{5}$$

with

$$M_{j1}(z_j(t)) = (z_j - \underline{z_j})\ (\overline{z_j} - \underline{z_j}) \quad M_{j2}(z_j(t)) = (\overline{z_j} - z_j)\ (\overline{z_j} - \underline{z_j}) \tag{6}$$

where

$$M_{j1}(z_j(t)) + M_{j2}(z_j(t)) = 1 \tag{7}$$

Then, the system matrices have the expressions

$$E_1 = \begin{bmatrix} 1 & 0 & 0 & 0 \\ 0 & 1 & 0 & 0 \\ 0 & 0 & \frac{4}{3}c_1 & \overline{z_1} \\ 0 & 0 & \overline{z_1} & \overline{z_2} \end{bmatrix} \quad E_2 = \begin{bmatrix} 1 & 0 & 0 & 0 \\ 0 & 1 & 0 & 0 \\ 0 & 0 & \frac{4}{3}c_1 & \overline{z_1} \\ 0 & 0 & \overline{z_1} & \underline{z_2} \end{bmatrix}$$

$$E_3 = \begin{bmatrix} 1 & 0 & 0 & 0 \\ 0 & 1 & 0 & 0 \\ 0 & 0 & \frac{4}{3}c_1 & \underline{z_1} \\ 0 & 0 & \underline{z_1} & \overline{z_2} \end{bmatrix} \quad E_4 = \begin{bmatrix} 1 & 0 & 0 & 0 \\ 0 & 1 & 0 & 0 \\ 0 & 0 & \frac{4}{3}c_1 & \underline{z_1} \\ 0 & 0 & \underline{z_1} & \underline{z_2} \end{bmatrix}$$

$$A_1 = \begin{bmatrix} 0 & 0 & 1 & 0 \\ 0 & 0 & 0 & 1 \\ \overline{z_3} & 0 & -c_3 & 0 \\ 0 & 0 & 0 & -c_6 \end{bmatrix} \quad A_2 = \begin{bmatrix} 0 & 0 & 1 & 0 \\ 0 & 0 & 0 & 1 \\ \underline{z_3} & 0 & -c_3 & 0 \\ 0 & 0 & 0 & -c_6 \end{bmatrix}$$

$v_k(z(t)) \geq 0$, $k \in \{1 \quad r_e\}$, $w_i(z(t)) \geq 0$, $i \in \{1 \quad r_a\}$. Therefore, the functions $v_k(z(t)) \geq 0$, $k \in \{1 \quad 4\}$, and $w_i(z(t)) \geq 0$, $i \in \{1\ 2\}$, are obtained by

$$\begin{aligned} &w_1(z) = M_{31}(z_3); \ w_2(z) = M_{32}(z_3) \\ &v_1(z) = M_{11}(z_1) \times M_{21}(z_2); \ v_2(z) = M_{11}(z_1) \times M_{22}(z_2) \\ &v_3(z) = M_{12}(z_1) \times M_{21}(z_2); \ v_4(z) = M_{12}(z_1) \times M_{22}(z_2) \end{aligned} \tag{8}$$

The set of 8 model rules is given in Table 1.

The control law used to stabilize the RIP in the upright position is the robust T-S descriptor stabilizing controller proposed in [12], which stabilizes the system in the

Table 1: Rules of T-S fuzzy descriptor model for the RIP.

Rules	*Membership functions*			*Matrices*
	$\mathbf{M_{1j}(z_1)}$	$\mathbf{M_{2j}(z_2)}$	$\mathbf{M_{3j}(z_3)}$	$\mathbf{E_k,A_i}$
1	M_{11}	M_{21}	M_{31}	E_1,A_1
2	M_{11}	M_{21}	M_{32}	E_1,A_2
3	M_{11}	M_{22}	M_{31}	E_2,A_1
4	M_{11}	M_{22}	M_{32}	E_2,A_2
5	M_{12}	M_{21}	M_{31}	E_3,A_1
6	M_{12}	M_{21}	M_{32}	E_3,A_2
7	M_{12}	M_{22}	M_{31}	E_4,A_1
8	M_{12}	M_{22}	M_{32}	E_4,A_2

operating range under uncertainties and distrubances. Then, the control input $u(t)$ is a fuzzy parallel distributed compensation (PDC) [12]:

$$u(t) = \sum_{k=1}^{4} \sum_{i=1}^{2} w_i(z(t)) v_k(z(t)) K_{ik} x(t) \tag{9}$$

with the following feedback gain matrices:

$$
\begin{aligned}
K_{11} &= \begin{bmatrix} 26\,8550 & 1\,4142 & 3\,8231 & 2\,0844 \end{bmatrix} \\
K_{12} &= \begin{bmatrix} 25\,1416 & 1\,4142 & 3\,5734 & 2\,0638 \end{bmatrix} \\
K_{13} &= \begin{bmatrix} 41\,6885 & 1\,4142 & 6\,0852 & 2\,0945 \end{bmatrix} \\
K_{14} &= \begin{bmatrix} 39\,0849 & 1\,4142 & 5\,7014 & 2\,0741 \end{bmatrix} \\
K_{21} &= \begin{bmatrix} 24\,9747 & 1\,4142 & 3\,7940 & 2\,1137 \end{bmatrix} \\
K_{22} &= \begin{bmatrix} 23\,4523 & 1\,4142 & 3\,5580 & 2\,0932 \end{bmatrix} \\
K_{23} &= \begin{bmatrix} 38\,7119 & 1\,4142 & 6\,0174 & 2\,1233 \end{bmatrix} \\
K_{24} &= \begin{bmatrix} 36\,3931 & 1\,4142 & 5\,6539 & 2\,1029 \end{bmatrix}
\end{aligned}
\tag{10}
$$

The observability of the system (4) requires that all the subsystems are observable, consider the following assumption.

Assumption 2.1 The system (4) satisfies the following rank test conditions for observability, ($k = 1 \quad r_e$ and $i = 1 \quad r_a$) [15]:

$$rank \begin{bmatrix} sE_k - A_i \\ C \end{bmatrix} = n \quad \forall s \in \mathbb{C} \tag{11}$$

$$rank \begin{bmatrix} E_k & A_i \\ 0 & E_k \\ 0 & C \end{bmatrix} = n + rank(E_k) \tag{12}$$

The objective of this paper is to design finite-time convergent observers of the velocities $\dot{\phi}$ and $\dot{\theta}$ for the RIP system, when only the positions ϕ and θ are measurable. The state vector x is estimated with the second-order sliding mode observers proposed in the following section.

3   Second-Order Sliding Mode Observer Design

3.1   Step-by-step sliding mode of order 2

Consider the sliding mode differentiator of order 2 (the super-twisting algorithm) [5]

$$\begin{cases} u(e_1) = u_1 + \lambda_1 |e_1|^{\frac{1}{2}} sign(e_1) \\ \dot{u}_1 = \alpha_1 sign(e_1) \end{cases} \tag{13}$$

where $e_1 = x_1 - \hat{x}_1$, and λ_1 and α_1 are positive tuning parameters of the differentiator whose output is u_1. The *sign* function is approximated by the saturation function with a high gain in the boundary layer. An important feature of the differentiator (13) is the fact that the output does not depend directly on discontinuous functions, but on an integrator output. So, high-frequency chattering is attenuated [5].

First, let us consider system (4). It can be rewritten into two subsystems in a triangular observable form as follows:

$$\Sigma_1 = \begin{cases} \dot{x}_1 = x_3 \\ \dot{x}_3 = \frac{3}{4c_1}(cx_1 - a\dot{x}_4 - c_3 x_3) = f_1(t \ x) \\ y_1 = x_1 \end{cases} \tag{14}$$

$$\Sigma_2 = \begin{cases} \dot{x}_2 = x_4 \\ \dot{x}_4 = \frac{1}{b}(c_7 u - c_6 x_4 - a\dot{x}_3) = f_2(t \ x \ u) \\ y_2 = x_2 \end{cases} \tag{15}$$

with

$$a = (v_1(z) + v_2(z))\overline{z_1} + (v_3(z) + v_4(z))\underline{z_1}$$
$$b = (v_1(z) + v_3(z))\overline{z_2} + (v_2(z) + v_4(z))\underline{z_2}$$
$$c = w_1(z)\overline{z_3} + w_2(z)\underline{z_3}$$

Applying the super-twisting algorithm (13) to the transformed system (14)-(15), the step-by-step sliding mode observers (Σ_{obs1}) and (Σ_{obs2}) are obtained, respectively, as

$$\Sigma_{obs1} = \begin{cases} \dot{\hat{x}}_1 = \tilde{x}_3 + \lambda_1 |x_1 - \hat{x}_1|^{\frac{1}{2}} sign(x_1 - \hat{x}_1) \\ \dot{\tilde{x}}_3 = \alpha_1 sign(x_1 - \hat{x}_1) \\ \dot{\hat{x}}_3 = \tilde{\theta}_1 + F_1 \lambda_2 |\tilde{x}_3 - \hat{x}_3|^{\frac{1}{2}} sign(\tilde{x}_3 - \hat{x}_3) \\ \dot{\tilde{\theta}}_1 = F_1 \alpha_2 sign(\tilde{x}_3 - \hat{x}_3) \end{cases} \tag{16}$$

$$\Sigma_{obs2} = \begin{cases} \dot{\hat{x}}_2 = \tilde{x}_4 + \lambda_3 |x_2 - \hat{x}_2|^{\frac{1}{2}} sign(x_2 - \hat{x}_2) \\ \dot{\tilde{x}}_4 = \alpha_3 sign(x_2 - \hat{x}_2) \\ \dot{\hat{x}}_4 = \tilde{\theta}_2 + F_2 \lambda_4 |\tilde{x}_4 - \hat{x}_4|^{\frac{1}{2}} sign(\tilde{x}_4 - \hat{x}_4) \\ \dot{\tilde{\theta}}_2 = F_2 \alpha_4 sign(\tilde{x}_4 - \hat{x}_4) \end{cases} \tag{17}$$

where $\hat{x}_i$, $i = 1 \quad 4$, are the state estimates and the functions F_i, $i = 1 \ 2$, are given by $F_i = 0$ if $e_i > \epsilon$ otherwise $F_i = 1$, where ϵ is a small positive constant.

Suppose that the system (14) is BIBS (Bounded Inputs Bounded State) in finite time, then the functions f_1, f_2 and their first-time derivatives are bounded by the known constants, for all $t > 0$,

$$\begin{aligned} |f_1| < K_1 \qquad |\dot{f}_1| < K_2 \\ |f_2| < K_3 \qquad |\dot{f}_2| < K_4 \end{aligned} \tag{18}$$

3.2   Convergence analysis

Consider the system (14) and the HOSM observer (16). Let us define the estimation errors as $e_i = \tilde{x}_i - \hat{x}_i$ $i = 1 \quad 4$, with $\tilde{x}_1 = x_1$ and $\tilde{x}_2 = x_2$.

Lemma 3.1 *For any initial conditions $(x_1(0) \ x_3(0))$, $(\hat{x}_1(0) \ \hat{x}_3(0))$ there exists a choice of λ_i and α_i such that the observer state $(\hat{x}_1 \ \hat{x}_3)$ converges in finite time to $(x_1 \ x_3)$.*

Proof. The convergence of the observation error is obtained in one step in finite time.
Step 1: Assume $e_1(0) \neq 0$, the error dynamics is given by

$$\begin{cases} \dot{e}_1 = x_3 - \tilde{x}_3 - \lambda_1 |e_1|^{\frac{1}{2}} sign(e_1) \\ \dot{\tilde{x}}_3 = \alpha_1 sign(e_1) \\ \dot{e}_3 = f_1 - \tilde{\theta}_1 - F_1 \lambda_2 |e_3|^{\frac{1}{2}} sign(e_3) \end{cases}$$

The second time derivative of e_1 is given by

$$\ddot{e}_1 = f_1 - \alpha_1 sign(e_1) - \frac{1}{2}\lambda_1 \dot{e}_1 |e_1|^{-\frac{1}{2}} \tag{19}$$

From [6], the sufficient conditions for the finite-time convergence on the second-order sliding set $\{e_1 = \dot{e}_1 = 0\}$ are

$$\begin{aligned} \alpha_1 &> K_1 \\ \lambda_1 &> \sqrt{2}\frac{K_1 + \alpha_1}{\sqrt{\alpha_1 - K_1}} \end{aligned} \tag{20}$$

The finite-time convergence to the second-order sliding set ensures that there exists a time $t_1 > 0$ such that for all $t > t_1$: $\hat{x}_1 = x_1$ and $\tilde{x}_3 = x_3$.
Step 2: For $t > t_1$, $F_1 = 1$ and the observer dynamics becomes

$$\begin{cases} \dot{e}_1 = 0 \\ \dot{e}_3 = f_1 - \tilde{\theta}_1 - \lambda_2 |e_3|^{\frac{1}{2}} sign(e_3) \\ \dot{\tilde{\theta}}_1 = \alpha_2 sign(e_3) \end{cases}$$

The second time derivative of e_3 has the form

$$\ddot{e}_3 = \dot{f}_1 - \alpha_2 sign(e_3) - \frac{1}{2}\lambda_2 \dot{e}_3 |e_3|^{-\frac{1}{2}}. \tag{21}$$

Thus, a sliding motion appears after a finite time on the sliding manifold $\{e_3 = \dot{e}_3 = 0\}$. The observer gains satisfy [6]

$$\begin{aligned} \alpha_2 &> K_2 \\ \lambda_2 &> \sqrt{2}\frac{K_2 + \alpha_2}{\sqrt{\alpha_2 - K_2}} \end{aligned} \tag{22}$$

Therefore, in the sliding mode, there exists a time $t_2 > t_1$ such that for all $t > t_2$: $\hat{x}_3 = \tilde{x}_3$ and $\dot{\tilde{\theta}}_1 = (\alpha_2 sign(e_3))_{eq}$.

According to a similar convergence analysis of the observer (16), the sufficient conditions of the observer (17) for the finite-time convergence to the sliding manifold $\{e_i = \dot{e}_i = 0\}$, $i = 2\ 4$, are

$$\alpha_3 > K_3$$
$$\lambda_3 > \sqrt{2}\frac{K_3 + \alpha_3}{\sqrt{\alpha_3 - K_3}} \tag{23}$$

$$\alpha_4 > K_4$$
$$\lambda_4 > \sqrt{2}\frac{K_4 + \alpha_4}{\sqrt{\alpha_4 - K_4}} \tag{24}$$

Thus, the convergence of the observer states $(\hat{x}_2\ \hat{x}_4)$ from (17) to the system state variables $(x_2\ x_4)$ in (15) occurs in finite time. $\square$

4   Experimental Results

Experimental results of the proposed observers (16) and (17) are presented in this section. A picture of the experimental setup of the considered RIP system is shown in Fig.2. The different parts include: a rotary inverted pendulum manufactured by Quanser, a VoltPAQ-X2 linear voltage amplifier, a PC with measurement computing PCI-QUAD04 quadrature encoder board and PCI-DAS6025 board. The development of the controller and observer systems is made in the MATLAB/Simulink environment. The numerical values of the mechanical and electrical system parameters for the RIP-model are provided in Table 2.
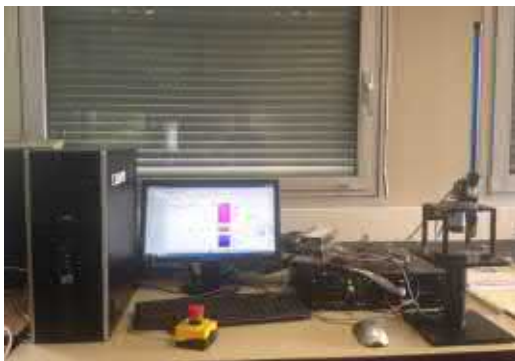
Figure 2: The experiment setup.

The T-S fuzzy descriptor system (4) approximates the RIP system in a range of $|\phi| \leq \phi_0$. For $\phi_0 = \frac{49\pi}{180}$ (rad), it follows that

$$\begin{array}{lll} \underline{z_1} = 0\ 003 & \underline{z_2} = 0\ 0111 & \underline{z_3} = 0\ 1813 \\ \overline{z_1} = 0\ 0045 & \overline{z_2} = 0\ 0131 & \overline{z_3} = 0\ 2054 \end{array} \tag{25}$$

and the state equation matrices are

$$E_1 = \begin{bmatrix} 1 & 0 & 0 & 0 \\ 0 & 1 & 0 & 0 \\ 0 & 0 & 0.0047 & 0.0045 \\ 0 & 0 & 0.0045 & 0.0131 \end{bmatrix}, \quad E_2 = \begin{bmatrix} 1 & 0 & 0 & 0 \\ 0 & 1 & 0 & 0 \\ 0 & 0 & 0.0047 & 0.0045 \\ 0 & 0 & 0.0045 & 0.0111 \end{bmatrix},$$

$$
E_3 = \begin{bmatrix} 1 & 0 & 0 & 0 \\ 0 & 1 & 0 & 0 \\ 0 & 0 & 0.0047 & 0.003 \\ 0 & 0 & 0.003 & 0.0131 \end{bmatrix}, \quad
E_4 = \begin{bmatrix} 1 & 0 & 0 & 0 \\ 0 & 1 & 0 & 0 \\ 0 & 0 & 0.0047 & 0.003 \\ 0 & 0 & 0.003 & 0.0111 \end{bmatrix},
$$

$$
A_1 = \begin{bmatrix} 0 & 0 & 1 & 0 \\ 0 & 0 & 0 & 1 \\ 0.2054 & 0 & -0.001 & 0 \\ 0 & 0 & 0 & -0.0729 \end{bmatrix},
$$

$$
A_2 = \begin{bmatrix} 0 & 0 & 1 & 0 \\ 0 & 0 & 0 & 1 \\ 0.1813 & 0 & -0.001 & 0 \\ 0 & 0 & 0 & -0.0729 \end{bmatrix}, \quad
B = \begin{bmatrix} 0 \\ 0 \\ 0 \\ 0.1282 \end{bmatrix}.
$$

Table 2: The mechanical and electrical system parameters [12].

| Symbol	Description	Value
m	Mass of the pendulum rod (kg)	0 125
l	Length of the pendulum rod (m)	0 335
r	Length of the pendulum arm (m)	0 215
J_{eq}	Equivalent moment of inertia of the pendulum arm and gears (kgm^2)	$3\ 5842 \times 10^{-3}$
J_m	Moment of inertia of the motor rotor (kgm^2)	$3\ 87 \times 10^{-7}$
B_a	Friction coefficient of the pendulum arm $(Nmsrad^{-1})$	0 004
B_r	Friction coefficient of the pendulum rod $(Nmsrad^{-1})$	0 0095
g	Gravity (ms^{-2})	9 81
K_t	Torque constant (NmA^{-1})	$7\ 67 \times 10^{-3}$
K_v	Back EMF constant $(Vsrad^{-1})$	$7\ 67 \times 10^{-3}$
R	Motor armature resistance (Ω)	2 6
K_g	Gearbox ratio	70
η_g	Gearbox efficiency	0 9
η_m	Motor efficiency	0 69

It is assumed that the pendulum starts in the stable downward position. First, the swing up control [12] swings the pendulum up till it reaches the inverted position. When the pendulum rod is within $\pm\phi_0$, it can then be caught in the upright position with the robust T-S fuzzy descriptor controller (9).

The initial values of the estimated states are $\hat{x}=[0\,0\,0\,0]^T$. The proposed HOSM observers (16) and (17) estimate the positions and velocities of the RIP. The observer gains are selected as in (20), (22)- (24) to ensure the convergence of the observers. The chosen gains $\lambda_1\ \alpha_1\ \lambda_2\ \alpha_2\ \lambda_3\ \alpha_3\ \lambda_4$ and α_4 are 40 1500 200 3000 40, 1500 200 and 3000, respectively. The behavior of the proposed observers is shown by the following experimental results. Fig. 3 shows the convergence of the estimated positions θ_{est}, ϕ_{est} to the real positions θ_{mes}, ϕ_{mes}, respectively. Fig. 4 shows the estimates of velocities $\hat{\dot{\theta}}$

and $\hat{\dot{\phi}}$. The results indicate the finite-time convergence and accuracy of estimates of the proposed observers.
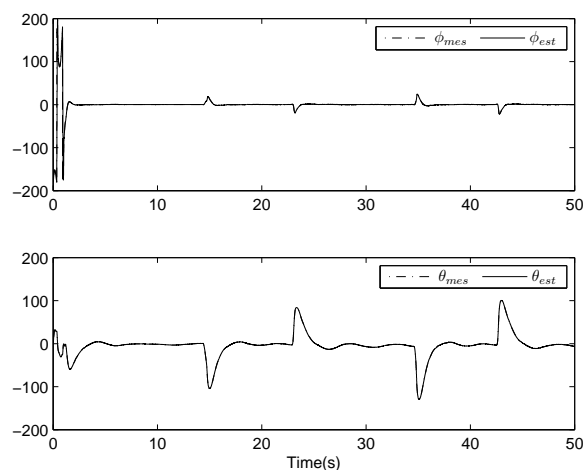
Figure 3: Pendulum rod's position (above) and pendulum arm's position (below): measured (dash-dotted), estimated (solid).
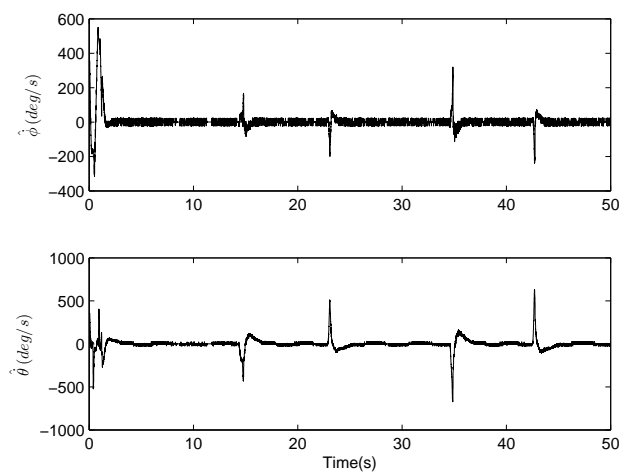
Figure 4: Pendulum rod's velocity estimate (above) and pendulum arm's velocity estimate (below).

Also, as is seen in Fig. 3, the RIP control system demonstrates good performance and maintains the pendulum in the upright position. The robustness is successfully realized by the robust T-S fuzzy descriptor controller in the presence of disturbances at time instants 14 4 s, 23 s, 34 6 s and 42 5 s. The oscillatory behavior observed in Fig. 4 is due to the backlash in the motor's gearbox.

5 Conclusion

This paper considers the state estimation of the T-S fuzzy descriptor system using a high-order sliding mode technique. Two second-order sliding mode observers based on the super-twisting algorithm have been proposed to reconstruct the states. The finite-time convergence and accuracy of estimates are demonstrated through experiments on a real-time example of the rotary inverted pendulum system.

References

[1] S. V. Drakunov and V. Utkin. Sliding Mode Observers, Tutorial. In: *Proc. Decision and Control Conf.* New Orleans, LA, 1995, 3376–3378.

[2] J.-P. Barbot and T. Floquet. Iterative higher order sliding mode observer for nonlinear systems with unknown inputs. *Dynamics of Continuous, Discrete and Impulsive Systems* **17** (6) (2010) 1019–1033.

[3] J. Davila, L. Fridman and A. Levant. Second-Order Sliding-Mode Observer for Mechanical Systems. *IEEE Transactions on Automatic Control* **50** (11) (2005).

[4] H. Rios, J. Davila and L. Fridman. High-order sliding mode observers for nonlinear autonomous switched systems with unknown inputs. *Journal of the Franklin Institute* **349** (10) (2012) 2975–3002.

[5] H. Saadaoui, N. Manamanni, M. Djemai, J.P. Barbot and T. Floquet. Exact differentiation and sliding mode observers for switched Lagrangian systems. *Nonlinear Analysis* **65** (2006) 1050–1069.

[6] T. Floquet and J.-P. Barbot. Super twisting algorithm based step-by-step sliding mode observers for nonlinear systems with unknown inputs. *International Journal of Systems Science* **38** (10) (2007).

[7] J.-P. Barbot, T. Boukhobza and M. Djemai. Sliding mode observer for triangular input form. In: *Proc. Decision and Control Conf.* Kobe, Japan, 2006.

[8] T. Takagi and M. Sugeno. Fuzzy identification of systems and its applications to modeling and control. *IEEE Transactions on SMC* **15** (1985) 116–132.

[9] K. Tanaka and H. O. Wang. *Fuzzy Control Systems and Design Analysis: A Linear Matrix Inequality Approach.* John Wiley & Sons, Inc, 2001.

[10] T. Taniguchi, K. Tanaka, and H. O. Wang. Fuzzy Descriptor Systems and Nonlinear Model Following Control. *IEEE Transactions on Fuzzy Systems* **8** (4) (2000) 442–452.

[11] K. Furuta, M. Yamakita, and S. Kobayashi. Swing-up control of inverted pendulum using pseudo-state feedback. *Journal of Systems and Control Engineering* **206** (6) (1992) 263–269.

[12] Q. V. Dang, B. Allouche, L. Vermeiren, A. Dequidt and M. Dambrine. Design and implementation of a robust fuzzy controller for a rotary inverted pendulum using the Takagi-Sugeno descriptor representation. In: *16th IFAC WC* Prague, Czech Republic, 2005.

[13] Y. Shtessel, C. Edwards, L. Fridman and A. Levant. *Sliding Mode Control and Observation.* Control Engineering, Springer, 2014.

[14] A. Choukchou-Braham, B. Cherki, M. Djemai and K. Busawon. *Analysis and Control of Underactuated Mechanical Systems.* Springer, Verlag, 2013.

[15] H. Hamdi, M. Rodrigues, C. Mechmeche and N. Benhadj Braiek. Observer based Fault Tolerant Control for Takagi-Sugeno Nonlinear Descriptor systems. In: *Proc. Control, Engineering & Information Technology Conf.*, 2013, 52–57.

Chaos Synchronization and Anti-Synchronization of Two Fractional-Order Systems via Global Synchronization and Active Control

M. Labid [1] and N. Hamri [2*]

[1] *Department of Mathematics, University Center of Mila, Mila 43000, Algeria*
[2] *Laboratory of Mathematics and Their Interactions,*
Department of Science and Technology, University Center of Mila, Mila 43000, Algeria.

Abstract: This paper investigates the phenomenon of chaos synchronization and anti-synchronization of two identical chaotic systems of the fractional-order lesser date moth model via the methods of global synchronization and active control. Numerical examples are provided to illustrate the results.

Keywords: *chaos; synchronization; anti-synchronization; active control; fractional-order systems.*

Mathematics Subject Classification (2010): 34H10, 37N35, 93C10, 93C15, 93C95.

1 Introduction

In recent years, the fractional calculus has become an excellent tool in modeling many physical phenomena and engineering problems [16]. One of the very important areas of application of fractional calculus is chaos theory. Chaos is a very interesting non-linear phenomenon that has been intensively studied over the past two decades. The chaos theory is found to be useful in many areas such as data encryption [14], financial systems [13], biology [17] and biomedical engineering [2], etc. Fractional-order chaotic dynamical systems have begun to attract a lot of attention in recent years and can be seen as a generalization of chaotic dynamic integer-order systems. Recently, the study of the synchronization of fractional-order chaotic systems has become an active area of

---

* Corresponding author: `mailto:mes.laabid@centre-univ-mila.dz`

research because of its potential applications in secure communication and cryptography [9, 10]. The synchronization of fractional-order chaotic systems was first studied by Deng and Li [18]. Then the idea of the synchronization is to use the output of the master (drive) system to control the slave (response) system so that the output of the slave system tracks asymptotically the output of the master system. In the past twenty years, various types of synchronization have been proposed and investigated, e.g., complete synchronization [20], lag synchronization [4], phase synchronization [8], project synchronization [15], generalized synchronization [6], etc. As a special case of generalized synchronization, anti-synchronization is achieved when the sum of the states of master and slave systems converges to zero asymptotically with time. In other words, the anti-synchronization is the use of the output of the master system to control the slave system so that the states of the slave system have the same amplitude but opposite signs as the states of the master system. In this paper, we apply global synchronization theory to synchronize two identical chaotic systems, we demonstrate the technique capability on the synchronization of fractional-order lesser date moth model [12] and we apply active control theory to synchronize and anti-synchronize two identical chaotic systems, we demonstrate the technique capability on the synchronization and anti-synchronization of fractional-order lesser date moth model.

The paper is organized as follows. In Section 2, we describe the problem statement and our methodology. In Section 3, a fractional-order lesser date moth model is presented. In Section 4, we discuss the chaos synchronization of two identical fractional-order lesser date moth models using global synchronization. In Section 5, we discuss the chaos synchronization of two identical fractional-order lesser date moth models using active control. In Section 6, we discuss the chaos anti-synchronization of two identical fractional-order lesser date moth models using active control. Section 7 gives the conclusion of this paper.

2 Problem Statement and Our Methodology

Consider the chaotic system described by the dynamics

$$D^\alpha x_1 = Ax_1 + g(x_1), \tag{1}$$

where $x_1 \in \mathbb{R}^n$ is the state vector, $A \in \mathbb{R}^{n \times n}$ is a constant matrix, $g(x_1)$ is a continuous nonlinear function, and D^α is the Caputo fractional derivative. We consider the system (1) as the master or drive system. As the slave or response system, we consider the following chaotic system described by the dynamics

$$D^\alpha x_2 = Ax_2 + g(x_2) + u, \tag{2}$$

where $x_2 \in \mathbb{R}^n$ is the state vector, $A \in \mathbb{R}^{n \times n}$ is a constant matrix, and $g(x_2)$ is a continuous nonlinear function and $u \in \mathbb{R}^n$ is the controller of the slave system.

The global chaos synchronization problem is to design a controller which synchronizes the states of the master system (1) and the slave system (2) for all initial conditions $x(0), y(0) \in \mathbb{R}^n$. The synchronization error is defined as

$$e = x_2 - x_1.$$

Then the synchronization error dynamics is obtained as

$$D^\alpha e = Ae + g(x_2) - g(x_1) + u. \tag{3}$$

Thus, the global synchronization problem is essentially to find a controller u so as to stabilize the error dynamics (3) for all initial conditions $e(0) \in \mathbb{R}^n$, i.e.,

$$lim_{t \to \infty} \|e(t)\| = 0$$

for all initial conditions $e(0) \in \mathbb{R}^n$.

Theorem 2.1 *[3] The following autonomous system:*

$$D^\alpha x = Ax, \ x(0) = 0,$$

where $0 < \alpha < 1$, $x \in \mathbb{R}^n$, $A \in \mathbb{R}^{n \times n}$, is asymptotically stable if and only if $|arg(eig)A| > \alpha \frac{\pi}{2}$. In this case, each component of the states decays towards 0 like $t^{-\alpha}$. Also, this system is stable if and only if $|arg(eig)A| \geq \alpha \frac{\pi}{2}$ and those critical eigenvalues that satisfy $|arg(eig)A| = \alpha \frac{\pi}{2}$ have geometric multiplicity one.

3 Fractional-Order Lesser Date Moth Model

Following [12], the model of biocontrol of the lesser date moth in palm trees can be written as follows:

$$\begin{cases} \frac{dP}{d\tau} = rP\left(1 - \frac{P}{K}\right) - \frac{bPL}{a+P}, \\ \frac{dL}{d\tau} = -dL + \frac{mPL}{a+P} - pLN, \\ \frac{dN}{d\tau} = -\mu N + qLN. \end{cases} \tag{4}$$

The model consists of three populations: the palm tree whose population density at time t is denoted by P; the pest (lesser date moth) whose population density is denoted by L; the predator whose population density is denoted by N. Here all the parameters r, K, b, a, d, m, p, μ, and q are positive. One can reduce the number of parameters in system (4) by using the following transformations: $P = Kx$, $L = \frac{Kr}{b}y$, $N = \frac{r}{p}z$, $\tau = \frac{t}{r}$, then we have the following dimensionless system:

$$\begin{cases} \frac{dx}{dt} = x(1-x) - \frac{xy}{\beta+x}, \\ \frac{dy}{dt} = -\delta y + \frac{\gamma xy}{\beta+x} - yz, \\ \frac{dz}{dt} = -\eta z + \sigma yz, \end{cases} \tag{5}$$

where $\beta = \frac{a}{K}$, $\delta = \frac{d}{r}$, $\gamma = \frac{m}{r}$, $\eta = \frac{\mu}{r}$ and $\sigma = \frac{qK}{b}$.

We introduce fractional order into the ODE model (5). The new system is described by the following set of fractional-order differential equations:

$$\begin{cases} D^\alpha x = x(1-x) - \frac{xy}{\beta+x}, \\ D^\alpha y = -\delta y + \frac{\gamma xy}{\beta+x} - yz, \\ D^\alpha z = -\eta z + \sigma yz, \end{cases} \tag{6}$$

where D^α is the Caputo fractional derivative.

The lesser date moth model is chaotic when the parameter values are taken as $\beta = 1.15$, $\delta = \eta = 1$, $\gamma = 3$, $\sigma = 3$, $\alpha = 0.95$. Figure 1 describes the state portrait of the lesser date moth model.
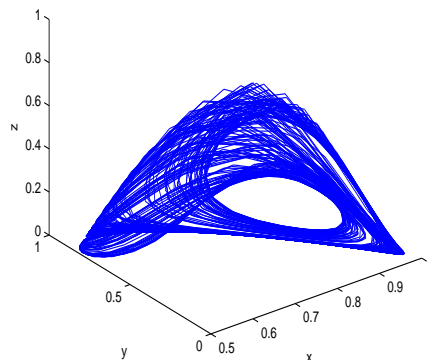
Figure 1: The state portrait of the lesser date moth model.

4 Synchronization of Identical Fractional-Order Lesser Date Moth Systems by Global Synchronization

In this section, we study chaos synchronization between two identical chaotic systems of the fractional-order lesser date moth model using the global synchronization. Thus, the master system is described by

$$
\begin{cases}
D^\alpha x_1 = x_1(1-x_1) - \frac{x_1 y_1}{\beta+x_1}, \\
D^\alpha y_1 = -\delta y_1 + \frac{\gamma x_1 y_1}{\beta+x_1} - y_1 z_1, \\
D^\alpha z_1 = -\eta z_1 + \sigma y_1 z_1,
\end{cases}
\tag{7}
$$

the equations of the slave system are

$$
\begin{cases}
D^\alpha x_2 = x_2(1-x_2) - \frac{x_2 y_2}{\beta+x_2} + k_1(x_1-x_2), \\
D^\alpha y_2 = -\delta y_2 + \frac{\gamma x_2 y_2}{\beta+x_2} - y_2 z_2 + k_2(y_1-y_2), \\
D^\alpha z_2 = -\eta z_2 + \sigma y_2 z_2 + k_3(z_1-z_2).
\end{cases}
\tag{8}
$$

Consider the case of the integer-order systems (when $\alpha = 1$), and then by subtracting (7) from (8), we obtain

$$
\begin{cases}
\dot{e}_1 = e_1 - (x_1+x_2)e_1 - (\frac{y_1}{\beta+x_1})e_1 + \frac{x_2 y_1}{(\beta+x_1)(\beta+x_2)}e_1 - \frac{x_2}{\beta+x_2}e_2 - k_1 e_1, \\
\dot{e}_2 = -\delta e_2 + [\frac{\gamma y_1}{\beta+x_1} - \frac{\gamma x_2 y_1}{(\beta+x_1)(\beta+x_2)}]e_1 - (z_2 - \frac{x_2}{\beta+x_2})e_2 - y_1 e_3 - k_2 e_2, \\
\dot{e}_3 = -\eta e_3 + \sigma(y_1 e_3 + z_2 e_2) - k_3 e_3,
\end{cases}
\tag{9}
$$

where $e_1 = x_1 - x_2, \quad e_2 = y_1 - y_2, \quad e_3 = z_1 - z_2$. In matrix form, (9) can be rewritten in the form

$$
\dot{e} = (A - K)e + M_{x_1,x_2}e,
\tag{10}
$$

i.e.,

$$\dot{e} = \left(\begin{bmatrix} 1 & 0 & 0 \\ 0 & -\delta & 0 \\ 0 & 0 & -\eta \end{bmatrix} - \begin{bmatrix} k_1 & 0 & 0 \\ 0 & k_2 & 0 \\ 0 & 0 & k_3 \end{bmatrix}\right)\begin{bmatrix} e_1 \\ e_2 \\ e_3 \end{bmatrix} +$$

$$\begin{bmatrix} -(x_1+x_2)-\frac{y_1}{\beta+x_1}+\frac{x_2y_1}{(\beta+x_1)(\beta+x_2)} & -\frac{x_2}{\beta+x_2} & 0 \\ \frac{\gamma y_1}{\beta+x_1}-\frac{\gamma x_2 y_1}{(\beta+x_1)(\beta+x_2)} & -z_2+\frac{\gamma x_2}{\beta+x_2} & -y_1 \\ 0 & \sigma z_2 & \sigma y_2 \end{bmatrix}\begin{bmatrix} e_1 \\ e_2 \\ e_{u_3} \end{bmatrix},$$

where

$$e = [e_1, e_2, e_3]^T, \quad K = \begin{bmatrix} k_1 & 0 & 0 \\ 0 & k_2 & 0 \\ 0 & 0 & k_3 \end{bmatrix},$$

$$M_{x_1,x_2} = \begin{bmatrix} -(x_1+x_2)-\frac{y_1}{\beta+x_1}+\frac{x_2y_1}{(\beta+x_1)(\beta+x_2)} & -\frac{x_2}{\beta+x_2} & 0 \\ \frac{\gamma y_1}{\beta+x_1}-\frac{\gamma x_2 y_1}{(\beta+x_1)(\beta+x_2)} & -z_2+\frac{\gamma x_2}{\beta+x_2} & -y_1 \\ 0 & \sigma z_2 & \sigma y_2 \end{bmatrix}, \quad (11)$$

$$A = \begin{bmatrix} 1 & 0 & 0 \\ 0 & -\delta & 0 \\ 0 & 0 & -\eta \end{bmatrix}. \quad (12)$$

From (11) and (12), we get
$$(A + M_{x_1,x_2}) + (A + M_{x_1,x_2})^T =$$

$$\begin{bmatrix} -2(x_1+x_2)-2\frac{y_1}{\beta+x_1}+2\frac{x_2y_1}{(\beta+x_1)(\beta+x_2)}+2 & -\frac{x_2}{\beta+x_2}+\frac{\gamma y_1}{\beta+x_1}-\frac{\gamma x_2 y_1}{(\beta+x_1)(\beta+x_2)} & 0 \\ \frac{\gamma y_1}{\beta+x_1}-\frac{\gamma x_2 y_1}{(\beta+x_1)(\beta+x_2)}-\frac{x_2}{\beta+x_2} & -2z_2+\frac{2\gamma x_2}{\beta+x_2}-2\delta & -y_1+\sigma z_2 \\ 0 & \sigma z_2 - y_1 & 2\sigma y_1 - 2\eta \end{bmatrix}. \quad (13)$$

By selecting the feedback control gains k_1, k_2 and k_3 that must satisfy the conditions given in [7], the two coupled integer-order lesser date moth systems are asymptotically synchronized, i.e., synchronization is achieved if the feedback control gains satisfy the following inequalities:

$$\begin{cases} k_1 \geq \frac{1}{2}[-2(x_1+x_2)-\frac{2y_1}{\beta+x_1}+\frac{2x_2y_1}{(\beta+x_1)(\beta+x_2)}+2+|-\frac{x_2}{\beta+x_2}+\frac{\gamma y_1}{\beta+x_1}-\frac{\gamma x_2 y_1}{(\beta+x_1)(\beta+x_2)}|-\mu], \\ k_2 \geq \frac{1}{2}[-2z_2+\frac{2\gamma x_2}{\beta+x_2}-2\delta+|-\frac{\gamma x_2 y_1}{(\beta+x_1)(\beta+x_2)}-\frac{x_2}{\beta+x_2}+\frac{\gamma y_1}{\beta+x_1}|+|-y_1+\sigma z_2|-\mu], \\ k_3 \geq \frac{1}{2}[-2\sigma y_1 - 2\eta + |\sigma z_2 - y_1| - \mu]. \end{cases} \quad (14)$$

Now, the coupled fractional-order lesser date moth systems (7) and (8) are integrated numerically with the parameter values $\gamma = 3$, $\delta = \eta = 1$, $\sigma = 3$, $\beta = 1.15$ and the same fractional order $\alpha = 0.95$. By selecting the feedback control gains as $k_1 = 1.2$, $k_2 = 2.45$, $k_3 = 0.7$, which satisfy the inequalities (14), the drive and response lesser date moth systems (7) and (8) are asymptotically synchronized. For the numerical simulations, we use some documented data for some parameters like $\gamma = 3$, $\delta = \eta = 1$, $\sigma = 3$, $\beta = 1.15$, $h = 0.85$, $\alpha = 0.95$, $\mu = -3.5$, then we have $(x_1, y_1, z_1) = (0.7, 0.3, 0.8)$ and $(x_2, y_2, z_2) = (0.98, 0.35, 0.65)$ and $k_1 = 1.2$, $k_2 = 2.45$, $k_3 = 0.7$. The simulation results are illustrated in Figure 2.
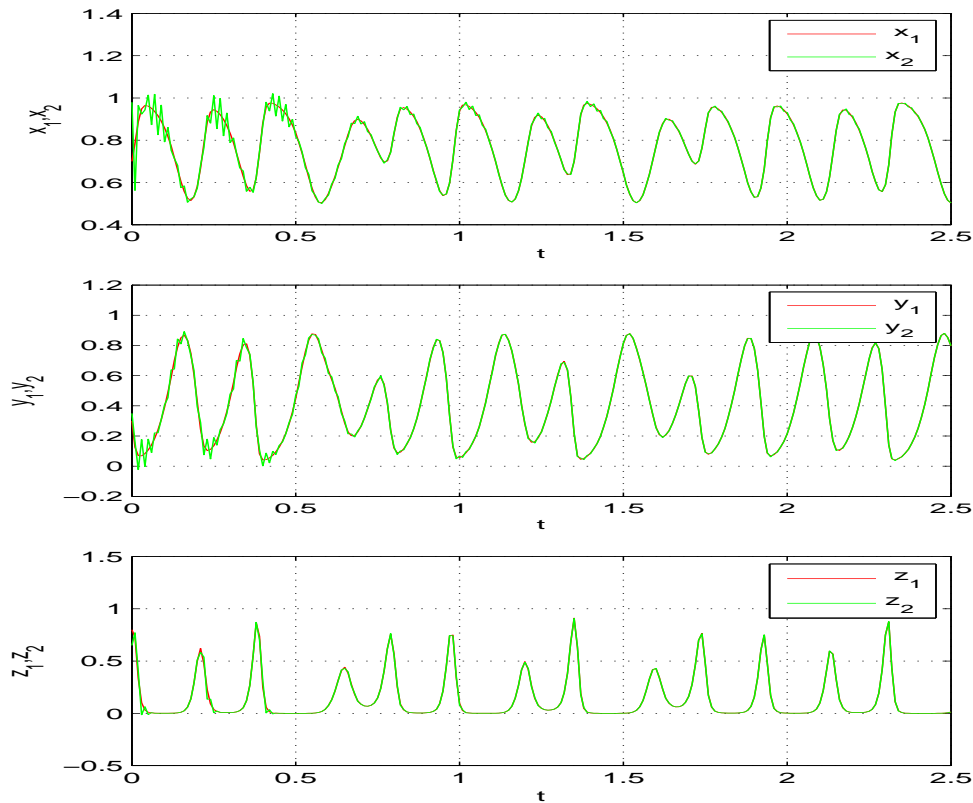
Figure 2: Synchronization of identical fractional-order lesser date moth model for

$$k_1 = 1.2, k_2 = 2.45,\ k_3 = 0.7.$$

5 Synchronization of Identical Fractional-Order Lesser Date Moth Systems by Active Control

In this section, we study chaos synchronization between two identical chaotic systems of the fractional-order lesser date moth model using the technique of active control [5]. Thus, the master system is described by

$$\begin{cases} D^\alpha x_1 = x_1(1 - x_1) - \frac{x_1 y_1}{\beta + x_1}, \\ D^\alpha y_1 = -\delta y_1 + \frac{\gamma x_1 y_1}{\beta + x_1} - y_1 z_1, \\ D^\alpha z_1 = -\eta z_1 + \sigma y_1 z_1, \end{cases} \tag{15}$$

the equations of the slave system are

$$
\begin{cases}
D^\alpha x_2 = x_2(1 - x_2) - \frac{x_2 y_2}{\beta + x_2} + u_1(t), \\
D^\alpha y_2 = -\delta y_2 + \frac{\gamma x_2 y_2}{\beta + x_2} - y_2 z_2 + u_2(t), \\
D^\alpha z_2 = -\eta z_2 + \sigma y_2 z_2 + u_3(t),
\end{cases}
\tag{16}
$$

where $u_1(t)$, $u_2(t)$, $u_3(t)$ are the active controls.

Subtracting (16) from (15) gives

$$
\begin{cases}
D^\alpha e_1 = e_1 - x_1^2 + x_2^2 - (\frac{y_2}{\beta + x_2})e_1 + \frac{x_1 y_2}{(\beta + x_1)(\beta + x_2)}e_1 - \frac{x_1}{\beta + x_1}e_2 + u_1(t), \\
D^\alpha e_2 = -\delta e_2 + [\frac{\gamma y_2}{\beta + x_2} - \frac{\gamma x_1 y_2}{(\beta + x_1)(\beta + x_2)}]e_1 - (z_2 - \frac{x_1}{\beta + x_1})e_2 - y_1 e_3 + u_2(t), \\
D^\alpha e_3 = -\eta e_3 + \sigma(y_1 e_3 + z_2 e_2) + u_3(t),
\end{cases}
\tag{17}
$$

where $e_1 = x_2 - x_1$, $e_2 = y_2 - y_1$, $e_3 = z_2 - z_1$.

We introduce a Lyapunov function in terms of the squares of these variables:

$$
V(e) = \frac{1}{2} \sum_{i=1}^{3} e_i^2.
\tag{18}
$$

The fractional-order derivative of the Lyapunov function is given as

$$
\begin{aligned}
D^\alpha V(e) &= e_1[e_1 - (x_2 + x_1)e_1 - (\frac{y_2}{\beta + x_2})e_1 + \frac{x_1 y_2}{(\beta + x_2)(\beta + x_1)}e_1 - \frac{x_1}{\beta + x_1}e_2] \\
&+ e_2[-\delta e_2 + (\frac{\gamma y_2}{\beta + x_2}e_1 - \frac{\gamma x_1 y_2}{(\beta + x_1)(\beta + x_2)})e_1 - (z_2 e_2 + \frac{\gamma x_1}{\beta + x_1})e_2 - y_1 e_3] \\
&+ e_3[-\eta e_3 + \sigma z_2 e_2 + \sigma y_1 e_3] + \sum_{i=1}^{3} u_i(t)e_i(t).
\end{aligned}
\tag{19}
$$

From this equation, we conclude that if the active control functions u_i are chosen such that

$$
\begin{aligned}
u_1(t) &= -[2e_1 - (x_1 + x_2)e_1 - (\frac{y_2}{\beta + x_2})e_1 + \frac{x_1 y_2}{(\beta + x_1)(\beta + x_2)}e_1 - \frac{x_1}{\beta + x_1}e_2], \\
u_2(t) &= -[(\frac{\gamma y_2}{\beta + x_2} - \frac{\gamma x_1 y_2}{(\beta + x_1)(\beta + x_2)})e_1 - (z_2 - \frac{\gamma x_1}{\beta + x_1})e_2 - y_1 e_3], \\
u_3(t) &= -[\sigma z_2 e_2 + \sigma y_1 e_3],
\end{aligned}
$$

equation (19) becomes

$$
D^\alpha V(e) = -(e_1^2 + \delta e_2^2 + \eta e_3^2) \le 0.
\tag{20}
$$

According to the inequality (18), the system is stable. For the numerical simulations, we use some documented data for some parameters like $\gamma = 3$, $\delta = \eta = 1$, $\sigma = 3$, $\beta = 1.15$, $h = 0.85$, $\alpha = 0.95$, then we have $(x_1, y_1, z_1) = (0.7, 0.3, 0.8)$ and $(x_2, y_2, z_2) = (0.12, 0.21, 0.13)$. The simulation results are illustrated in Figure 3.
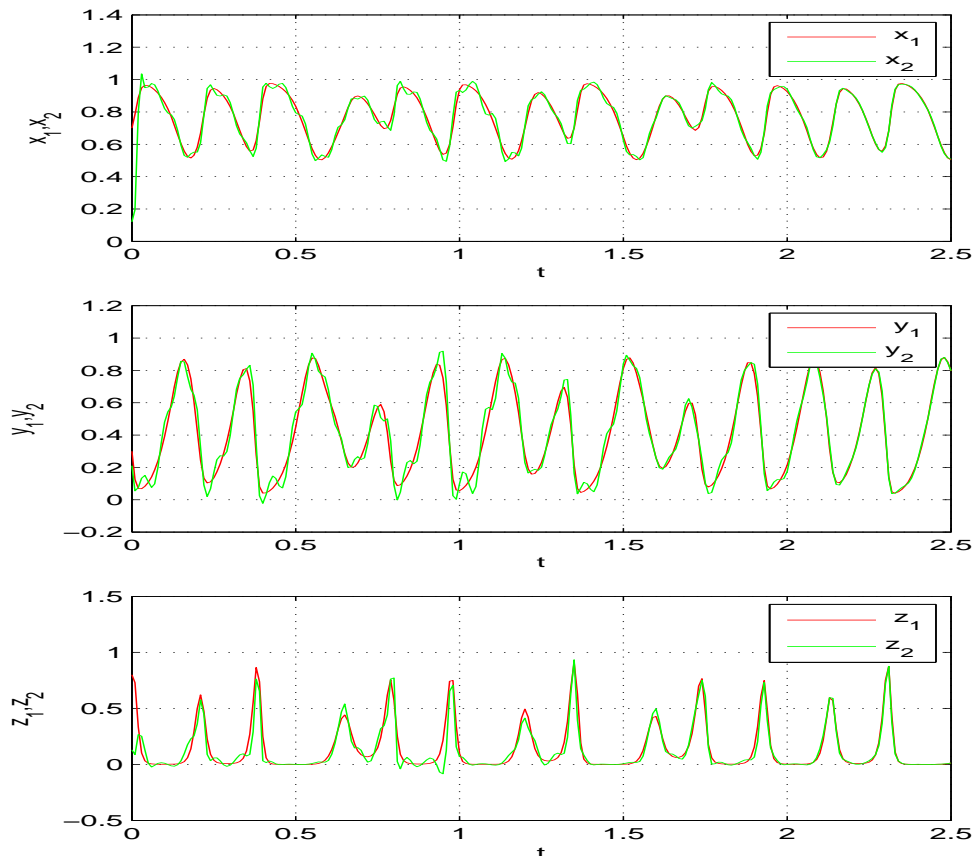
Figure 3: Synchronization of identical fractional-order lesser date moth model.

6   Anti-Synchronization of Identical Fractional-Order Lesser Date Moth Systems by Active Control

In this section, we study chaos anti-synchronization between two identical chaotic systems of the fractional-order lesser date moth model using the technique of active control. Thus, the drive system is described by

$$
\begin{cases}
D^\alpha x_1 = x_1(1 - x_1) - \frac{x_1 y_1}{\beta + x_1}, \\
D^\alpha y_1 = -\delta y_1 + \frac{\gamma x_1 y_1}{\beta + x_1} - y_1 z_1, \\
D^\alpha z_1 = -\eta z_1 + \sigma y_1 z_1;
\end{cases}
\tag{21}
$$

the equations of the response system are

$$
\begin{cases}
D^\alpha x_2 = x_2(1 - x_2) - \frac{x_2 y_2}{\beta + x_2} + u_1(t), \\
D^\alpha y_2 = -\delta y_2 + \frac{\gamma x_2 y_2}{\beta + x_2} - y_2 z_2 + u_2(t), \\
D^\alpha z_2 = -\eta z_2 + \sigma y_2 z_2 + + u_3(t),
\end{cases}
\tag{22}
$$

where u_1, u_2, u_3 are the active controls.

The anti-synchronization error is defined as

$$\begin{cases} e_1 = x_1 + x_2, \\ e_2 = y_1 + y_2, \\ e_3 = z_1 + z_2. \end{cases} \tag{23}$$

A simple calculation gives the error dynamics

$$\begin{cases} D^\alpha e_1 = e_1 - x_2^2 - x_1^2 - \frac{x_2 y_2}{\beta + x_2} - \frac{x_1 y_1}{\beta + x_1} + u_1(t), \\ D^\alpha e_2 = -\delta e_2 + \frac{\gamma x_1 y_1}{\beta + x_1} + \frac{\gamma x_2 y_2}{\beta + x_2} - z_2 y_2 - y_1 z_2 + u_2(t), \\ D^\alpha e_3 = -\eta e_3 + \sigma y_1 z_1 + \sigma y_2 z_2 + u_3(t). \end{cases} \tag{24}$$

We consider the active nonlinear controller defined by

$$\begin{cases} u_1(t) = x_2^2 + x_1^2 + \frac{x_2 y_2}{\beta + x_2} + \frac{x_1 y_1}{\beta + x_1} - 2e_1, \\ u_2(t) = -\frac{\gamma x_1 y_1}{\beta + x_1} - \frac{\gamma x_2 y_2}{\beta + x_2} + z_2 y_2 + y_1 z_2, \\ u_3(t) = -\sigma y_2 z_2 - \sigma y_1 z_1. \end{cases} \tag{25}$$

Substitution of (25) into (24) yields the linear error dynamics

$$\begin{cases} D^\alpha e_1 = -e_1, \\ D^\alpha e_2 = -\delta e_2, \\ D^\alpha e_3 = -\eta e_3. \end{cases} \tag{26}$$

We consider the quadratic Lyapunov function defined by

$$V(e) = \frac{1}{2} e^T e = \frac{1}{2}(e_1^2 + e_2^2 + e_3^2), \tag{27}$$

which is a positive definite function on $\mathbb{R}^3$. The fractional-order derivative of the Lyapunov function is given as

$$D^\alpha V(e) = -e_1^2 - \delta e_2^2 - \eta e_3^2 \leq 0. \tag{28}$$

According to the inequality (27), the system is stable. For the numerical simulations, we use some documented data for some parameters like $\gamma = 3$, $\delta = \eta = 1$, $\sigma = 3, \beta = 1.15$, $h = 0.85$, $\alpha = 0.95$, then we have $(x_1, y_1, z_1) = (0.7, 0.3, 0.8)$ and $(x_2, y_2, z_2) = (-0.99, -0.11, -0.15)$. The simulation results are illustrated in Figure 4.

7 Conclusion

In this paper, we have studied the phenomenon of chaos synchronization and anti-synchronization between two identical chaotic systems of the fractional-order lesser date moth model. Our results demonstrate that if one uses the technique of global synchronization and the technique of active control, chaos synchronization can be achieved between two identical chaotic systems. On the other hand, if one uses the technique of active control, chaos anti-synchronization can be achieved between two identical chaotic systems.
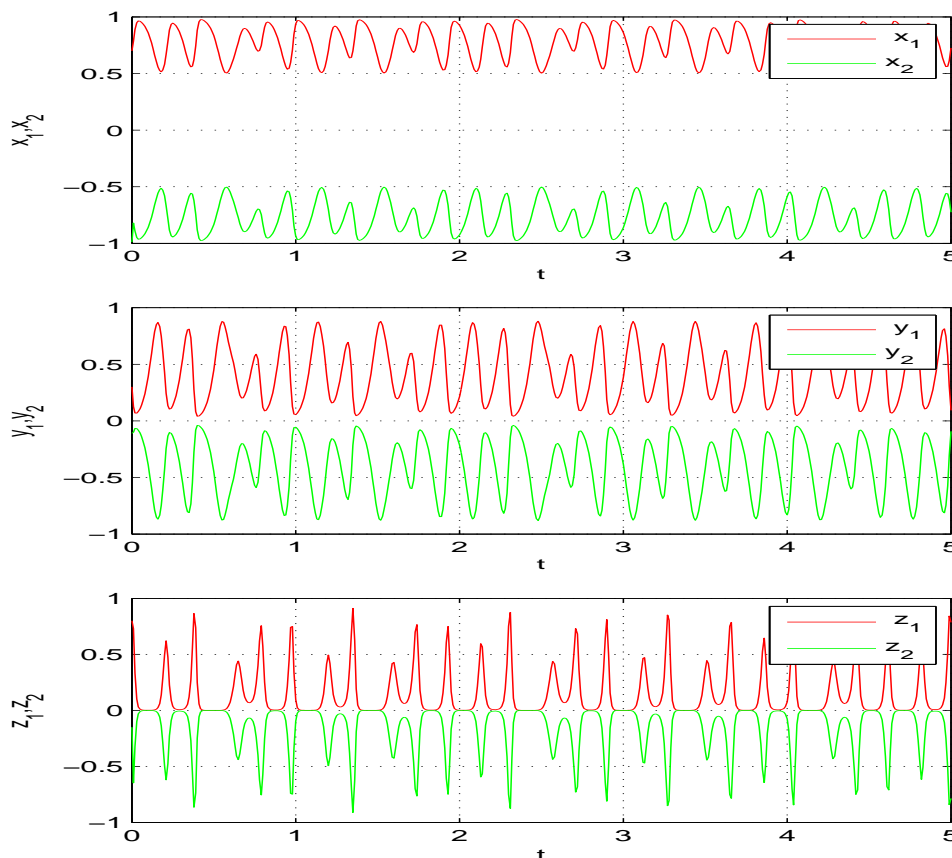
Figure 4: Anti-synchronization of identical fractional-order lesser date moth model.

References

[1] A. E. Matouk. Chaos, feedback control and synchronization of a fractional-order modified autonomous Van der Pol-Duffing circuit. *Commun Nonlinear Sci. Numer. Simulat.* **16** (2011) 975–986.

[2] B. Zsolt. Chaos theory and power spectrum analysis in computerized cardiotocography. *Eur. J. Obstet. Gynecol. Reprod. Biol.* **71** (2) (1997) 163–168.

[3] D. Matignon. Stability result on fractional differential equations with applications to control processing. *Computational Engineering in Systems and Application multi-conference, IMACS, In: IEEE-SMC Proceedings, Lille, France* **2** (1996) 963–968.

[4] D. Pazo, M. A. Zaks and J. Kurths. Role of unstable periodic orbit in phase and lag synchronization between coupled chaotic oscillators. *Chaos* **13** (2003) 309–318.

[5] E. W. Bai and K. E. Lonngren. Synchronization of two Lorenz systems using active control. *Chaos, Solitons and Fractals*, **9** (1998) 1555–1561.

[6] G. Alvarez, S. Li, F. Montoya, G. Pastor and M. Romera. Breaking projective chaos synchronization secure communication using filtering and grneralized synchronization. *Chaos, Solutons and Fractals* **24** (2005) 775–783.

[7] G. P. Jiang, K. S. Tang and G. Chen. A simple global synchronization criterion for coupled chaotic systems. *Chaos, Solitons and Fractals* **15** (2003) 925–935.

[8] H. Targhvafard and G. H. Enjace. Phase and anti-phase synchronization of fractional-order chaotic systems via active control. *Commun. Nonlinear Sci. Numer. Simul.* **16** (2011) 4079–4408.

[9] K. Murali and M. Lakshmanan. Secure communication using a compound signal from generalized synchronizable chaotic system. *Phys. Letters A* **241** (1998) 303–310.

[10] L. Kocarev and U. Parlitz. General approach for chaotic synchronization with applications to communication. *Phys. Rev. Lett.* **74** (1995) 5028–5030.

[11] L. M. Pecora and T. L. Carroll. Synchronization in chaotic systems. *Phys. Rev. Lett.* **64** (1990) 821–824.

[12] M. El-Shahed, Juan J. Nieto, A. M. Ahmed and I. M. E. Abdelstar. Fractional-order model for biocontrol of the lesser date moth in palm trees and its discretization. *Advance in Difference Equations* (2017) 2017–2295.

[13] N. Laskin. Fractional market dynamics. *Physica A* **287** (2000) 482–492.

[14] N. Zhou, Y. Wang, L. Gong, H. He and J. Wu. Novel single-channel color image encryption algorithm based on chaos and fractional Fourier transform. *Optics Communications* **284** (2011) 2789–2796.

[15] R. Mainieri and J. Rehacek . Projective synchronization in three dimensional chaotic systems. *Phys. Rev. Lett.* **82** (1999) 3042–3045.

[16] S. H. Strogatz. *With Applications to Physics, Biology, Chemistry and Engineering.* Nonlinear Dynamics and Chaos, Perseus Books Pub., 1994.

[17] S. Vaidyanathan. Lotka-Volterra two-species mutualistic biology models and their ecological monitoring. *Pharm. Tech. Research* **8** (2015) 199–212.

[18] W. H. Deng and C.P. Li. Chaos synchronization of the fractional Lü system. *Physica A* **353** (2005) 61–72.

[19] W. Laouira and N. Hamri. Feedback Control of Chaotic systems by Using Jacobian Matrix Conditions. *Nonlinear Dynamics and Systems Theory* **18** (3) (2018) 285–295.

[20] Y. Zhang and J. Sun. Chaotic synchronization and anti-synchronization based on suitable separation. *Physics Letters A* **330** (2004) 442–447.

Comparison of Quadrotor Performance Using Forwarding and PID-Backstepping Control

F. Ouendi [1,3*], S. Houti [2] and M. Tadjine [1]

[1] *Process Control Laboratory, Department of Electrical Engineering, National Polytechnic School of Algiers, 10 avenue Pasteur, Hassan Badi, BP 182, El Harrach, Algiers, Algeria.*
[2] *University of Versailles Saint Quentin, France.*
[3] *University of Mouloud Mammeri Tizi-Ouzou, Algeria.*

Abstract: The purpose of this paper is to discuss a comparative evaluation of the performance of two different controllers, namely a controller based on the forwarding control and a hybrid controller based on the PID-backstepping control in the quadrotor dynamic system which is a sub-system actuated with a high non-linearity. As only four states can be controlled at the same time in the quadrotor, the trajectories are designed on the basis of the four states while the position and the three-dimensional rotation along the axis, called yaw movement, are taken into account.

This paper deals with the forwarding controller and the hybrid controller composed of PID controllers for attitude control and backstepping for controlling the position. The forwarding approach is applied for the nonlinear model of the quadrotor to track the trajectories. Meanwhile the hybrid controller approach for nonlinear model is designed on the basis of a linear model for the PID controller and a nonlinear model for the controller backstepping quadrotor because the performance of the linear model and the nonlinear model around some nominal points is almost similar. Simulink and MATLAB software are used to design the controllers and evaluate the performance of both controllers.

Keywords: *nonlinear systems; feedback control; perturbations; stability; boundedness; simulation.*

Mathematics Subject Classification (2010): 93C10; 93B52; 93C73; 70K20; 34C11.

---

* Corresponding author: mailto:fatima_ouendi@yahoo.fr

1 Introduction

Quadrotors are flying robots that have been investigated in recent years, this is due to their low manufacturing cost as well as their maneuverability, their ability to execute vertical takeoffs and landings and their large fields of application, both military and civil, and, in particular, when human intervention becomes difficult or dangerous [5]. The quadrotors consist of four rotors; two of these rotors rotate in one direction and the two others in the opposite direction. By varying the rotational speeds of these rotors, the quadrotor can make different movements both in translation and in rotation [9].

The quadrotor is classified in the category of the most complex flying systems given the number of physical effects that affect its dynamics, namely aerodynamic effects, gravity, gyroscopic effects, friction and moment of inertia [7]. This complexity results essentially from the fact that the expression of these effects differs for each flight mode. The operation of the quadrotor is so particular. While varying astutely rotors throttles, it is possible to make it go up/go down, to incline it on the left/right (rolling motion: rotation around the x-axis) or forward /back (pitching motion: rotation around the y-axis) or to make it swivel on itself (yaw motion: rotation around the z-axis) The desired roll and pitch angles are deduced from nonholonomic constraints [6].

Finally, all synthesized control laws are validated by simulations for the complete model [6]. A quadrotor is a dynamic vehicle with four input forces, six output coordinators, highly coupled and unstable dynamics [5]. Hence the design of a control law is an interesting challenge [15]. Based on the dynamical system of UAV, many researchers focus on the stability of the attitude control. This is because the moving of the UAV depends on the torque, and the torque has a strong relationship with the UAV attitude [15]. [4] presented the optimized PID method to control the UAV attitude. [13] proposed the fuzzy-PD controller structure with the purpose of combining the behaviors of several PD controller configurations. [3] developed a hybrid optimal backstepping and adaptive fuzzy control for the quadrotor with time-varying disturbance. [18] proposed the synthesis control method to perform the position and attitude tracking control of the dynamical model of the small quadrotor. [7] has combined the backstepping control with the sliding mode control.

Several linear methods, such as the PID and LQR control methods have been applied to control a quadrotor [5, 9, 10]. Since the quadrotor is a nonlinear system, and for a good performance, the nonlinear control methods have been attempted such as the feedback linearization, sliding mode [19], and backstepping control [2, 9, 15]. In [17] the authors used the backstepping strategy and BP nerual network. [9] proposed a PID cascade control of a quadrotor path tracking problem when velocity and acceleration are small. [20] has developed a forwarding algorithm for designing a tracking controller for a high-order nonlinear system in the presence of bounded unknown disturbances. [8] has developped an adaptive backstepping controller design for a quadrotor with unknown disturbances. [15] proposed a trajectory tracking control method for a quadrotor, by using the backstepping control and the dual-loop cascade control.

This paper presents two control techniques applied to a quadrotor for developing a reliable control system for stabilization and trajectory tracking.

A nonlinear forwarding control technique forces the whole system to be able to drive the quadrotor to the desired trajectory of the Cartesian position and yaw angle [20]. A forwarding control algorithm was proposed to stabilize the desired trajectory of position and attitude. Then, we present a control technique based on the development

and the synthesis of a control algorithm based upon a hybrid approach, which combines the backstepping and the PID classic regulation controls to navigate a quadrotor. The backstepping controller was developed to ensure the Lyapunov stability and to follow the desired trajectories [15].

2 Dynamics Models

The quadrotor essentially contains a reticulated rigid structure with four independent rotors propellers launched. Three basic movements are needed to describe all the movements of a quadrotor. The rotational movement about the x-axis is described as a roll motion (φ) and about the y-axis is noted as a pitching motion (θ). The roll motion and the pitching motion can be achieved by balancing the motor speed 2 and 4 and motor 1 and 3, respectively. Lateral and longitudinal acceleration are possible, respectively, by changing the angle φ and θ.

Let $E = \{\overrightarrow{E}_x, \overrightarrow{E}_y, \overrightarrow{E}_z\}$ be the fixed inertial reference, and $B = \{\overrightarrow{B}_x, \overrightarrow{B}_y, \overrightarrow{B}_z\}$ be the reference associated with the center of mass of the quadrotor (see Figure 1).
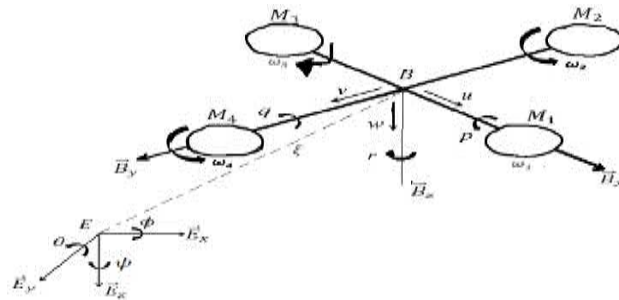

Figure 1: Definition of the frame.

3 The Transformation Matrix

Since it is necessary to deal with two different coordinate systems, namely an inertial marker and a reference linked to the quadrotor's center of mass to explain the position and motion of a quadrotor, a matrix transformation must be used. Here, R is the required transformation matrix that can describe the position and movement of the earth-inertial frame to the fixed frame of the body [9].

The rotation matrix connecting the two marks is defined by the orthogonal matrix: $R(h) : B \rightarrow E; R(h) = R_\Psi R_\theta R_\Phi$ in which : C_x and S_x denote $cos(x)$ and $sin(x)$, respectively, and :

$$R_\Psi = \begin{bmatrix} C_\Psi & -S_\Psi & 0 \\ S_\Psi & C_\Psi & 0 \\ 0 & 0 & 1 \end{bmatrix}, \ R_\theta = \begin{bmatrix} C_\theta & -S_\Psi & S_\theta \\ 0 & 1 & 0 \\ -S_\theta & 0 & C_\theta \end{bmatrix}, \ R_\Phi = \begin{bmatrix} 1 & 0 & 0 \\ 0 & C_\Phi & -S_\Phi \\ 0 & S_\Phi & C_\Phi \end{bmatrix}.$$

(1)

So
$$R(h) = \begin{bmatrix} C_\theta C_\Psi & S_\Phi S_\theta C_\Psi - C_\Phi S_\Psi & C_\Phi S_\theta C_\Psi + S_\Phi S_\Psi \\ C_\theta S_\Psi & S_\Phi S_\theta S_\Psi + S_\Phi C_\Psi & C_\Phi S_\theta S_\Psi - S_\Phi C_\Psi \\ -S_\theta & S_\Phi C_\theta & C_\Phi C_\theta \end{bmatrix}. \tag{2}$$

4 Translational Movement

The gravitational force (F_g) and the aerodynamic drag force (F_a) must be introduced to describe the translational motion of a quadrotor while these forces must be overcome by the thrust of the engines (F_{tb}) to achieve any horizontal motion or movement lace. Here, the translational motion of the quadrotor is described by Newton's second law as follows:

$$m \begin{pmatrix} \ddot{x} \\ \ddot{y} \\ \ddot{z} \end{pmatrix} = \begin{pmatrix} 0 \\ 0 \\ mg \end{pmatrix} + R \begin{pmatrix} 0 \\ 0 \\ -U_1 \end{pmatrix} - k_t \begin{pmatrix} \dot{x} \\ \dot{y} \\ \dot{z} \end{pmatrix}. \tag{3}$$

5 Rotary Mouvement

The Newton-Euler method is used to obtain rotational motion equations for the quadrotor [10].

$$I_w = - \begin{pmatrix} p \\ q \\ r \end{pmatrix} \times I \begin{pmatrix} p \\ q \\ r \end{pmatrix} - \begin{pmatrix} p \\ q \\ r \end{pmatrix} \times \begin{pmatrix} 0 \\ 0 \\ I_r w_r \end{pmatrix} + \begin{pmatrix} IU_2 \\ IU_3 \\ IU_4 \end{pmatrix} - k_r \begin{pmatrix} p \\ q \\ r \end{pmatrix}. \tag{4}$$

The state model of the quadrotor is given as follows: $[x \quad y \quad z \quad \dot{x} \quad \dot{y} \quad \dot{z} \quad \Phi \quad \theta \quad \Psi \quad \dot{\Phi} \quad \dot{\theta} \quad \dot{\Psi}]^T$. A representation of the state space can be obtained as follows by considering equations (1) for the dynamic model :

$$\begin{cases} \dot{x}_1 = x_4, \\ \dot{x}_2 = x_5, \\ \dot{x}_3 = x_6, \\ \dot{x}_4 = \dfrac{U_1}{m} U_x, \\ \dot{x}_5 = \dfrac{U_1}{m} U_y, \\ \dot{x}_6 = \dfrac{U_1}{m}(Cx_7 Cx_8) - g, \\ \dot{x}_7 = x_{10}, \\ \dot{x}_8 = x_{11}, \\ \dot{x}_9 = x_{12}, \\ \dot{x}_{10} = a_1 x_{11} x_{12} + b_1 U_2 \quad with : a_1 = \dfrac{j_y - j_x}{j_x}, a_2 = \dfrac{j_{rz}}{j_x}, b_1 = \dfrac{d}{j_x}, \\ \dot{x}_{11} = a_3 x_{10} x_{12} + b_2 U_3 \quad with : a_3 = \dfrac{j_z - j_x}{j_y}, a_4 = -\dfrac{j_{rz}}{j_y}, b_2 = \dfrac{d}{j_y}, \\ \dot{x}_{12} = a_5 x_{10} x_{11} + b_3 U_4 \quad with : a_5 = \dfrac{j_x - j_y}{j_z}, b_3 = \dfrac{1}{j_z}, \end{cases} \tag{5}$$

where w_i represents the speed of the engine, $U_x = Cx_7Sx_8Cx_9 + Sx_7Sx_9$ and $U_y = Cx_7Sx_8sx_9 - Sx_7Cx_9$. So, we end up with the following dynamic model:

$$\begin{cases} \dot{x}_1 = x_4, \\ \dot{x}_2 = x_5, \\ \dot{x}_3 = x_6, \\ \dot{x}_4 = \dfrac{U_1}{m}(Cx_7Sx_8Cx_9 + Sx_7Sx_9), \\ \dot{x}_5 = \dfrac{U_1}{m}(Cx_7sx_8sx_9 - sx_7Cx_9), \\ \dot{x}_6 = \dfrac{U_1}{m}(Cx_7Cx_8) - g, \\ \dot{x}_7 = x_{10}, \\ \dot{x}_8 = x_{11}, \\ \dot{x}_9 = x_{12}, \\ \dot{x}_{10} = a_1x_{11}x_{12} + b_1U_2, \\ \dot{x}_{11} = a_3x_{10}x_{12} + b_2U_3, \\ \dot{x}_{12} = a_5x_{10}x_{11} + b_3U_4. \end{cases} \tag{6}$$

The writing of the control inputs according to the rotational speeds of the rotors is as follows:

$$\begin{bmatrix} U_1 \\ U_2 \\ U_3 \\ U_4 \end{bmatrix} = \begin{bmatrix} b & b & b & b \\ 0 & -Ib & 0 & Ib \\ -Ib & 0 & Ib & 0 \\ d & -d & d & -d \end{bmatrix} \begin{bmatrix} w_1^2 \\ w_2^2 \\ w_3^2 \\ w_4^2 \end{bmatrix}, \tag{7}$$

where w_i represents the speed of the rotor i. Notice that from the equation of u_x and u_y we find $\Phi_d = arcsin(U_x sin(\Psi_d) - U_y cos(\Psi_d))$ and $\theta_d = arcsin(U_x cos(\Psi_d) + U_y sin(\Psi_d))/(cos(\Phi_d))$.
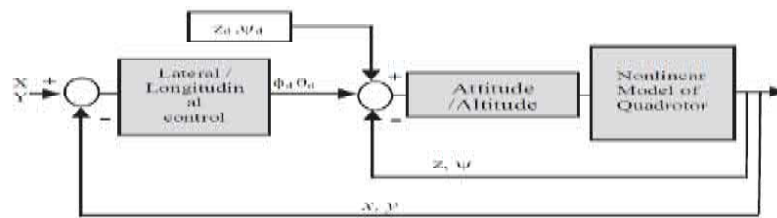
Figure 2: General structure of the quadrotor control system.

In what follows, we develop two strategies to stabilize the orientation and position

of the quadrotor. Their performance is then compared in the next section, based on the numerical simulation results.

6 Strategy of Control

State and output feedback controllers design for dynamic systems with the prescribed and desired properties is a key problem of the strategy of control. At the same time, the properties of control systems such as asymptotic stability, robustness and optimality of the performance indexes are in the foreground [1].

7 The Forwarding Control

It is a non-linear control technique that is considered robust; the synthesis of such a control is done in a systematic way and based on the Lyapunov approach as well as the control in a recursive way for a system that can be written in the following form [14] :

$$
\begin{cases}
\dot{x}_1 = f_1(x_2, \cdots, x_n) + g_1(x_2, \cdots, x_n)u, \\
\dot{x}_2 = f_1(x_2, \cdots, x_n) + g_1(x_2, \cdots, x_n)u, \\
\vdots \\
\dot{x}_{n-1} = f_{n-1}(x_n) + g_{n-1}(x_n)u, \\
\dot{x}_n = u,
\end{cases}
\tag{8}
$$

where $x \in R^n, u \in R$ and $g = [g_1, \cdots, g_{n-1}, 1]^T$.

The aim is to determine a control law that ensures the overall stabilization of the system. This is done in several steps. First, we try to stabilize x_n through u. Taking a function of Lyapunov V_n which is positive definite on R, one seeks to find a return of state $u = a_n(x_n)$ to stabilize x_n. The next step is to increase the system from x_n to x_{n-1}, and replace the control u, with $u = a_n(x_n) + V_{n-1}$. By taking a function of Lyapunov V_{n-1} being positive definite on R^2, one seeks to find a return of state $V_{n-1} = a_{n-1}$ which stabilizes the augmented system. The same procedure is repeated until the last step, where a control u which makes it possible to have an overall stabilization of the system, will be calculated.

8 The Steps of the Synthesis

The synthesis of the control law for the system is carried out in several steps [14].

8.1 First step

We take the system $\dot{x}_n = u$. Let the function of Lyapunov be $V_n = \frac{1}{2}x_n^2$. Its derivative is given by $\dot{V}_n = x_n u$. To make $\dot{V}_n$ negative definite, we can take $u = a_n(x_n) = -\lambda_n LgV_n = -\lambda_n x_n$ with $\lambda_n \geq 0$, which gives $\dot{V}_n = -\lambda_n x_n^2$ which is negative definite on R.

8.2 Second step

Let the system be increased:

$$
\begin{cases}
\dot{x}_{n-1} = f_{n-1}(x_n) + g_{n-1}(x_n)u, \\
\dot{x}_n = u.
\end{cases}
\tag{9}
$$

For $u = a_n(x_n)$, the system becomes

$$
\begin{cases}
\dot{x}_{n-1} = \phi_{n-1}(x_n), \\
\dot{x}_n = -\lambda_n(x_n), \\
\phi_{n-1}(x_n) = f_{n-1}(x_n) - \lambda_n g_{n-1}(x_n)x_n.
\end{cases}
\tag{10}
$$

The term ϕ_{n-1} is called the interconnection term. The temporal solution of the previous system will be : $\widetilde{x}_n(t) = x_n(0)e^{-\lambda_n t}$, $\widetilde{x}_{n-1}(t) = \int_0^t (f_{n-1}(\widetilde{x}_n) - \lambda_n g_{n-1}(\widetilde{x}_n)\widetilde{x}_n)dt + x_{n-1}(0)$. The new control input for the system (9) will be [14]: $u = a_n(x_n) + v_{n-1}$.

The function of Lyapunov for the system is given by [14]

$$
\begin{aligned}
V_{n-1} &= V_n + \frac{1}{2}x_{n-1}^2 + \int_0^\infty \widetilde{x}_{n-1}(t)\phi_{n-1}(\widetilde{x}_n(t))dt \\
&= V_n + \frac{1}{2}lim_{t\longrightarrow\infty}\widetilde{x}_{n-1}^2(t).
\end{aligned}
\tag{11}
$$

9   Synthesis of the Control Laws for the Quadrotor

All tracking errors are written in the following form:

$$
e_i = \begin{cases}
x_i - x_{id}, & i \in 1,2,3,7,8,9; \\
x_i - \dot{x}_{(i-1)d}, & i \in 4,5,6,10,11,12.
\end{cases}
\tag{12}
$$

All the functions of Lyapunov take the form

$$
V_i = \begin{cases}
\frac{1}{2}e_i^2, & i \in \{4,5,6,10,11,12\}; \\
V_{i+1} + \frac{1}{2}lim_{t\longrightarrow\infty}\widetilde{e}_i^2, & i \in \{1,2,3,7,8,9\},
\end{cases}
\tag{13}
$$

where e_i presents the temporal solution of the system. The steps of the order summary will be shown for the subsystem

$$
\begin{cases}
\dot{x}_7 = x_{10}, \\
\dot{x}_{10} = a_1 x_{11} x_{12} + b_1 U_2.
\end{cases}
\tag{14}
$$

Let the tracking error be defined by $e_7 = x_7 - x_{7d}$. Its dynamics is described by $\dot{e}_7 = x_{10} - \dot{x}_{7d}$. If we set $e_{10} = x_{10} - \dot{x}_{7d}$, the system (14) becomes

$$
\dot{e}_7 = e_{10}, \quad \dot{e}_{10} = a_1 x_{11} x_{12} - \ddot{x}_{7d} + b_1 U_2.
\tag{15}
$$

The synthesis is done in two steps.

9.1   The first step

We consider only the second equation of the system (15). Let the function of Lyapunov be $V_{10} = \frac{1}{2}e_{10}^2$. Its derivative is $\dot{V}_{10} = e_{10}\dot{e}_{10}$. To make $\dot{V}_{10}$ negative definite, we can choose the control

$$
U_2 = a_{10}(x) = \frac{1}{b_1}(-a_1 x_{11} x_{12} - \lambda_{10}e_{10} + \ddot{x}_{7d})\lambda_{10} \geq 0.
\tag{16}
$$

We will have $\dot{V}_{10} = -\lambda_{10}e_{10}^2$ which is negative on R. This control will ensure the convergence of e_{10} towards the origin.

9.2   The second step

By replacing the control found in the previous step in the system (15), we get $\dot{e}_7 = e_{10}$ and $\dot{e}_{10} = -\lambda_{10}e_{10}$. The temporal solution of this system is $\widetilde{e}_7(t) = -\frac{1}{\lambda_{10}}e_{10}(0)e^{\lambda_{10}t} + e_7(0) + \frac{1}{\lambda_{10}}e_{10}(0)$, $\widetilde{e}_{10}(t) = e_{10}(0)e^{-\lambda_{10}t}$. We put $e_{10}(0) = e_{10}$ and $e_7(0) = e_7$. Let the function of Lyapunov be $V_7 = V_{10} + \frac{1}{2}lim_{t\longrightarrow\infty}\widetilde{e}_7^2(t)$. So, $V_7 = \frac{1}{2}[e_{10}^2 + (e_7 + \frac{1}{\lambda_{10}}e_{10})^2]$. If we put $U_2 = a_{10}(x) + w_{10}$, the derivative of V_7 will be $\dot{V}_7 = -\lambda_{10}e_{10}^2 + [\frac{e_7}{\lambda_{10}} + (\frac{1}{\lambda_{10}^2} + 1)e_{10}]b_1 w_{10}$. To make $\dot{V}_7$ negative, we can take

$$w_{10} = -\frac{\lambda_7}{b_1}[\frac{e_7}{\lambda_{10}} + (\frac{1}{\lambda_{10}^2} + 1)e_{10}], \quad \lambda_7 \geq 0. \tag{17}$$

The control U_2 becomes $U_2 = \frac{1}{b_1}(-a_1 x_{11} x_{12} - \frac{\lambda_7}{\lambda_{10}}e_7 - (\frac{\lambda_7}{\lambda_{10}^2} + \lambda_7 + \lambda_{10})e_{10} + \ddot{x}_{7d}$.

This control will stabilize the system (14). The same steps are taken to determine U_1, U_3, U_4, U_x, U_y. The system controls with forwarding are given as follows:

$$\begin{cases} U_2 = \dfrac{1}{b_1}(-a_1 x_{11} x_{12} - \dfrac{\lambda_7}{\lambda_{10}}e_7 - (\dfrac{\lambda_7}{\lambda_{10}^2} + \lambda_7 + \lambda_{10})e_{10} + \ddot{x}_{7d}, \\[2mm] U_3 = \dfrac{1}{b_2}(-a_1 x_{11} x_{12} - \dfrac{\lambda_8}{\lambda_{11}}e_8 - (\dfrac{\lambda_8}{\lambda_{11}^2} + \lambda_8 + \lambda_{11})e_{11} + \ddot{x}_{8d}, \\[2mm] U_4 = \dfrac{1}{b_3}(-a_5 x_{10} x_{11} - \dfrac{\lambda_9}{\lambda_{12}}e_9 - (\dfrac{\lambda_9}{\lambda_{12}^2} + \lambda_9 + \lambda_{12})e_{12} + \ddot{x}_{9d}, \\[2mm] U_1 = \dfrac{m}{cx_7 cx_8}(g - \dfrac{\lambda_3}{\lambda_6}e_3 - (\dfrac{\lambda_3}{\lambda_6^2} + \lambda_3 + \lambda_6)e_6 + \ddot{x}_{3d}, \\[2mm] U_x = \dfrac{m}{U_1}(-\dfrac{\lambda_1}{\lambda_4}e_1 - (\dfrac{\lambda_1}{\lambda_4^2} + \lambda_1 + \lambda_4)e_4 + \ddot{x}_{1d}, \\[2mm] U_y = \dfrac{m}{U_1}(-\dfrac{\lambda_2}{\lambda_5}e_2 - (\dfrac{\lambda_2}{\lambda_5^2} + \lambda_2 + \lambda_5)e_5 + \ddot{x}_{2d}, \end{cases} \tag{18}$$

with $\lambda_i \geq 0$ for $i \in [1,12]$.

10   The PID-Backstepping Controller

The PID regulator (proportional-integral-derivative) serves to reduce the error between the measurement and the set point; it is used in most industrial processors thanks to its simplicity and efficiency especially in linear systems. It is based on three operations [12]: proportional action (P): in which a gain K_p is applied to the error, an integral action (I): in which we integrate the error, and we multiply the result by a gain K_i, and a derivative action (D): in which one derives the error, and one multiplies the result by a gain K_d.

The architecture of the cascade PID has been extended to the non-linear case by separating the translation and rotation dynamics from the equations of motion. A linear control is then applied to the dynamics of rotation and a nonlinear control has been applied to the dynamics translation by the backstepping control.

11   Attitude and Altitude Control by PID:

The linear control by a PID is well adapted to the quasi-stationary flight, for which the angles of inclination of the vehicle are small. This makes it possible to obtain a decoupled

model in several SISO (Single Input Single Output) chains of the dynamics of the drone. Let $e_\phi = \phi_d - \phi$, and $U_2 = K_{p\phi}e_\phi(t) + K_{I\phi}\int_0^t e_\phi(\tau)d\tau + K_{D\phi}\frac{de_\phi(t)}{dt}$.

The same applies to the pitch and yaw angle and altitude control

$$\begin{cases} e_\theta = \theta_d - \theta, \\ U_3 = K_{p\theta}e_\theta(t) + K_{I\theta}\int_0^t e_\theta(\tau)d\tau + K_{D\theta}\frac{de_\theta(t)}{dt}, \end{cases} \tag{19}$$

and

$$\begin{cases} e = \Psi_d - \Psi, \\ U_4 = K_{p\Psi}e_\Psi(t) + K_{I\Psi}\int_0^t e_\Psi(\tau)d\tau + K_{D\Psi}\frac{de_\Psi(t)}{dt}, \end{cases} \tag{20}$$

and

$$\begin{cases} e = z_d - z, \\ U_1 = K_{pz}e_z(t) + K_{Iz}\int_0^t e_z(\tau)d\tau + K_{Dz}\frac{de_z(t)}{dt}. \end{cases} \tag{21}$$

The parameters K_{px}, K_{Ix}, K_{Dx}, respectively, define the proportional, integral and derivative gains of the angles ϕ, θ, Ψ and altitude Z.

12 Control in Position with the Backstepping Controller

The backstepping represents a recursive method that allows to build a control law which guarantees, at any time, the stability of the system. Writing states in pure parametric form highlights the subsystems. For each of these parts, it is necessary to find, using a Lyapunov function, a control which makes it possible to stabilize this subsystem [11].

To do this, the next state is considered as the new controller input (the virtual control). The order of the subsystem is then increased and the previous development is restarted. At the end, a control law is obtained [5].

13 The Steps of the Synthesis

The backstepping is, in fact, only the construction of the Lyapunov function as well as the step-by-step control for a system that can be written in the form, called cascade, as follows:

$$\begin{cases} \dot{x}_1 = x_2 + \phi_1(x_1), \\ \dot{x}_2 = x_3 + \phi_2(x_1, x_2), \\ \vdots \\ \dot{x}_{n-1} = x_n + \phi_{n-1}(x_1, x_2, \cdots, x_{n-1}), \\ \dot{x}_n = u + \phi_n(x_1, x_2, \cdots, x_n), \\ y = x_1, \end{cases} \tag{22}$$

where $x \in R^n$ and $u \in R$.

The aim is to find a law of control which ensures the continuation of a reference y_d. It is carried out in several stages. In our case, we applied the backstepping control to stabilize the position of the quadrotor along the x and y axes, so we apply it to these two subsystems in cascade [16]. We used backstepping control to stabilize the outer loop and the PID to stabilize the inner loop. The steps of the synthesis are: The first subsystem is given by the following equations:

$$\begin{cases} \dot{x}_1 = x_4, \\ \dot{x}_4 = C_{x7} * S_{x8} * \dfrac{U_1}{m}. \end{cases} \tag{23}$$

Consider $e_1 = x_d - x_1$ as a tracking error of the x-axis, and its time derivative $\dot{e}_1 = \dot{x}_d - \dot{x}_1$. The analysis of stability is treated by Lyapunov's theorem considering a positive definite function $V(e_1)$ and its negative semi-definite temporal derivative. Put $V_1 = \frac{1}{2}(x_d - x_1)^2$ and $\dot{V}_1 = (x_d - x_1)(\dot{x}_d - \dot{x}_1) = (x_d - x_1)(\dot{x}_d - x_4)$. To ensure stability for this equation let us take $x_4 = \phi_4 = -\lambda(x_d - x_1) + \dot{x}_{1d}$. The desired new reference will be the control variable for the preceding subsystem $x_4 = \phi_4$.

The regulation error is $e_2 = \phi_4 - x_4$. Its derivative is $\dot{e}_2 = \dot{\phi}_4 - \dot{x}_4$. The extended Lyapunov function for this system is $V_4 = V_1 + \frac{1}{2}e_2^2$, and

$$V_4 = \frac{1}{2}(e_1^2 + e_2^2). \tag{24}$$

Its derivative is : $\dot{V}_4 = \dot{V}_1 + e_2\dot{e}_2$ and

$$\begin{aligned} \dot{V}_4 &= (x_d - x_1)(\dot{x}_d - \dot{x}_1) + (\phi_4 - x_4)(\dot{\phi}_4 - \dot{x}_4) \\ &= (x_d - x_1)(\dot{x}_d - \phi_4) + (\phi_4 - x_4 - \dot{\phi}_4 - C_{x7} * S_{x8} * \frac{U_1}{m}) \end{aligned} \tag{25}$$

and $C_{x7} * S_{x8} * \frac{U_1}{m} = -\lambda_4(\phi_4 - x_4) + (x_{1d} - x_1) + \dot{\phi}_4 - x_1 + x_{1d}$, in which $\theta_d = x_8^* = arcsin[([-\lambda_4(\phi_4 - x_4) + (x_d - x_1) + \dot{\phi}_4 - x_1 + x_{1d}] * m)/(C_{x7} * U_1)]$. In the same way for the subsystem

$$\begin{cases} \dot{x}_2 = x_5, \\ \dot{x}_5 = -S_{x8} * \dfrac{U_1}{m}. \end{cases} \tag{26}$$

We end up with the control that stabilizes x_5, which is $\phi_5 = -\lambda_2(x_{2d} - x_2) + \dot{x}_2$, and $\phi_d = x_7^* = arcsin[(-m[-\lambda_5(\phi_5 - x_5) + \dot{\phi}_5 - x_2 + x_{2d}])/(U_1)]$.

14   Simulation Results

The parameters of the quadrotor are given as follows: mass (m = 0.650 Kg), moment of inertia of the quadrotor compared to x (j_x = 7.5e-3 $Kg.m^2$), moment of inertia of the quadrotor compared to y (j_y = 7.5e-3 $Kg.m^2$), moment of inertia of the quadrotor compared to z (j_z = 1.3e-2 $Kg.m^2$), coefficient of lift (b = 3.13e-5 Ns^2), coefficient of drag (k = 7.5e-5 Nms^2), moment of inertia of the rotor compared to z (j_{rz} = 6e-5 $Kg.m^2$), distance between the rotor and the center of gravity (d = 0.23 m).

In order to validate the robustness and disturbance resistance of the proposed controls schemes for stabilizing the quadrotor at trajectory tracking, the simulation is conducted

in MATLAB SIMULINK 2016, a programming environment on an Intel Core i5 - PC running under Windows 10. Similarly, linear and aleatory disturbances are added to the outputs of the quadrotor.

The two control techniques, the forwarding controller and the PID-backstepping hybrid controller, were implemented on a non-linear model of the quadcopter. Numerical simulation was performed using MATLAB SIMULINK software. The resolution of the systems of differential equations was made by the Runge-Kutta method of order 4 with a simulation step t = 0.0001 sec, and a final time tf = 20 sec.

The control parameters of the PID controllers are tuned by the tune function of SIMULINK.
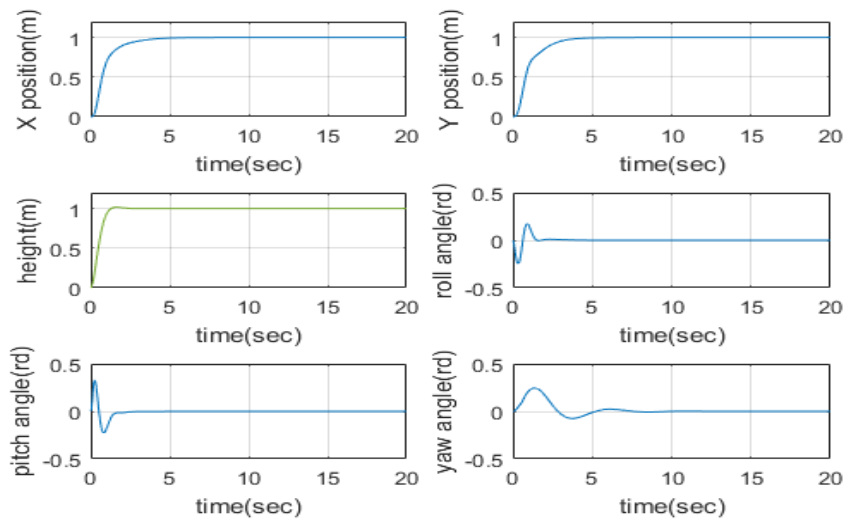
Figure 3: The forwarding system response.

15 Disturbance Rejection with the Forwarding Control

We introduced a disturbance of the order of 10% on the outputs x, y, z and Ψ and the results are given in the figures below. We note that this control was able to eliminate the effect of the disturbance which confirms its robustness. The control parameters of the PID controllers are tuned by the tune function of SIMULINK. The tuned parameters are given as follows using a unit step response case: altitude : (K_{Pz}=132.3356, K_{Iz}=205.1444, K_{Dz}=20.9622), roll : ($K_{P\phi}$ =0.6054, $K_{I\phi}$=0.2834, $K_{D\phi}$ =0.3175), pitch : ($K_{P\theta}$=0.6054, $K_{I\theta}$=0.2834, $K_{D\theta}$=0.3175), yaw : ($K_{P\psi}$=24.1383, $K_{I\psi}$ =113.0029, $K_{D\psi}$ =1.2660.

The responses of the quadrotor to the PID control and backstepping are given in the following figures. To test the robustness of this control, we introduced a disturbance of the order of 10% of the input signal on the outputs x, y, z and Ψ from the 10th second, we obtain the following response.   In the comparative simulation, the quadrotor follows a referenced trajectory of x, y, z and Φ and θ are equal to zero, which is shown in the figures above. Linear and noise signals are applied at the 10th second. From the result, the response of the forwarding is slightly faster than that of the PID-backstepping. As the noise signal increases, the tracking error becomes bigger. Nevertheless, it is obvious
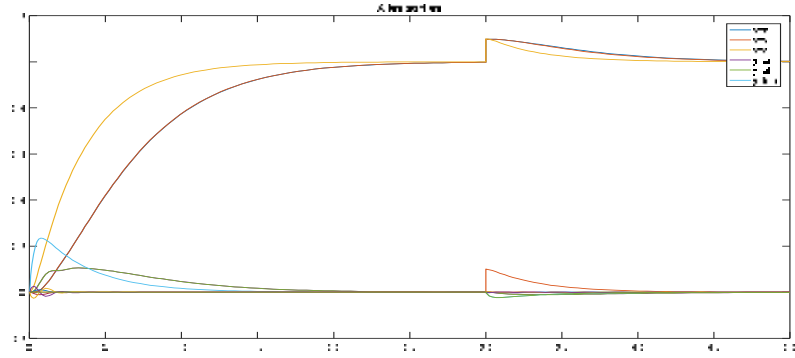
**Figure 4**: Rejection of the disturbance applied at the moment of 30 sec.
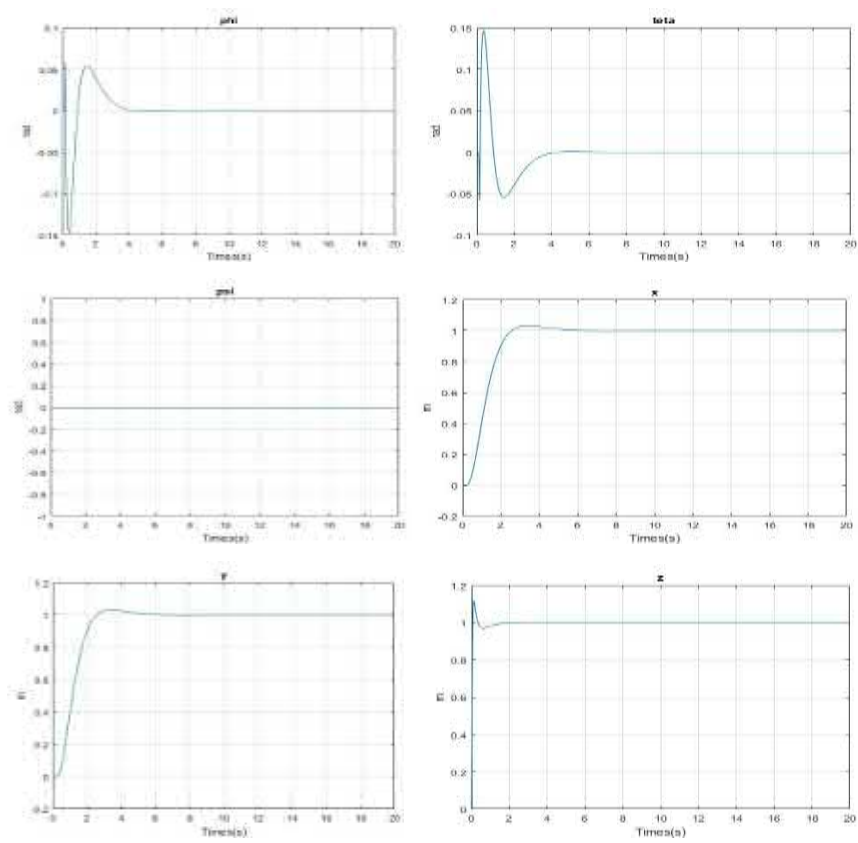
Figure 5: The system response with the PID-backstepping control.
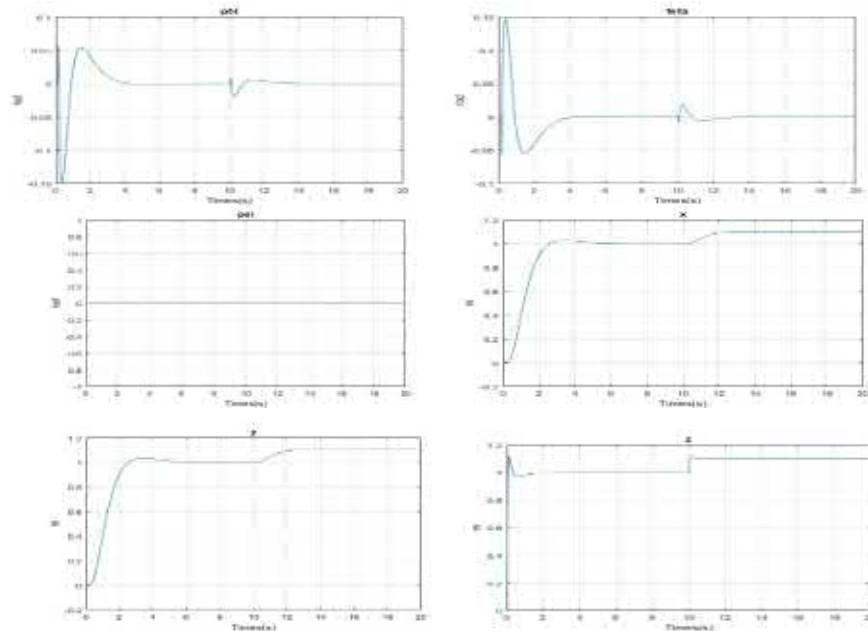
Figure 6: The system response with the PID-backstepping control with disturbances.

that the steady state error of forwarding is smaller than that of PID-backsteppig. In conclusion, the forwarding has a strong ability of disturbance compensation.

16   Conclusion

In this paper, we presented a control law of stabilization of the trajectory of a quadrotor synthesized by the forwarding control based primarily on the development of the dynamic model of the quadrotor, all this by taking into account the different forces and couples that can influence the evolution of this drone and the development of non-holonomic constraints of high order imposed on the movements of the system. These control laws allowed the follow-up of the different desired trajectories expressed in terms of coordinates of the center of mass of the system in spite of the complexity of the proposed model. The forwarding control gave satisfactory results of the follow-up of the imposed trajectories and the rejects of disturbances. The simulations show the good performance of the proposed controller.

To ensure the robustness of the forwarding control we compared its performance with another hybrid control that is based on the PID-backstepping control. Unlike the forwarding control, the PID-backstepping control gives satisfactory results as long as we are close to the operating point where the effect of disturbances on system responses is studied by different simulations. The proposed approaches have proved their robustness and efficiency in simulation for the stability of the position and attitude of the system. Our perspectives are to test the effectiveness of these strategies on the real system.
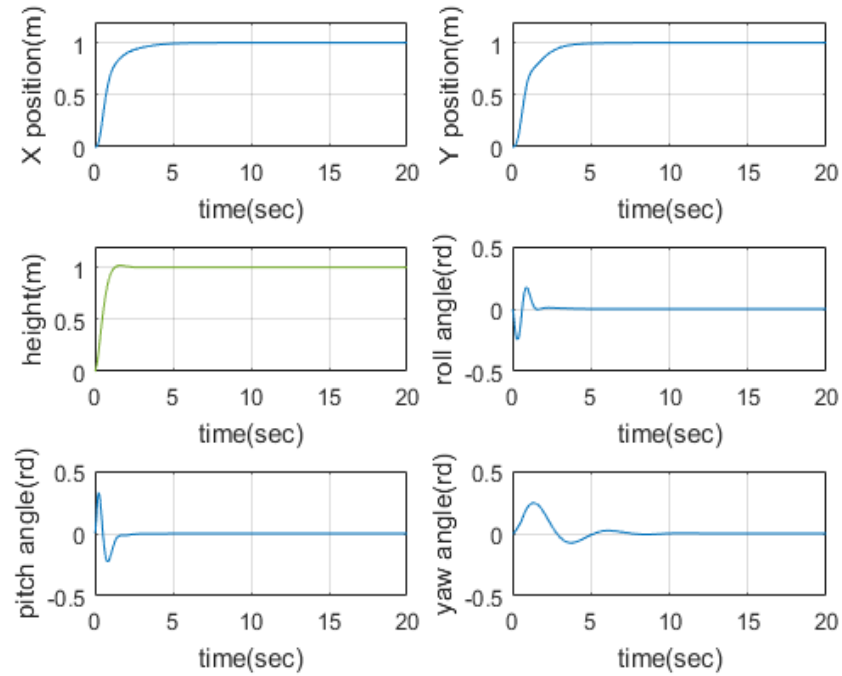
**Figure 7**: The system response with the forwarding control with variation of parameters.
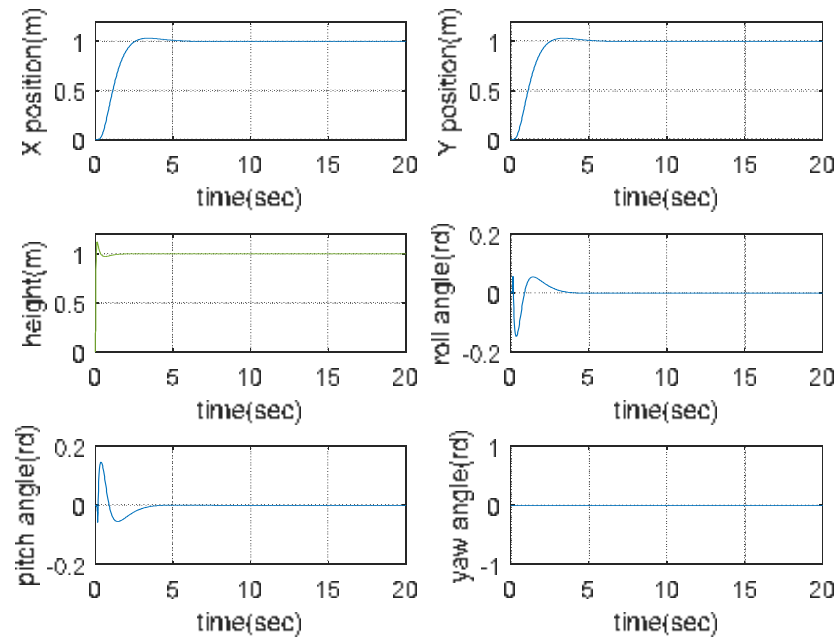
Figure 8: The system response with the PID-backstepping control with variation of parameters.
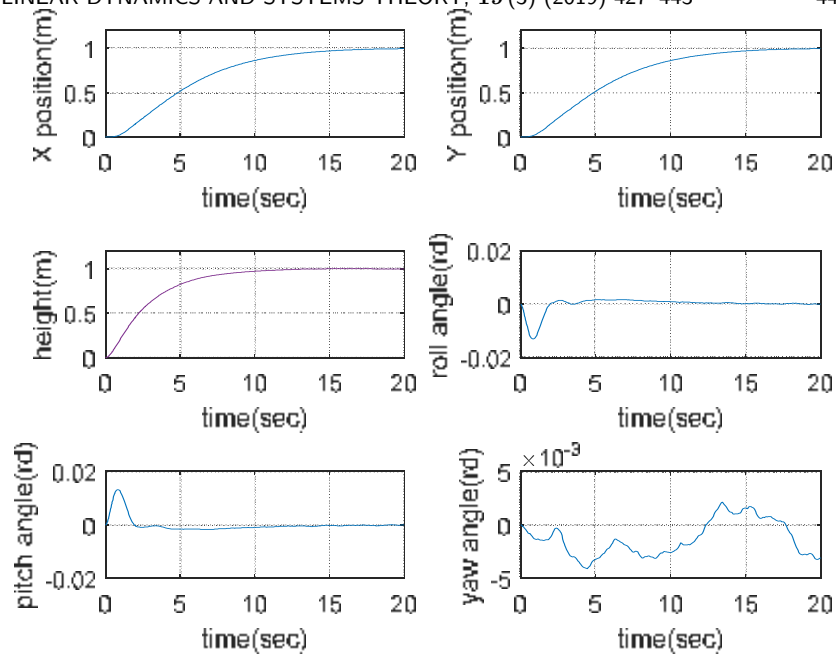
Figure 9: The system response with the forwarding control with aleatory disturbances.
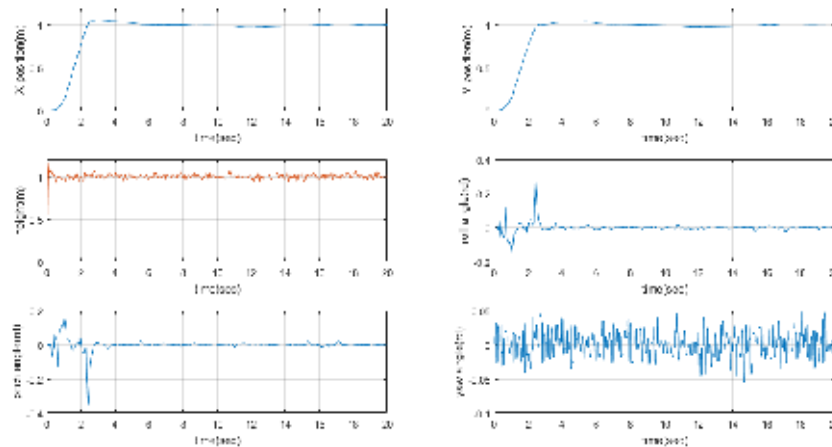

Figure 10: The system response with the PID-backstepping control with aleatory disturbances.

References

[1] A. Y. Aleksandrov, E. B. Aleksandrova, A. V. Platonov, and M. V. Voloshin. On the global asymptotic stability of a class of nonlinear switched systems. *Nonlinear Dynamics and*

Systems Theory **2** (17) (2017) 107–120.

[2] R. Ashton & M. Maggiore. A class of position controllers for underactuated VTOL vehicles. *IEEE Transactions on Automatic Control* **59** (9) (2014) 2580–2585.

[3] M. A. M. Basri, A. R. Husain and K. A. Danapalasingam, A hybrid optimal backstepping and adaptive fuzzy control for autonomous quadrotor helicopter with time-varying disturbance. *J. Aerospace Engineering* **229** (12) (2015) 2178–2195.

[4] H. Bolandi, M. Rezaei, R. Mohsenipour, H. Nemati and S. M. Smailzadeh. Attitude control of a quadrotor with optimized pid controller. *Intelligent Control and Automation* **04** (3) (2013) 342–349.

[5] S. Bouabdallah, A. Noth and R. Siegwart. PID vs LQ control techniques applied to an indoor micro quadrotor. In: *Proc. of the IEEE International Conference on Intelligent Robots and Systems (IROS)* (2004) 2451–2456.

[6] H. Bouadi, M., Bouchoucha, and M. Tadjine. Modelling and Stabilizing Control Laws Design Based on Sliding Mode for an UAV Type-Quadrotor. *Engineering Letters* **15** (2) (2007) 15–24.

[7] F. Chen, R. Jiang, K. Zhang, B. Jiang, G. Tao. Robust Backstepping Sliding-Mode Control and Observer-Based Fault Estimation for a Quadrotor UAV. *IEEE Transactions on Industrial Electronics* **63** (8) (2016) 5044–5056.

[8] Z. Dong, H. Fan, Y. Wang, L. Xu and W. Wang. Adaptive backstepping controller design for quadrotor aircraft with unknown disturbance. In: *Control, Automation, Robotics and Vision (ICARCV), 2016 14th International Conference*, (2016, November), 1–5.

[9] M. Idres, O., Mustapha and M. Okasha. Quadrotor trajectory tracking using PID cascade control. In: *IOP Conference Series: Materials Science and Engineering*, IOP Publishing **270** (1) (2017, December), 10–12.

[10] M. Islam, M. Okasha and M. M. Idres, Trajectory tracking in quadrotor platform by using PD controller and LQR control approach. In: *IOP Conference Series: Materials Science and Engineering*, IOP Publishing **260** (1) (2017, November), 012–026.

[11] A. G. Mazko. Robust Output Feedback Stabilization and Optimization of Control Systems *Nonlinear Dynamics and Systems Theory* **17** (1) (2017) 42–59.

[12] J. P. Ortiz, L. I. Minchala, and M. J. Reinoso. Nonlinear robust h-infnity PID controller for the multivariable system quadrotor. *IEEE Latin America Transactions* **14** (3) (2016) 1176–1183.

[13] J. A. Paredes, C. Jacinto, R. Ramrez, I. Vargas and L. Trujillano. Simplified fuzzy-PD controller for behavior mixing and improved performance in quadcopter attitude control systems. In: *ANDESCON, 2016 IEEE*, (2016, October), 1–4.

[14] R. Sepulchre, M. Jankovic, and P. Kokotovic. *Constructive Nonlinear Control*. Springer-Verlag. London, 1997.

[15] X. Shi, B., Hu, C., Yin, Y., Cheng and X. Huang. Design of trajectory tracking controller with backstepping method for quadrotor unmanned aerial vehicles. Chinese Control and Decision Conference (CCDC), (2018, June), 3124–3128.

[16] L. Wang, H. Jia. The trajectory tracking problem of quadrotor UAV: Global stability analysis and control design based on the cascade theory. *Asian Journal of Control* **16** (2) (2014) 574–588.

[17] X. Wang, X. Lin, Y. Yu, Q. Wang and C. Sunl. Backstepping Control for Quadrotor with BP Nerual Network Based Thrust Model. *32nd Youth Academic Annual Conference of Chinese Association of Automation (YAC)* (2017) 292–297.

[18] J. Xiong and E. H. Zheng. Position and attitude tracking control for a quadrotor UAV. *ISA transactions* **53** (3) (2014) 725–731.

[19] C. Yin, X. Huang, Y. Chen, S. Dadras, S. M. Zhong and Y. Cheng. Fractional-order exponential switching technique to enhance sliding mode control. *Applied Mathematical Modelling* **44** (2017) 705–726.

[20] X. Zhang, X. Huang, and H. Lu. Forwarding-based Trajectory Tracking Control for Nonlinear Systems with Bounded Unknown Disturbances. *International Journal of Control, Automation and Systems* **14** (5) (2016) 1–13.

CAMBRIDGE SCIENTIFIC PUBLISHERS

Lyapunov Exponents and Stability Theory
Stability, Oscillations and Optimization of Systems: Volume 6,
317 pp, 2012   ISBN   £55/$100/€80

N.A. Izobov

Institute of Mathematics, National Academy of Sciences of Belarus,
Minsk, Belarus

This monograph deals with one of two basic methods of stability investigation of solutions to differential systems – the method of characteristic Lyapunov indices. It provides necessary knowledge from modern theory of Lyapunov indices and presents results of the author who is a leading expert in this field. Main attention is focused on the following areas:

- the theory of low Perrone indices, general Bole indices, central Vinograd indices and the author's exponential indices
- the freezing method
- investigation of effect of exponentially decreasing perturbations on characteristic indices of linear differential systems
- stability of characteristic indices of linear systems with respect to small perturbations
- Lyapunov problem on investigation of asymptotic stability with respect to linear approximation
- Millionschikov method of turnings and its methodical application in modern theory of Lyapunov indices

Requiring only a fundamental knowledge of general stability theory, this book serves as an excellent text for graduate students studying ordinary differential equations and stability theory as well as a useful reference for analysts interested in applied mathematics.

CONTENTS